

**Regional Groundwater Modelling for Flow Analysis and Investigation of Alternative Water  
Resources in the Edmonton Region, Alberta, Canada**

By

Marcus Henry Kehler

A thesis submitted in partial fulfillment of the requirements for the degree of

Master of Science

Department of Earth and Atmospheric Sciences  
University of Alberta

© Marcus Henry Kehler, 2022

## **Abstract**

Water resources in the Edmonton region are expected to be increasingly threatened by climate change and/or contamination in the coming decades. Currently, the sole source of water for the city of Edmonton is the North Saskatchewan River (NSR). This makes Edmonton vulnerable to changes in water supply from drought or contamination. A potential temporary secondary water source is groundwater. The groundwater resource in the Edmonton region with the most favourable prospects for large scale water withdrawal is buried valleys (channels). A steady state groundwater model is used to understand regional groundwater flow and the role of buried valleys in groundwater flow in the region. It includes dipping bedrock geology and surficial geology together with recently mapped buried valley extents. Findings help to characterize groundwater flow in the area, highlighting flow system features such as discharge areas, groundwater-surface water interactions and buried valley's role in a regional flow context. The steady state model also provides a starting point for transient simulations. Transient simulations focus on the Onoway, Beverly and Stony channels. Results indicate the Beverly channel is the most favourable for large scale water extraction followed by the Onoway and the Stony channels respectively. The Beverly channel was able to supply 190 ML/day for 365 days, followed by the Onoway channel at 190 ML/day for 30 days, with the smallest extraction rate sustained by the Stony channel at 10 ML/day for 365 days.

## Preface

This thesis is organized into 4 chapters. Chapters 2 and 3 represent the body of the thesis and cover the steady state and transient groundwater models respectively. Chapters 2 and 3 are intended to be submitted for publication in peer reviewed journals at a later date. Chapters 1 and 4 represent the introduction and summary/conclusions respectively. Chapters 1-4 are co-authored by Drs. Brian Smerdon, Ben Rostron, and Daniel Alessi, who assisted by providing constructive feedback and editorial comment throughout the formulation of this thesis. I (Marcus Kehler) designed the framework of the thesis, wrote most of the text contained in it and created all figures.

## **Acknowledgements**

I would like to thank my supervisors, Drs. Ben Rostron, Brian Smerdon, and Daniel Alessi for guiding me through this thesis. They actively encouraged me to work independently while also providing much needed guidance when necessary. I have gained so much valuable experience not just in hydrogeology but professionally under their supervision. They have helped me become a better educated, more confident, and more competent earth scientist and for that I am forever grateful.

Thank you to Alberta Innovates and EPCOR for providing the funding and support needed to complete this thesis. Without their generous support this project would not be possible. Thank you to Mike Christensen, Heather Zarski, and Steph Neufeld at EPCOR for providing crucial data and feedback for the project.

Thank you to my family and friends who have supported me throughout this academic endeavor. I could not have done it without their support. Most of all, thank you to my partner, Jasmine, for encouraging and supporting me through challenging moments.

## Table of Contents

<b>Abstract .....</b>	ii
<b>Preface .....</b>	iii
<b>Acknowledgements.....</b>	iv
<b>Table of Contents .....</b>	v
<b>List of Tables .....</b>	viii
<b>List of Figures.....</b>	ix
<b>Chapter 1: Introduction.....</b>	1
<b>1.1 Background.....</b>	1
<b>1.2 Thesis Organization and Objectives.....</b>	4
<b>1.3 References .....</b>	5
<b>Chapter 2: Steady State Model.....</b>	8
<b>2.1 Introduction .....</b>	8
<b>2.2 Hydrogeologic Setting.....</b>	11
<b>2.2.1 Climate.....</b>	11
<b>2.2.2 Geology .....</b>	11
<b>2.2.3 Hydrogeology.....</b>	19
<b>2.3 Model Design.....</b>	22
<b>2.3.1 Steady State Representation .....</b>	22
<b>2.3.2 Model Domain .....</b>	25
<b>2.3.3 Grid Design.....</b>	29
<b>2.3.4 Layer Types .....</b>	31
<b>2.3.5 Model Boundary Conditions .....</b>	31

<b>2.3.6. Parameterization .....</b>	36
<b>2.4. Calibration .....</b>	39
<b>2.4.1 Calibration Method .....</b>	39
<b>2.4.2 Sources of Error in Calibration Data .....</b>	43
<b>2.5 Model Results and Sensitivity Analysis.....</b>	44
<b>2.5.1 Hydraulic Head Distribution .....</b>	44
<b>2.5.2 Sensitivity Analysis.....</b>	51
<b>2.6 Discussion.....</b>	55
<b>2.6.1 Bedrock and Surficial hydraulic head distributions .....</b>	55
<b>2.6.2 Groundwater flow patterns and directions .....</b>	58
<b>2.6.3 Groundwater Discharge Areas .....</b>	61
<b>2.6.4 Buried valleys and the North Saskatchewan River .....</b>	62
<b>2.7 Conclusions and recommendations.....</b>	67
<b>2.8 References .....</b>	69
<b>Chapter 3: Transient Model .....</b>	77
<b>3.1 Introduction .....</b>	77
<b>3.2 Methods.....</b>	80
<b>3.2.1 Model Area .....</b>	80
<b>3.2.2 Geology .....</b>	82
<b>3.2.3 Hydrogeology.....</b>	82
<b>3.2.4 Numerical model Set-Up .....</b>	89
<b>3.2.5 Pumping Scenarios .....</b>	92
<b>3.3 Results .....</b>	100

<b>3.4 Discussion.....</b>	108
<b>3.4.1 Pumping rates.....</b>	108
<b>3.4.2 Drawdown trends in buried valley aquifers .....</b>	111
<b>3.4.3 Implications of three-dimensional hydrogeologic setting for buried valleys.....</b>	112
<b>3.5 Conclusions .....</b>	119
<b>3.6 References .....</b>	121
<b>Chapter 4: Conclusions and Future Research .....</b>	128
<b>4.1 Conclusions .....</b>	128
<b>4.2 Future Research.....</b>	130
<b>Bibliography.....</b>	133

## List of Tables

<b>Table 2.0.</b> Stratigraphic column for model area (Bayrock & Hughes, 1962; Fenton et al., 2013; Kathol & Mcpherson, 1975; Prior et al., 2013) .....	18
<b>Table 2.1.</b> Summary of boundary conditions to represent large lakes in the model area.....	35
<b>Table 2.2.</b> Model hydraulic conductivity compared with literature values. ....	38
<b>Table 3.0.</b> Hydraulic conductivity model values compared literature reported values. ....	87
<b>Table 3.1.</b> Storage parameters compared literature reported values. ....	88
<b>Table 3.2.</b> Number and location of wells used the in each model pumping scenario. ....	95
<b>Table 3.3.</b> Relative probability table of tested pumping scenarios. ....	110

## List of Figures

<b>Figure 2.0.</b> Digital elevation model (DEM) (Alberta Environment and Parks, 2017) of the study area with buried valley extents from Rubin (2022) .....	10
<b>Figure 2.1.</b> Bedrock geology in study area modified from Prior et al. (2013). Note, The Scollard Formation is mapped separately from the Edmonton Group due to its ability to be mapped at this scale.....	12
<b>Figure 2.2.</b> Surficial Geology modified from Andriashuk et al., (1979), Bayrock (1972), and Fenton et al. (2013) in the study area. Buried valley extents (Empress Formation) from Rubin (2022).....	13
<b>Figure 2.3.</b> Location of active GOWN wells in model area with AWWID IDs listed. Buried valley extents from Rubin (2022).....	23
<b>Figure 2.4.</b> Hydrographs of active GOWN wells in study area with AWWID IDs Posted. ....	24
<b>Figure 2.5.</b> Model Boundary superimposed with HUC watersheds boundaries (Alberta Environment and Parks, 2014).....	26
<b>Figure 2.6</b> Surficial Static water level map based off data from the AWWID database (Government of Alberta, n.d.a).....	27
<b>Figure 2.7.</b> Bedrock static water level map based off data from the AWWID database (Government of Alberta, n.d.a).....	27
<b>Figure 2.8.</b> Model boundary with local groundwater divides modified from Bibby (1974b), Ceroici (1979b), Tokarsky (1971), Stein (1976b), and Stein & Carlson (1982) superimposed....	28
<b>Figure 2.9.</b> Example of discretizing dipping layers in finite difference grid.....	30
<b>Figure 2.10.</b> Recharge distribution in the model area. .....	33
<b>Figure 2.11.</b> Evapotranspiration distribution in model area. .....	34
<b>Figure 2.12.</b> Digital Elevation Model (DEM) with locations of ET applied by model. .....	41
<b>Figure 2.13.</b> Calibration data with 1:1 line in black.....	42

<b>Figure 2.14.</b> Simulated water table.....	46
<b>Figure 2.15a.</b> Hydraulic head in layer 2 (surficial deposits without buried valleys).....	47
<b>Figure 2.15b.</b> Hydraulic head in layer 4 (surficial deposits including buried valleys).....	48
<b>Figure 2.15c.</b> Hydraulic head in layer 6 (shallow bedrock) .....	49
<b>Figure 2.15d.</b> Hydraulic head in layer 8 (deep bedrock).....	50
<b>Figure 2.16.</b> Percent change in RMS error for surficial sensitivity analysis.....	52
<b>Figure 2.17.</b> Percent change in RMS error for bedrock sensitivity analysis.....	53
<b>Figure 2.18.</b> Percent change in RMS error for recharge sensitivity analysis.....	54
<b>Figure 2.19.</b> Surficial aquifers superimposed on Layer 4 hydraulic head distribution.....	57
<b>Figure 2.20.</b> Water table contours superimposed on topography with interpreted flow arrows. .	60
<b>Figure 2.21a.</b> Areas with a favourable head gradient for upwards groundwater flow.....	63
<b>Figure 2.21b.</b> Areas with a favourable head gradient for upwards groundwater flow with observed spring and flowing wells. ....	64
<b>Figure 2.21c.</b> Areas with a favourable head gradient for upwards GW with interpreted GW discharge areas.....	65
<b>Figure 2.21d.</b> Relative baseflow variation across the NSR.....	66
<b>Figure 3.0.</b> Study area map with reference cities and digital elevation model (DEM) (Alberta Environment and Parks, 2017). Buried valley extents from Rubin (2022).....	81
<b>Figure 3.1.</b> Bedrock geology in layers 5 to 20 of model, modified from Prior et al. (2013). .....	84
<b>Figure 3.2.</b> Surficial geology in layers 1 and 2 of model, modified from Andriashek et al., (1979), Bayrock (1972), and Fenton et al. (2013). .....	85
<b>Figure 3.3.</b> Surficial geology in layers 3 and 4 of model, modified from Andriashek et al., (1979), Bayrock (1972), Fenton et al. (2013), and Rubin (2022).....	86

<b>Figure 3.4.</b> Calibration chart for steady state model with 1:1 line in black. ....	91
<b>Figure 3.5.</b> Areas of interest within chosen channels.....	94
<b>Figure 3.6.</b> Pumping well network for 10 ML/day scenarios (3 and 30 days). .....	96
<b>Figure 3.7.</b> Pumping well network for 10 ML/day scenario, with two wells in the Stony channel (365 days).....	97
<b>Figure 3.8.</b> Pumping well network for seven pumping wells in each of the Beverly and Onoway channels for the 190 and 375 ML/day scenarios (3 days).....	98
<b>Figure 3.9.</b> Pumping well network for thirteen wells in each of the Beverly and Onoway channels for the 190 and 375 ML/day scenarios (30 and 365 days).....	99
<b>Figure 3.10.</b> Model area with location of interest in red.....	101
<b>Figure 3.11.</b> Drawdown contours after 3 days pumping at 10 ML/day. ....	102
<b>Figure 3.12.</b> Drawdown contours after 30 days pumping at 10 ML/day. ....	103
<b>Figure 3.13.</b> Drawdown contours after 365 days pumping at 10 ML/day. ....	104
<b>Figure 3.14.</b> Drawdown contours after 3 days pumping at 190 ML/day. Note that 190 ML/day could not be pumped from the Stony Valley.....	105
<b>Figure 3.15.</b> Drawdown contours after 30 days pumping at 190 ML/day. Note that 190 ML/day could not be pumped from the Stony Valley.....	106
<b>Figure 3.16.</b> Drawdown contours after 365 days pumping at 190 ML/day. Note that 190 ML/day could not be pumped from the Stony and Onoway valleys.....	107
<b>Figure 3.17.</b> How transmissivity effects the shape of the drawdown cone showing A) Low transmissivity (T). B) High T. After Freeze & Cherry (1979). ....	114
<b>Figure 3.18.</b> Drawdown trends in buried valley aquifers at 10 ML/day. ....	115
<b>Figure 3.19.</b> Drawdown trends in buried valley aquifers at 190 ML/day. ....	116

**Figure 3.20.** Drawdown extent from layer 4 in the Beverly channel after 30 days with an extraction rate of 190 ML/day with A. layer 4 geology and B. layers 1 and 2 geology overlain.....117

**Figure 3.21.** Drawdown extent from layer 4 in the Beverly channel after 365 days with an extraction rate of 190 ML/day with A. layer 4 geology and B. layers 1 and 2 geology overlain.....118

## **Chapter 1: Introduction**

### **1.1 Background**

Climate change is expected to negatively impact water resources across much of North America in the coming decades (Marvel et al. 2019; Organisation for Economic Co-operation and Development (OECD), 2013). Alberta's water resources are especially vulnerable due to its location in the semi-arid prairies of Western Canada. The Canadian Prairies are projected to have increasingly frequent and long-lasting drought as climate change progresses (Natural Resources Canada, 2020), which can have the added impact of increased contaminant concentrations as water levels decline (Organisation for Economic Co-operation and Development (OECD), 2013). However, contamination can also occur suddenly (e.g., chemical spills) regardless of climate change. Either contamination or water scarcity may threaten the water security of growing prairie cities. For example, the sole water source for the city of Edmonton, Alberta is the North Saskatchewan River (NSR) (Edmonton Power Corporation (EPCOR), 2020). Lack of alternative water supplies means Edmonton is vulnerable to drought and contamination in the future.

In response to lack of alternative water supplies for Edmonton, a multidisciplinary research project at the University of Alberta was initiated in 2020. Integrated watershed modelling, water chemistry, aquifer characterization and regional groundwater (GW) modelling were used to understand both the NSR and alternative water sources. Integrated watershed modelling involved creation of a coupled SWAT-MODFLOW model for the North Saskatchewan River Basin (NSRB) (Zaremehrjardy et al., 2022). This watershed scale model simulated future climatic scenarios for the NRB, informing how surface water and groundwater availability may be impacted in response to climate change. Water chemistry research involves utilizing hydrogen and oxygen isotopes in addition to major and minor element chemistry to understand interactions between the NSR and groundwater sources, along with enhancing aquifer characterization. Additional isotopic tracers have the added benefit of potentially differentiating GW and surface water (SW) contributions to the NSR. Finally, significant work was done on regional aquifer characterization and representation through modelling. In the Edmonton area, regional aquifer delineation and mapping was completed by Rubin (2022). That work enabled subsequent work to be done using Electrical Resistivity Tomography (ERT) and groundwater modelling. ERT work was completed simultaneously to better delineate buried channels of interest in data sparse regions. Groundwater

modelling focused on representing the regional aquifers and the groundwater flow system (GFS), while also defining limits on groundwater extraction. The focus of this thesis will be on the groundwater modelling portion of the research project.

Groundwater is often considered less vulnerable than surface water to drought or contamination (Zektser & Everett, 2006). Thus, groundwater may provide a valuable defense in the case of NSR water scarcity. Regional characterization of groundwater starts with delineation and mapping of aquifers. As noted previously, Rubin (2022) mapped the most extensive regional aquifers in terms of spatial distribution and ability to supply water in the Edmonton region. These aquifers are termed buried valleys/channels. Buried valleys are preglacial channels incised into bedrock and subsequently buried by glacial deposits (Cummings et al., 2012). They are often filled with high hydraulic conductivity (K) sand and gravel sediment and are regionally extensive in nature, spanning much of Alberta (Cummings, et al., 2012; Rubin, 2022). Because of this, they have been noted to have a significant role in groundwater transport and storage (Farvolden et al., 1963). Research from the 1970s through to the early 2000s focused on jurisdictionally bounded groundwater mapping and reports (Bibby 1974a, 1974b, 1974c; Ceroici, 1979a, 1979b; Hydrogeological Consultants Ltd, 1998a, 1998b, 1998c, 1999, 2001; Ozoray, 1972; Stein, 1976a, 1976b; Stein, 1982; Stein & Carlson, 1982). These reports outlined the geology, hydrogeology, and estimated groundwater yields based on field observations and subsequent professional interpretation for various hydrogeological units. This earlier work provided a framework for future investigations that used a regional approach to map groundwater (Riddell et al., 2014; WorleyParsons, 2009). However, conformation to jurisdictional boundaries may exclude important parts of a GFS, while regional approaches may lack necessary detail depending on size.

Each previous groundwater study in the Edmonton region provides valuable information, but from the perspective of a GFS, a limitation was the scale and spatial boundaries. For the Edmonton area, the studies are either too small scale to capture important GFS's and hydrogeologic units or too large and lack sufficient detail. Boundaries that follow municipal or county jurisdictions often ignore cross jurisdictional continuity of groundwater flow. However, a GFS based approach provides a solution to this as it includes the necessary hydraulic continuity between important hydrogeology while also conforming to groundwater flow principles (Tóth, 1963). Notwithstanding, a GFS based study investigating the role of buried valley aquifers on flow

systems in the Edmonton area has not been completed. Likewise, a more holistic GFS based approach has not been used to study maximum city scale groundwater availability and extraction limits. This presents two important knowledge gaps, the first being the role of buried valleys in groundwater flow in the Edmonton region, the second being the theoretical availability of groundwater from buried valleys for large scale water withdrawal. This thesis aims to investigate each of these knowledge gaps, in turn providing a regional understanding of buried valleys role in the GFS and as a water source.

To address the first knowledge gap: the role of buried valleys in groundwater flow systems in the Edmonton area, a steady state groundwater model was produced. A steady state model uses a single timestep with computed heads, fluxes, storage parameters, etc., constant through time to balance inflows with outflows for an area of interest (Anderson et al., 2015). For a conceptualization that imitates real world conditions, including complex hydrogeology and geology, a model can help to understand flow patterns, flow rates, fluxes, gradients, etc. The creation of the model presents a unique opportunity to deliver a large scale, conceptual understanding of groundwater flow in the Edmonton area with buried valleys as a focal point.

To address the second knowledge gap, a transient model was produced. Currently, it is unknown whether groundwater could be a primary or supplementary water source for a large metropolitan area such as the city of Edmonton. As noted previously, buried valleys provide the most promising groundwater resource. To better understand groundwater as a resource, a quantification of the upper limits of how much water buried valleys could provide is necessary. Using water volumes provided from EPCOR (water provider for Edmonton), hypothetical pumping scenarios are developed for three buried valleys close to the city of Edmonton. This is done using a transient groundwater model that utilizes starting conditions from the aforementioned steady state model. Transient models account for changes in response to stress through time, such as pumping that perturbs the natural static starting conditions from the steady state model (Anderson et al., 2015). Each buried valley investigated has characteristically different hydrogeological conditions, and because of this may provide different volumes of water. This allows for hierarchization and characterization of buried valleys of interest on a regional scale, providing a first order understanding of maximum extractable volumes from these unique aquifers under idealized conditions.

## **1.2 Thesis Organization and Objectives**

This thesis focuses on examining the steady state flow patterns and transient pumping scenarios related to buried valleys around Edmonton, Alberta. This was achieved by developing steady state and transient MODFLOW-2005 models respectively. Both models involved data mining, processing, preparation, and post-processing. The objectives of this thesis are to:

- 1) Identify and evaluate the role of buried valleys in groundwater flow systems in the Edmonton area;
- 2) Develop a first order regional scale hierarchization and characterization for large scale water extraction from buried valleys in the Edmonton area;

This thesis is divided into four papers/chapters including this introductory chapter, which provides a brief overview of the broader project and hydrogeological problems being addressed. Chapter 2 covers the background information for the model area, steady state model development, results, and conclusions. It focuses on evaluating the influence of buried valley aquifers on groundwater flow directions, paths, and GW-SW interactions. Chapter 3 uses the same steady state model as chapter 2 but in transient mode. The transient model is used to examine various pumping rates for buried valleys of interest. Three buried valleys are ranked according to their ability to produce water. Chapter 4 provides a summary of both the steady state and transient model conclusions and includes recommendations for future work.

### 1.3 References

- Anderson, M. P., Woessner, W. W., & Hunt, R. J. (2015). *Applied groundwater modeling: Simulation of flow and Advective Transport*. Elsevier, Academic Press.
- Bibby, R. (1974a). *Hydrogeology of the Edmonton area (northwest segment), Alberta*. (ARC/AGS Earth Sciences Report 1974-10). Edmonton, AB: Alberta Research Council.
- Bibby, R. (1974b). *Hydrogeological map of the Edmonton area, northwest segment, Alberta, NTS 83H (part)*. (Map 108). Edmonton AB: Alberta Geological Survey.
- Bibby, R. (1974c). *Regional chemistry and water level distribution of the near-surface groundwaters of the Edmonton area (northwest segment) Alberta*. (ARC/AGS Earth Sciences Report 1974-06). Edmonton AB, Alberta Research Council.
- Ceroici, W.J. (1979a). *Hydrogeology of the southwest segment, Edmonton, Alberta*. (ARC/AGS Earth Sciences Report 1978-05). Edmonton AB: Alberta Research Council.
- Ceroici, W. J. (1979b). *Hydrogeological map of the Edmonton area (southwest segment), Alberta, NTS 83H (part)*. (Map 117). Edmonton AB: Alberta Geological Survey.
- Cummings, D. I., Russell, H. A., & Sharpe, D. R. (2012). *Buried valleys and till in the Canadian Prairies: Geology, hydrogeology, and origin*. (Current research 2012-4 - Geological Survey of Canada). Ottawa, ON: Natural Resources Canada.
- Edmonton Power Corporation (EPCOR). (2020). *Edmonton 2020 Source Water Protection Plan*. (Report). Edmonton, AB.
- Farvolden, R., N., Meneley, W., A., Le Breton, E., G., Lennox, D., H., Meyboom, P. (1963). *Early Contributions to the Groundwater Hydrology of Alberta*. (Bulletin 12). Edmonton AB: Alberta Research Council.
- Hydrogeological Consultants Ltd. (1998a). *County of Lamont No. 30 Part of the North Saskatchewan River Basin Parts of Tp 051 to 058, R 15 to 20, W4M Regional Groundwater Assessment*. (Report No. 97-100). Agriculture and Agri-Food Canada, Prairie Farm Rehabilitation.

Hydrogeological Consultants Ltd. (1998b). *Lac Ste. Anne County Parts of the North Saskatchewan and Athabasca River Basins Parts of Tp 053 to 059, R 01 to 09, W5M Regional Groundwater Assessment*. (Report No. 97-112). Agriculture and Agri-Food Canada, Prairie Farm Rehabilitation.

Hydrogeological Consultants Ltd. (1998c). *Parkland County Part of the North Saskatchewan and Athabasca River Basins Parts of Tp 050 to 054, R 25, W4M to R 08, W5M Regional Groundwater Assessment*. (Report No. 97-202). Agriculture and Agri-Food Canada, Prairie Farm Rehabilitation.

Hydrogeological Consultants Ltd. (1999). *Leduc County Part of the North Saskatchewan River Basin Parts of Tp 047 to 051, R 21 to 28, W4M and R 01 to 04, W5M Regional Groundwater Assessment*. (Report No. 98-130). Agriculture and Agri-Food Canada, Prairie Farm Rehabilitation.

Hydrogeological Consultants Ltd. (2001). *Sturgeon County Part of the North Saskatchewan River Basin Parts of Tp 053 to 058, R 20 to 28, W4M & Tp 054 to 057, R 01, W5M Regional Groundwater Assessment*. (Report No. 01-100). Agriculture and Agri-Food Canada, Prairie Farm Rehabilitation.

Marvel, K., Cook, B. I., Bonfils, C., Durack, P. J., Smerdon, J. E., & Williams, A. P. (2019). Twentieth-century emergence of an externally forced signal in global hydroclimate. *Nature*, 569, 59–65.

Natural Resources Canada. (2020, July 14). Government of Canada. Retrieved September 09, 2020, from <https://www.nrcan.gc.ca/climate-change/impacts-adaptations/climate-change-impacts-forests/forest-change-indicators/drought/17772>

Organisation for Economic Co-operation and Development (OECD). (2013). Chapter 3: Climate change adaptation for water systems in OECD countries. In *Water and climate change adaptation: Policies to navigate Uncharted Waters*. <https://doi.org/10.1787/9789264200449-7-en>

Ozoray, G.F. (1972). *Hydrogeology of the Wabamun Lake area, Alberta* (RCA/AGS Earth Sciences Report 1972-08). Edmonton, AB, Research Council of Alberta.

- Rubin, A. D. (2022). *Pre-Laurentide and Deglacial History of the Edmonton Region, Alberta, Canada* (master's thesis). Edmonton, AB: University of Alberta.
- Riddell, J.T.F., Moktan, H. and Jean, G. (2014). *Regional hydrology of the Edmonton–Calgary Corridor, Alberta* (AER/AGS Open File Report No. 2014-02). Edmonton, AB: Alberta Energy Regulator. Retrieved from <https://ags.aer.ca/publication/ofr-2014-02>
- Stein, R. (1976a). *Hydrogeology of the Edmonton area, (northeast segment), Alberta* (ARC/AGS Earth Sciences Report 1976-01). Edmonton, AB, Alberta Energy and Utilities Board.
- Stein, R. (1976b). *Hydrogeological map of the Edmonton area (northeast segment), Alberta, NTS 83H* (Map 112). Edmonton, AB: Alberta Energy and Utilities Board.
- Stein, R. (1982). *Hydrogeology of the Edmonton area (southeast segment), Alberta* (ARC/AGS Earth Sciences Report 1979-06). Edmonton, AB, Alberta Research Council.
- Stein, R., Carlson, V. A., (1982). *Hydrogeological map of the Edmonton area (southeast segment), Alberta, NTS 83H* (Map 152). Edmonton, AB: Alberta Energy and Utilities Board.
- Tóth, J. (1963). A theoretical analysis of groundwater flow in small drainage basins. *Journal of Geophysical Research*, 68(16), 4795–4812. <https://doi.org/10.1029/jz068i016p04795>
- WorleyParsons. (2009). *North Saskatchewan River Basin Overview of Groundwater Conditions, Issues, and Challenges* (Report No. E00088100). Edmonton, AB, North Saskatchewan Watershed Alliance.
- Zaremehrjady, M., Victor, J., Park, S., Smerdon, B., Alessi, D. S., & Faramarzi, M. (2022). Assessment of snowmelt and groundwater-surface water dynamics in mountains, foothills, and plains regions in northern latitudes. *Journal of Hydrology*, 606, 127449. <https://doi.org/10.1016/j.jhydrol.2022.127449>
- Zektser I. S., & Everett, L. G. (2006). *Ground Water Resources of the world and their use*. National Ground Water Association Press.

## Chapter 2: Steady State Model

### 2.1 Introduction

Groundwater (GW) is often the hidden/forgotten resource. It is equally important as a drinking water source as it is to maintain natural ecosystem functions (Freeze & Cherry, 1979). To describe groundwater completely, in context of its place, conceptual models bring together geological frameworks and hydraulics (Tóth, 1970). In turn, conceptual models are the basis for quantitative models that utilize the principles of fluid flow to address groundwater flow problems (Anderson et al., 2015). Models are useful to determine GW recharge/discharge areas, GW interaction with surface water (SW), the directions of GW movement, GW availability, and key hydrostratigraphy. Models are important tools to understand hydrogeology within a specific area/region due to their incorporation of GW flow principles and ability to represent problems across a range of spatial scales.

The first step in a hydrogeological characterization for the purposes of modelling is to choose the size and shape of the study area. In the Edmonton region of Alberta, Canada, research over the past five decades has been done using spatial boundaries ranging from legal boundaries to watershed boundaries (Barker et al., 2011; Bibby, 1974a; Bibby 1974c; Ceroici, 1979a; Hydrogeological Consultants Ltd, 1998a, 1998b, 1998c, 1999, 2001; Ozoray, 1972; Stein 1976a; Stein 1982; WorleyParsons, 2009). Municipal or legal boundaries are a poor choice for hydrogeological studies as natural systems and their flow boundaries do not conform to legal boundaries. Watershed boundaries may be a logical choice, but these too can suffer from a lack of conformity to a groundwater flow system (GFS) (Enviroatlas, n.d.; Seaber et al., 1987). Conformity to GFS boundaries can be achieved by choosing a model boundary that follows groundwater divides. A groundwater divide is a plane where groundwater does not cross, forming a no-flow boundary (Hubbert, 1940). Regional topographic or water table highs and lows provide the ideal groundwater divides as they encompass smaller intermediate to local flow systems, ensuring that no natural flow system is truncated by chosen model boundaries (Tóth, 1963). A GFS based approach provides conformity to groundwater flow principles and because of this, includes vital hydrogeological components unique for the study area.

The Edmonton area has several important hydrogeologic features to be included. Regionally extensive aquifers are of primary interest due to their ability to transmit water across relatively

large areas. Some of the most regionally extensive aquifers in the Edmonton area are buried valleys (Cummings et al., 2012). These are channels formed from late Tertiary rivers in response to episodic tectonic uplift of the Rocky Mountains to the west (Cummings et al., 2012). This formed large channels filled with sand and quartzite gravels that have eroded or down-cut into the bedrock deposits (Cummings et al., 2012). Subsequent glaciation led to glacial deposits blanketing the preglacial channels or burying the ancient river valleys/channels (Cummings et al., 2012). Buried valleys form anastomosing networks spanning 100's of km, while also being kms wide and, 10's of meters deep (Andriashek, 2019; Cummings et al., 2012; Rubin, 2022). The predominant composition of sand and gravel causes them to be some of the highest hydraulic conductivity (K) deposits in the area (Cummings et al., 2012). Because of the high K values and extent of buried valleys, they are crucial to understand as they are likely to have a significant influence on groundwater flow in Edmonton and the surrounding area.

To represent the groundwater flow system in the Edmonton area, I developed a three-dimensional finite difference steady state model using MODFLOW-2005 (Harbaugh et al., 2017). A 15,967 km<sup>2</sup> area is represented by the model, which includes surficial geological deposits, recently mapped buried valley extents from Rubin (2022), and dipping bedrock geology (Figure 2.0) to a depth of 500 m. Simulation of the steady state groundwater flow system provided insight into lateral and vertical regional scale hydraulic head distributions, groundwater flow patterns, recharge/discharge areas, and generalized interaction with the North Saskatchewan River (NSR) that flows through the study area. Additionally, through the model creation process, a greater understanding of the hydrogeologic system was achieved. This includes the identification of significant hydrostratigraphic units that control GW flow and GW yield, hydraulic properties, recharge distributions, and potential lake-groundwater interactions. By understanding the steady state groundwater flow system, valuable information about the circulation of groundwater in the Edmonton area and relation to the buried valleys can be achieved.

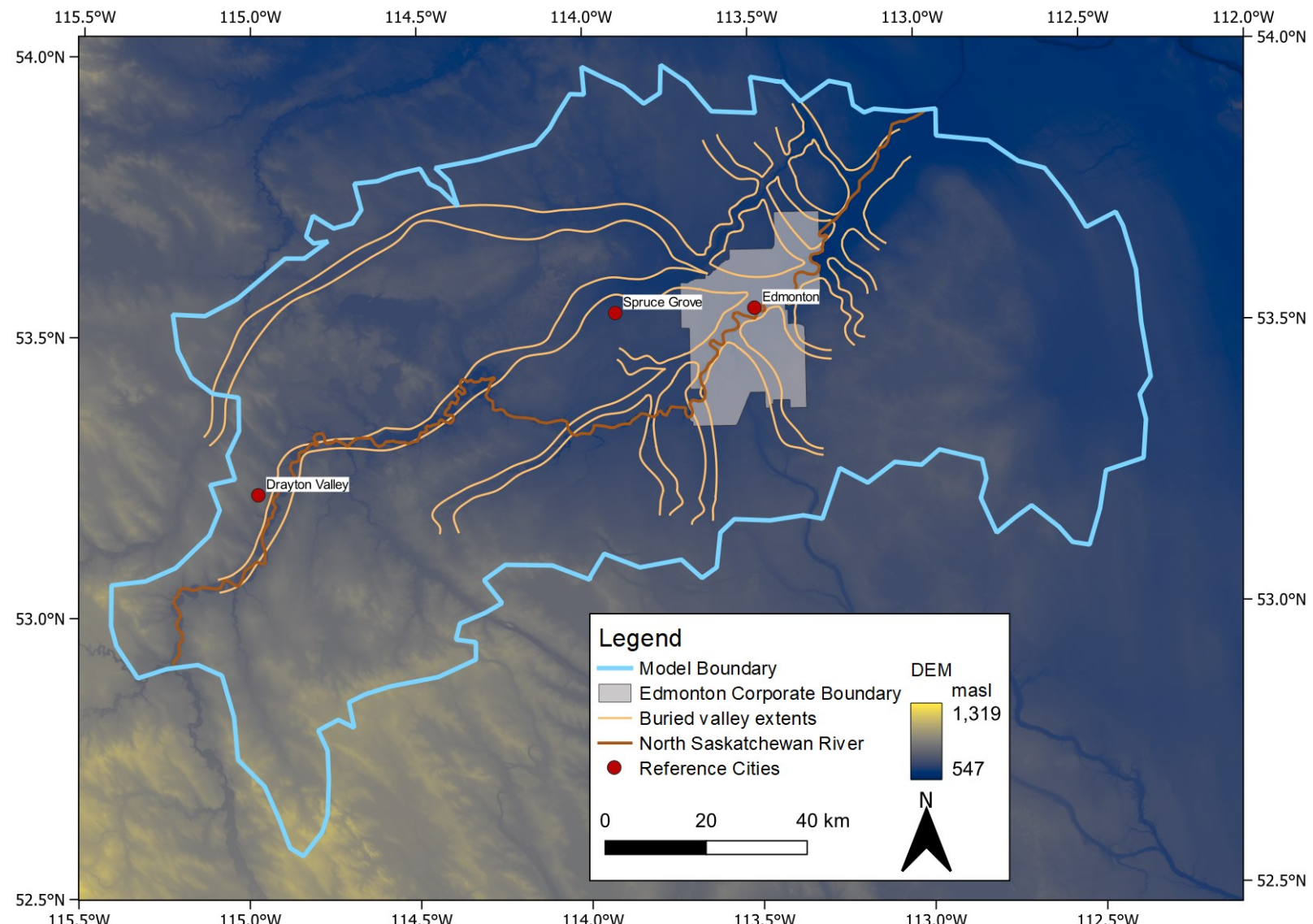


**Figure 2.0.** Digital elevation model (DEM) (Alberta Environment and Parks, 2017) of the study area with buried valley extents from Rubin (2022).

## **2.2 Hydrogeologic Setting**

The hydrogeologic setting of Edmonton consists of three main components in this study, i) Climate, ii) Geology, and iii) Hydrogeology.

### **2.2.1 Climate**

The climate in the Edmonton area is humid continental, which implies large variations in temperatures between days, seasons, and years (Kathol & McPherson, 1975). Moderate precipitation occurs throughout the year with cold winters and short, warm summers (Kathol & McPherson, 1975). Average monthly temperatures remain below 0°C from November through March only rising above 0°C consistently in April and reaching peak temperature in July (Environment and Climate Change Canada, 2022). The monthly average temperatures from the period 1982–2010 at the Edmonton Stony Plain weather station show an average temperature of 17°C in the warmest month, July, to -9.9°C in the coldest month, January (Environment and Climate Change Canada, 2022). Average yearly precipitation from 1982–2010 is 487.2 mm/year, with the majority (75%) occurring as rainfall from April to October at 371.2 mm/year. The remainder 116.0 mm/year of precipitation results from melting of 132.0 cm/year of snowfall (Environment and Climate Change Canada, 2022).

### **2.2.2 Geology**

Geology can be divided into bedrock formations of the Western Canada Sedimentary Basin (WCSB) that dip towards the southwest (Figure 2.1) and the overlying surficial deposits (Figure 2.2).

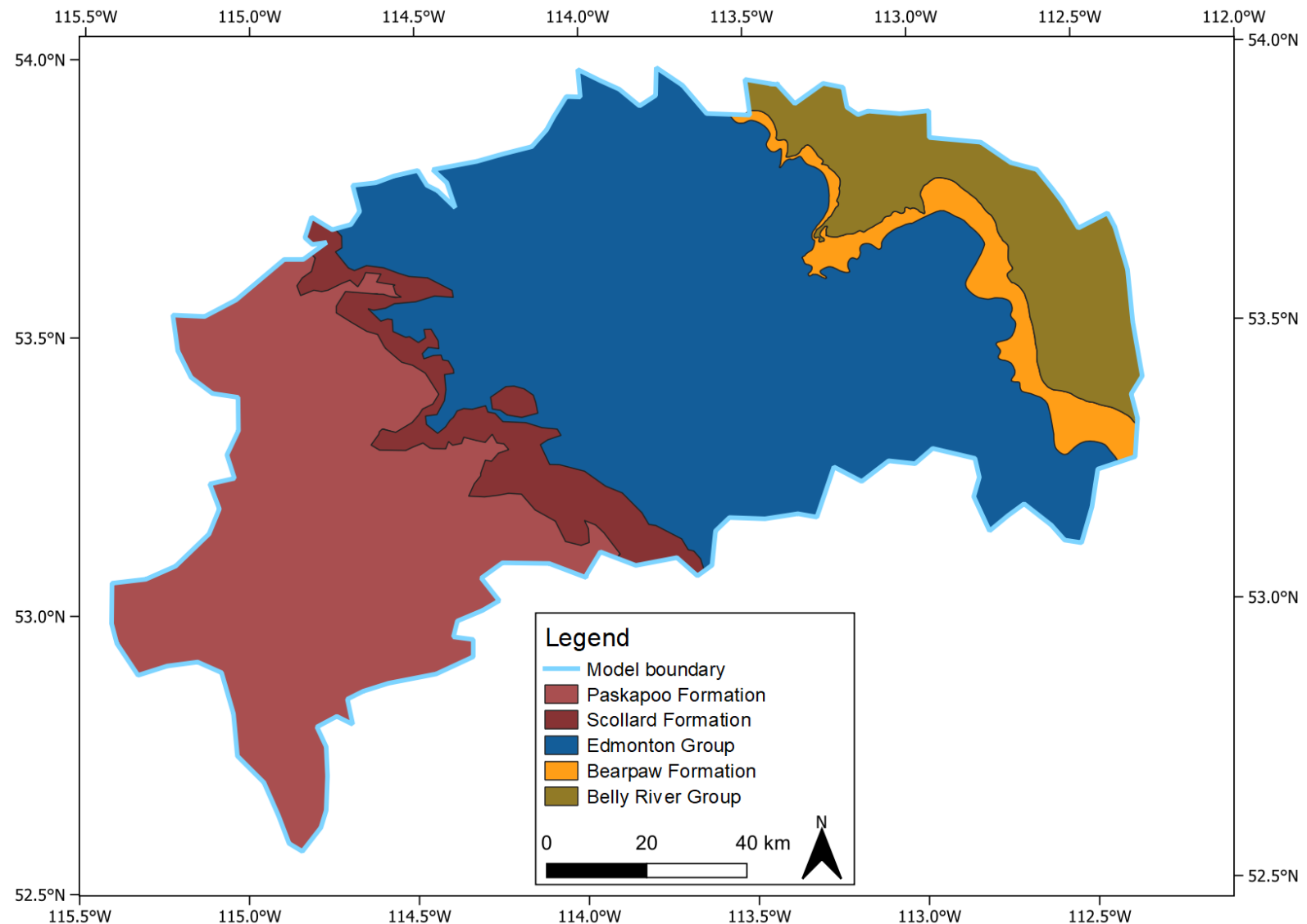


**Figure 2.1.** Bedrock geology in study area modified from Prior et al. (2013). Note, The Scollard Formation is mapped separately from the Edmonton Group due to its ability to be mapped at this scale.

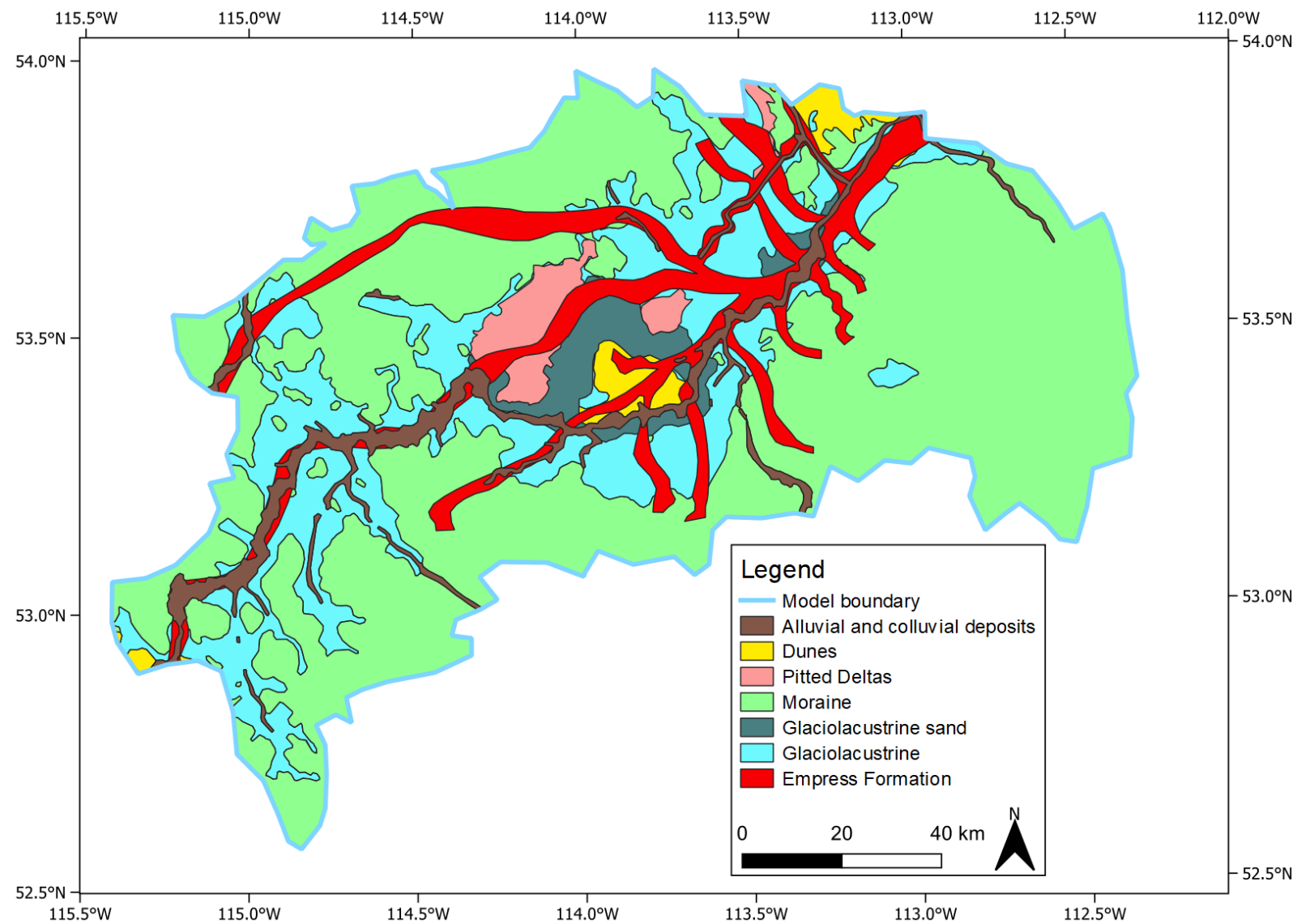


**Figure 2.2.** Surficial Geology modified from Andriashuk et al., (1979), Bayrock (1972), and Fenton et al. (2013) in the study area.

Buried valley extents (Empress Formation) from Rubin (2022).

## **Bedrock Geology**

The Belly River Group is the lowermost bedrock unit in the study area (Table 2.0). It is a late Cretaceous clastic wedge that thins eastward and in southern to central Alberta can be divided into 3 Formations: the Dinosaur Park Formation, the Oldman Formation, and the Foremost Formation (Brown et al., 2013; Glombick, 2010). Lithologies vary from thick bedded sandstone to siltstone and mudstone with lesser extents of coal and ironstone (Andriashuk, 1988; Glombick, 2010; Kathol & McPherson, 1975). In the study area, the formation is generally described as similar in sedimentological character to the Edmonton group albeit slightly sandier (Andriashuk, 1988; Glombick, 2010; Kathol & McPherson, 1975).

Overlying the Belly River Group is the Bearpaw Formation (Table 2.0). While part of the Edmonton Group, the Bearpaw Formation is large enough to be mapped separately at this scale (Figure 2.1). The dominant lithology of the Bearpaw Formation in the Edmonton region is shale to silty shale with less frequent glauconitic sandstones, thin ironstone, and bentonitic beds (Andriashuk, 1988). The formation is characteristically thin ranging from less than a metre to 63 m with the average thickness roughly 45 m (Kathol & McPherson, 1975).

The Edmonton Group (Table 2.0) is composed of the Bearpaw Formation, Horseshoe Canyon Formation, Battle Formation, and the Scollard Formation. The Bearpaw Formation is described previously as a separate unit due to its ability to be mapped separately. The Horseshoe Canyon Formation is a late Cretaceous primarily non-marine deposit, overlying the Bearpaw Formation with thicknesses ranging from approximately 140 m to 190 m (Andriashuk, 1988; Kathol & McPherson, 1975). The composition varies from clayey sandstone to bentonitic mudstone and carbonaceous shale with concretionary ironstone beds and coal scattered throughout (Andriashuk, 1988; Godfrey, 2001; Kathol & McPherson, 1975). Beds within the Horseshoe Canyon Formation can be highly variable and frequently pinch out over relatively short distances, creating difficulties delineating vertical and horizontal continuity (Kathol & McPherson, 1975). The Battle Formation consists of dark grey black bentonitic shale and can range from 0-9 m in thickness (Irish & Havard, 1968). Since the Scollard Formation is large enough to be mapped separately (Figure 2.1) at this scale, it is described in the following paragraph as a separate unit.

The Scollard Formation (Table 2.0) is a non-marine late Maastrichtian to early Paleocene clastic unit of fluvial origin; it consists of siltstone and sandstone with olive green mudstone and coal interbeds (Mossop et al., 1994; Khidir & Catuneanu, 2010). The Scollard Formation disconformably overlies the Battle Formation (Mossop et al., 1994; Khidir & Catuneanu, 2010), which in the study area is included with the Edmonton Group (Prior et al., 2013). Only two members can be distinguished in the Scollard Formation, an upper member with abundant coal and a lower member that is largely devoid of coal deposits (Mossop et al., 1994).

The Paskapoo Formation (Table 2.0) is a Paleogene to early Eocene fluvial deposit that unconformably overlies the Scollard Formation in Alberta (Grasby et al., 2008). The fluvial nature of this sediment makes it highly heterogenous (Burns et al., 2010); the formation consists of lithologies ranging from mudstone and siltstone to sandstone, with sandstone making up channels interspersed between the mudstone/siltstone (Burns et al., 2010; Grasby et al., 2008). The Paskapoo Formation is divided into three members (Demchuk & Hills, 1991): the lowermost being the Haynes member, which is overlayed by the Lacombe member, and the Dalehurst member on top. The Haynes member consists of massive, stacked, medium to coarse grained channel sandstones (Burns et al., 2010; Grasby et al., 2008). The Lacombe member is made up of siltstone, mudstone, and some coal comprising floodplain deposits that fill the spaces between anastomosing lenticular channel sandstones (Burns et al., 2010; Grasby et al., 2008). The Dalehurst member being the uppermost, is distinguished from the Haynes member by several thick coal deposits throughout (Burns et al., 2010; Grasby et al., 2008). However, this member is normally only found in Northwestern Alberta and the foothills, outside the study area (Burns et al., 2010; Grasby et al., 2008).

## **Surficial Deposits**

Incised into the bedrock is the early Pleistocene Empress Formation (Figure 2.2; Table 2.0), it originates from pre-glacial anastomosing fluvial channels (buried valleys) infilled with quartzite sand and gravel sediments then subsequently covered with glacial deposits (Bayrock & Hughes, 1962; Kathol & McPherson, 1975). Buried valleys can be up to 75 m thick, hundreds of kilometres long, and kilometres wide (Cummings et al., 2012). The main buried valleys in the study area are the Beverly, Onoway and Drayton valleys along with a series of smaller tributaries that intersect these valleys such as the Stony and Warburg valleys (Andriashuk, 2019). While Andriashuk (2019)

delineated valley thalwegs, Rubin (2022) took this a step further and delineated not just updated thalwegs but also mapped the buried valley extents. Additionally, Rubin (2022) helped to illuminate various sediment sources within the buried valleys, showing distinct differences in the hinterland of sediments between buried valleys.

Glacial moraine sediment is also present throughout the study area (Table 2.0), characterized as a highly variable mixture of sand, silt, and clay (Andriashuk, 1988; Feltham, 1993). Moraine is the dominant surficial deposit in the study area, except for the central area where glaciolacustrine sediments follow SW–NE trend of the NSR valley (Figure 2.2). Several distinct kinds of till are seen in the study area; these include moraine, fluted moraine, stagnant ice moraine, and ice-thrust moraine (Fenton et al., 2013). This reflects the highly variable nature of moraine sediments that not only have a variety of categories of moraine in the study area but are also highly heterogenous within a specific unit (Feltham, 1993; Fenton et al., 2013).

Pitted deltas (Table 2.0) are formed at locations where supraglacial rivers flowed off glacial ice and into Glacial Lake Edmonton (Bayrock & Hughes, 1962). These deposits are predominantly sand and gravel with clay to silt interbeds (Andriashuk, 1988; Bayrock & Hughes 1962). They commonly form distinctive pit and kettle type topography produced by melting of sediment surrounded/covered ice blocks left as the ice sheet retreated (Bayrock & Hughes 1962). Most of the pitted delta deposits are located near the centre of the study area (Figure 2.2).

Much of the Edmonton Area is draped with a thick layer of glaciolacustrine sediments (Figure 2.2; Table 2.0), the remnants of glacial lake Edmonton (Bayrock & Hughes, 1962). These sediments are a mix of stratified clay, silt, and sand; a highly variable mixture that despite stratification is discontinuous, making correlations difficult (Andriashuk, 1988; Bayrock & Hughes, 1962). The thickness is also variable but generally the sediments in the centre of the deposit around Edmonton are thicker as it gradually tapers towards its margins in the NW and SE (Bayrock & Hughes, 1962).

Sand dunes are present in the study area, also largely centrally located (Figure 2.2; Table 2.0). The sand is usually fine to medium grained and originates from glacial outwash (Kathol & McPherson, 1975). Formed after the Laurentide ice sheet retreated, the parabolic or longitudinal shape of the sand dunes indicates a dominate wind direction to the northeast during Formation (Bayrock & Hughes, 1962; Kathol & McPherson, 1975). At present day, these dunes are covered and stabilized with vegetation.

Recent alluvial to colluvial deposits line the modern-day NSR valley and associated tributaries (Figure 2.2; Table 2.0). Lithologically, alluvial deposits are mostly sand and gravel but change in character towards the flood plain of the river where the sand/gravel is draped with silt and clay (Bayrock & Hughes, 1962). Colluvial deposits are made of slumped glacial and bedrock material along river valley edges and as a result they contain a chaotic mixture to clay to sand material (Kathol & McPherson, 1975). Alluvial deposits commonly are found in sediment bar morphologies within the river and terraces towards the periphery of the river valleys (Bayrock & Hughes, 1962). Gravel tends to dominate in alluvial deposits associated with the NSR whereas silt, clay, and sand dominate the tributaries and smaller rivers depending on location (Bayrock & Hughes, 1962).

Era	Period	Epoch	Formation/Deposit
Cenozoic	Quaternary	Holocene	Alluvial/Colluvial
			Sand Dunes
		Pleistocene	Glaciolacustrine
			Pitted Delta
			Moraine
			Empress Formation
	Paleogene	Paleocene	Paskapoo Formation
			Scollard Formation
Mesozoic	Cretaceous		Edmonton Group
			Bearpaw Formation
			Belly River Group

**Table 2.0.** Stratigraphic column for model area (Bayrock & Hughes, 1962; Fenton et al., 2013; Kathol & Mcpherson, 1975; Prior et al., 2013).

## **2.2.3 Hydrogeology**

### **Groundwater Flow Distribution**

Groundwater flow within bedrock deposits in the study area is primarily controlled by topography with geological variations only effecting local scale hydrogeology (Bibby, 1974a; Ceroici, 1979a; Stein, 1976a; Stein, 1982, WorleyParsons, 2009). In each bedrock Formation/Group, groundwater preferentially follows high K flow pathways such as sandstone and fractured coal seams, except for the Bearpaw Formation which serves as a regional aquitard (Bibby, 1974a; Ceroici, 1979a; Hydrogeological Consultants Ltd, 1998a; Stein, 1976a; Stein, 1982). While these high K flow pathways exist throughout the Paskapoo, Scollard, Edmonton Group, and Belly River Group they do not cause a noticeable impact on topography driven flow patterns in the bedrock due to their small scale (Research Council of Alberta, 1978). The dominant flow direction in the bedrock is unchanged and flows according to topography towards the NSR as this occupies a regional low in the landscape (Bibby, 1974a; Ceroici, 1979a; Stein, 1976a; Stein, 1982; WorleyParsons, 2009). However, local to intermediate scale topographic variations also produce associated local to intermediate scale flow systems, often discharging in lakes or streams occupying topographic lows across the study area (Bibby, 1974a; Ceroici, 1979a; Stein, 1976a; Stein, 1982, WorleyParsons, 2009). This generates nested flow systems in the bedrock that are primarily controlled by topography on the scale of this study.

General hydraulic head patterns in surficial deposits follow topographic variations but are modified by geology (Bibby, 1974a; Ceroici, 1979a; Stein, 1976a; Stein, 1982). Regional groundwater flow is directed towards to NSR, with local-intermediate flow systems superimposed on regional flow patterns (Bibby, 1974a; Ceroici, 1979a; Stein, 1976a; Stein, 1982, WorleyParsons, 2009). Buried valleys have a noticeable impact on surficial flow patterns, as they are composed of the highest K sand and gravel sediments in the study area (Bibby, 1974a; Ceroici, 1979a; Cummings et al., 2012; Stein, 1976a; Stein, 1982). Because of their high K and regionally extensive distribution, buried valleys induce groundwater flow from the surrounding surficial and bedrock geology (Bibby, 1974a; Ceroici, 1979a; Research Council of Alberta, 1978; Stein, 1976a; Stein, 1982).

### **Bedrock Hydraulic Properties**

The Belly River Group yields approximately  $\sim$ 10 m<sup>3</sup>/day to  $\sim$ 150 m<sup>3</sup>/day depending on the location and aquifer targeted (Hydrogeological Consultants Ltd., 1998a; Hydrogeological Consultants Ltd., 2001; Stein, 1982). TDS values vary widely depending on location and depth/distance down dip (i.e., increasing downdip) ranging from <500 mg/L to over 2000 mg/L (Hydrogeological Consultants Ltd., 1998a; Hydrogeological Consultants Ltd., 2001). According to Stein (1976a) average hydraulic conductivity values vary from  $\sim$ 5.79E-7 m/s to  $\sim$ 5.79E-8 m/s with isolated individual sandstones being as high as  $\sim$ 8.45E-5 m/s.

More permeable portions of the Bearpaw Formation are called the Bearpaw aquifer and yield <10 m<sup>3</sup>/day to up to 100 m<sup>3</sup>/day; though many wells have insufficient water or are dry due to the low permeability of the formation (Hydrogeological Consultants Ltd., 1998a; Hydrogeological Consultants Ltd., 2001; Stein, 1982). TDS in the Bearpaw ranges from 500 mg/L to over 2000 mg/L, increasing downdip (Hydrogeological Consultants Ltd., 1998a; Hydrogeological Consultants Ltd., 2001). Data regarding the bulk hydraulic conductivity are sparse for the Bearpaw Formation given its thickness and lithology. However, the Colorado Group of which the Bearpaw is a part has K values varying from 1E-11 m/s to 1E-14 m/s (Pétré et al., 2015).

The Horseshoe Canyon Formation typically yields 10–100 m<sup>3</sup>/day and has a TDS <1500 mg/L (Hydrogeological Consultants Ltd., 1998c; Hydrogeological Consultants Ltd., 1999). Hydraulic conductivity measurements taken from core vary from 4.4E-10 m/s to 3.6E-6 m/s with an average value of 3.8E-7 m/s (Smerdon et al., 2017). Fractured coal seams in the Horseshoe canyon Formation may act as potential aquifers as found by Stein (1982), whereby the K of these coal seams can increase up to 5.1E-4 m/s.

The upper Scollard Formation yields 10–100 m<sup>3</sup>/day while the lower Scollard yields 1–10 m<sup>3</sup>/day (Hydrogeological Consultants Ltd., 1998b; Hydrogeological Consultants Ltd., 1998c). TDS in the upper/lower Scollard is typically <1500 mg/L (Hydrogeological Consultants Ltd., 1998b; Hydrogeological Consultants Ltd., 1998c). Hydraulic conductivity values originating from core samples have an average K value of  $\sim$ 3.5E-7 m/s with a low of 9.3E-10 m/s and a high of 3.5E-6 m/s (Smerdon et al., 2017).

The Paskapoo Formation consists of generally low K values with high K variations sometimes referred to collectively as the Paskapoo aquifer (Hydrogeological Consultants Ltd., 1998b; Hydrogeological Consultants Ltd., 1998c). The long-term yield of the water wells is between 10

and 100 m<sup>3</sup>/day with a total dissolved solids (TDS) concentration that varies between 500–1000 mg/L (Hydrogeological Consultants Ltd., 1998b; Hydrogeological Consultants Ltd., 1998c). Hydraulic conductivity estimates vary from 1.1E-10 m/s to 1.0E-3 m/s depending on measurement method and location (Hughes et al., 2017). The average hydraulic conductivity for sandstones is ~1.2E-4 m/s while the average hydraulic conductivity for siltstone/mudstone is ~4.4E-9 m/s.

## **Surficial Hydraulic Properties**

The Empress Formation can be informally divided into the upper sand and gravel aquifer and the lower sand and gravel aquifer in the study area based on water well records (Hydrogeological Consultants Ltd., 1998b; Hydrogeological Consultants Ltd., 1998c). The upper sand and gravel aquifer typically has yields of less than 100 m<sup>3</sup>/day while the lower sand and gravel aquifer has yields of 100–500 m<sup>3</sup>/day (Hydrogeological Consultants Ltd., 1998b; Hydrogeological Consultants Ltd., 1998c). In some cases, yields can be 2300 m<sup>3</sup>/day as is the case for the town of Stony Plain which has pumped at this rate for ~20 years prior to 1998 without any appreciable declines in water in the aquifer (Hydrogeological Consultants Ltd., 1998b; Hydrogeological Consultants Ltd., 1998c). Hydraulic conductivity values for the sand and gravel can be as high as 0.01 m/s for the gravel deposits to 1E-4 m/s for the sand deposits (Kathol & McPherson, 1975).

Glacial moraine, glaciolacustrine deposits and aeolian dune deposits yield ~8.6 m<sup>3</sup>/day to ~36 m<sup>3</sup>/day (Kathol & McPherson, 1975; Stein, 1982). Groundwater yields come from gravel/sand lenses that are interspersed within the till/glaciolacustrine deposits while yields are relatively homogenous throughout aeolian deposits (Kathol & McPherson, 1975; Stein, 1982). The variable nature of moraine and glaciolacustrine deposits not only makes it difficult to predict where sand and gravel lenses are but also to extrapolate short term pumping tests into the future (Stein, 1982). TDS can vary from <1000 mg/L to >4000mg/L depending upon location of surficial deposits in local and regional flow systems (Stein, 1982). Hydraulic conductivity is less than 1E-5 m/s for till and glaciolacustrine deposits, while it is significantly higher in Aeolian dune deposits at 1E-4 to 1E-3 m/s (Kathol & McPherson, 1975).

Pitted delta deposits offer a slightly higher yield than other surficial deposits at 7.2–36 m<sup>3</sup>/day (Kathol & McPherson, 1975). TDS can be between 200–1500 mg/L with the majority of the groundwater being of calcium-magnesium-bicarbonate or sodium-bicarbonate type (Hydrogeological Consultants Ltd., 1998c). Hydraulic conductivity for sand in pitted delta

deposits ranges from 0.01 m/s to 1E-4 m/s while silt is between 1E-5 and 1E-7 m/s (Kathol & McPherson, 1975).

Recent alluvial and river terrace sediments can contain large proportions of sand and gravel which make good aquifers when present (Kathol & McPherson, 1975; Stein, 1976a). TDS can be between 200–1500 mg/L, however significant amounts of geologically recent deposits have TDS below 200 mg/L (Hydrogeological Consultants Ltd., 1998c). Hydraulic conductivity varies from 0.01 m/s for gravel deposits to 1E-8 m/s for clay sediments (Kathol & McPherson, 1975).

## 2.3 Model Design

### 2.3.1 Steady State Representation

A steady state model was created to replicate observed water levels in the model area as relatively small changes in hydraulic head are observed over long periods.

Wells from the Groundwater Observation Well Network (GOWN) (Government of Alberta, n.d.b) were selected because of their accuracy, availability of long term water level data, and based on whether water levels were actively measured in 2020. The chosen GOWN piezometers in the study area illustrate that large changes in hydraulic head are uncommon in the study area (Figure 2.4). Most of the observation wells have seasonal variations of 1–2 m, with isolated short-lived variations around 6 m (Figure 2.4). Given that error in the DEM can vary from less than 5 m to up to 8 m (Land Information Services Division, 1988), seasonal variations of 1–2 m are deemed negligible, and modelling efforts were focused on matching the long term water level averages. With regards to larger short-lived, transient events (~6 m), the goal of the model was not to examine localized, isolated events, but rather represent regional groundwater flow for a relatively large area.

A second method to examine the validity of a steady state simulation is to examine the range of elevation values in the model area as a proxy for the range in potential water levels (Hubbert, 1940). Since the range in elevation spans ~558 m, a variation of 1–2 m is ~ 0.2–0.4 % of the total elevation range and 6 m is ~1.1% of the total range of hydraulic head measurements. Because the potential water level variation is a relatively small proportion of the total range of measurements, this supports the notion that replicating average water levels in a regional basin should be treated as a steady state problem (Tóth, 1963).

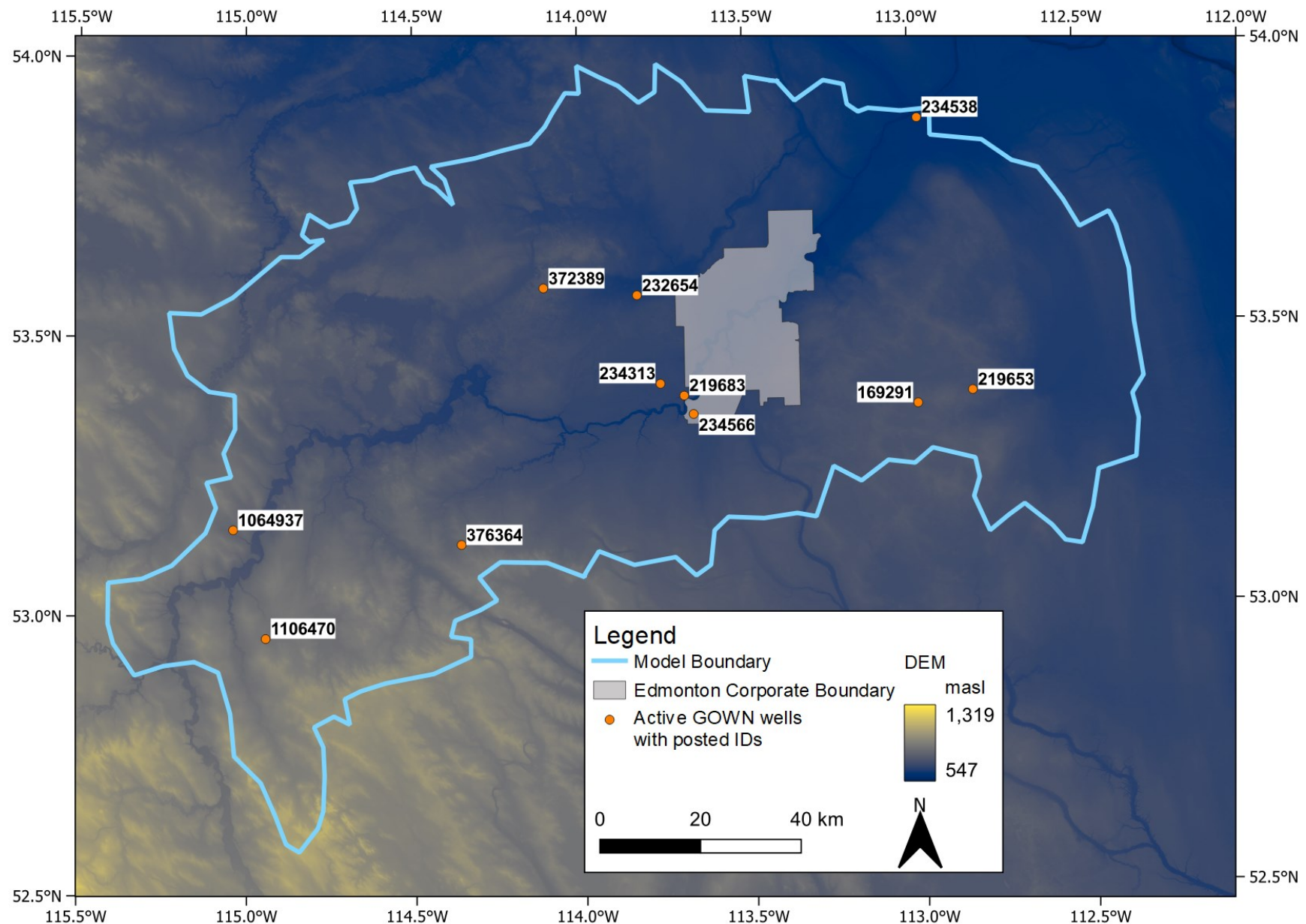
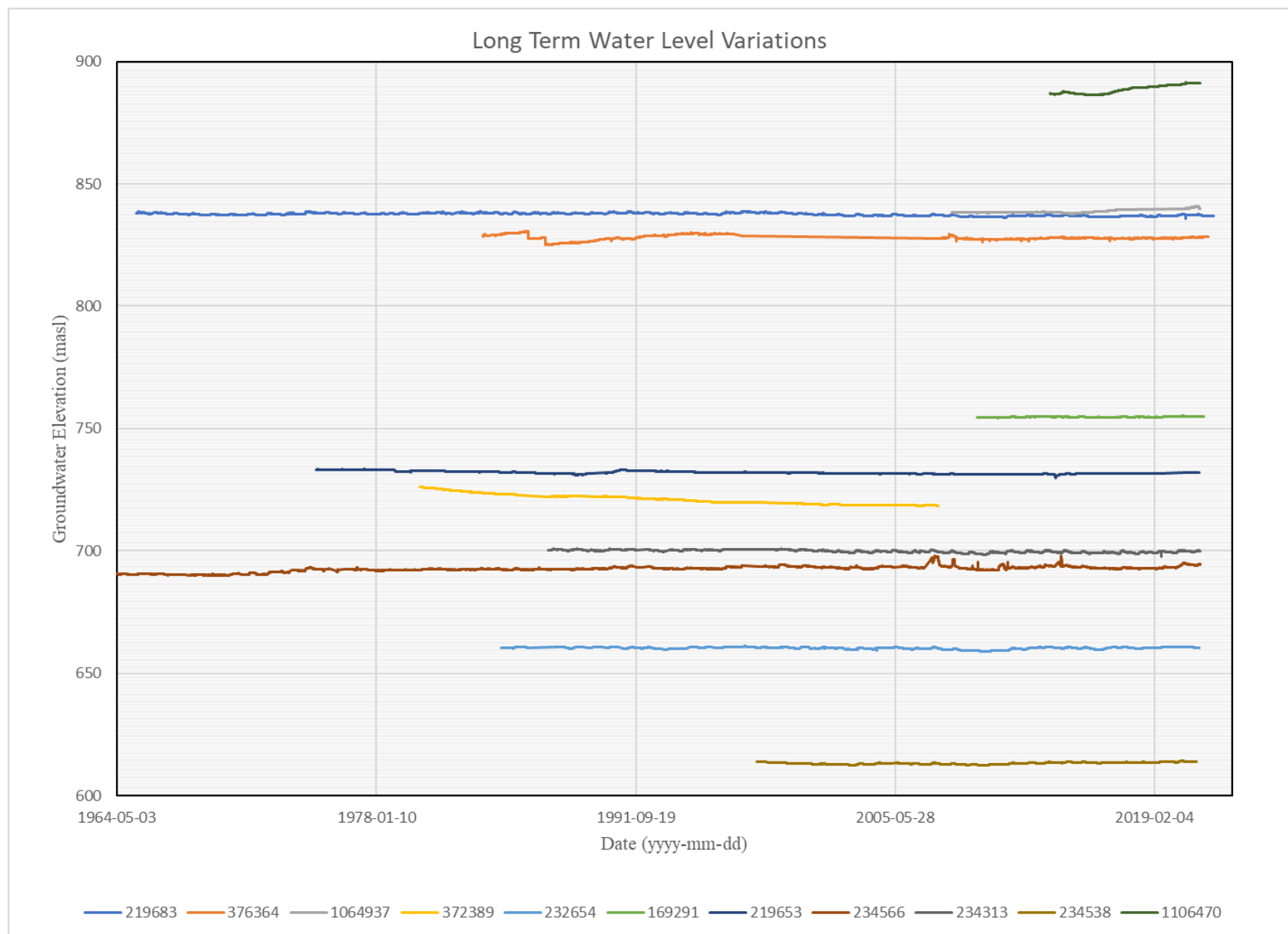


Figure 2.3. Location of active GOWN wells in model area with AWWID IDs listed. Buried valley extents from Rubin (2022).



**Figure 2.4.** Hydrographs of active GOWN wells in study area with AWWID IDs Posted.

### **2.3.2 Model Domain**

The model boundary was chosen to align with published watershed boundaries such as Hydrological Unit Code (HUC) watersheds (Figure 2.5). This allows for some level of standardization and comparison. However, it is important to note, HUC watersheds do not always align with groundwater flow principles so there are small areas where the model boundary may deviate from HUC boundaries (Enviroatlas, n.d.; Seaber et al., 1987).

To verify the model boundary, two static maps of hydraulic head were made using water wells compiled in the Alberta Water Well Information Database (AWWID) (Government of Alberta, n.d.a) for the surficial and bedrock units respectively. Data was culled to fit the study area, with lithology, and pumping test data required, as static water levels are reported as part of a pumping test. The respective surficial and bedrock wells were then interpolated by kriging, resulting in the maps shown in Figure 2.6 and Figure 2.7. The static water level maps show the model boundary broadly follows surficial and bedrock water level highs (Figure 2.6; Figure 2.7). This provides confirmation that the model boundary is valid, since groundwater flow boundaries also are present at regional water level highs (Tóth, 1962). Additional examination of historical mapping of local groundwater divides (as opposed to regional) shows a good fit where local and regional boundaries coincide (Figure 2.8). This provided a final form of verification for the model boundary.

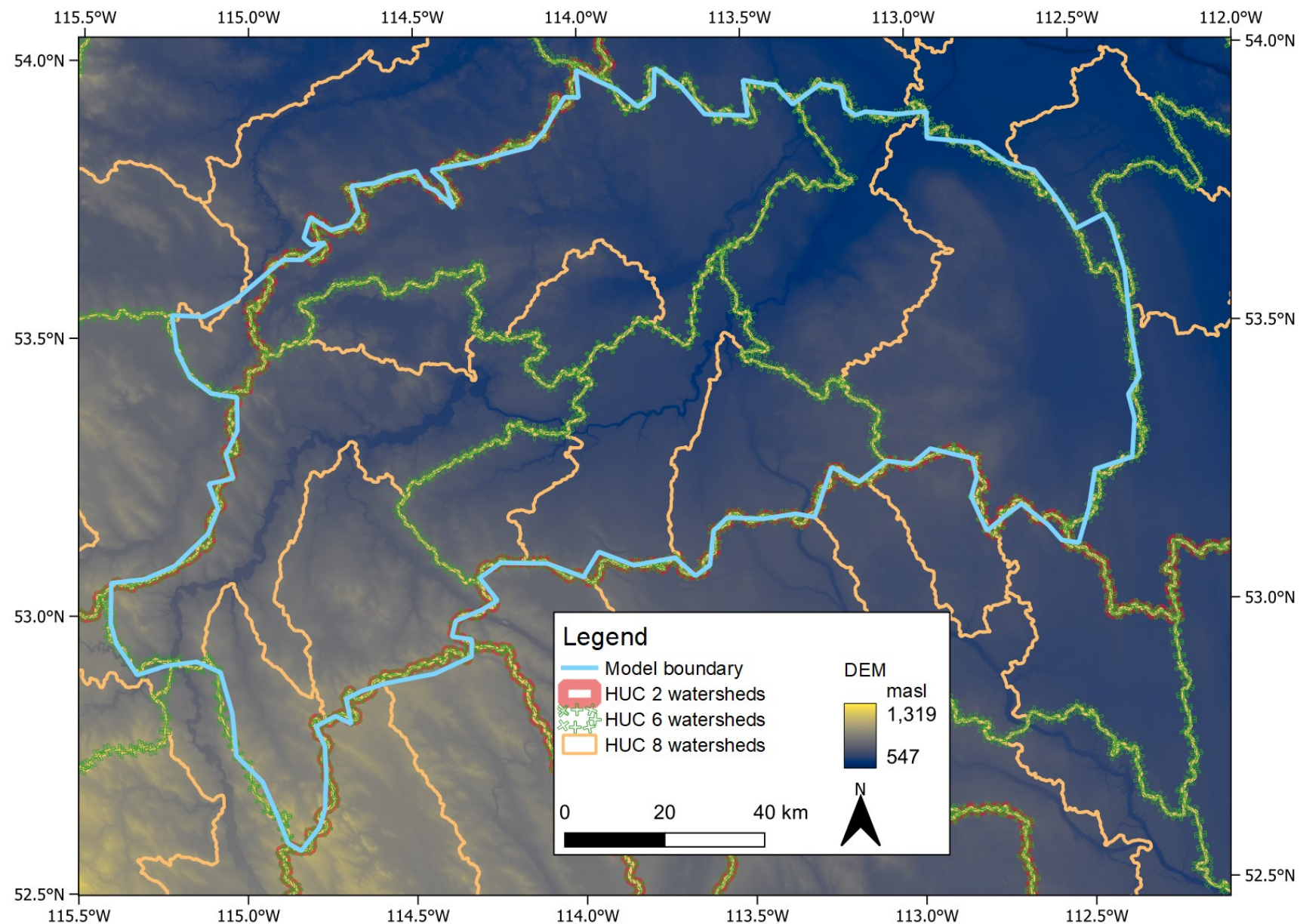


**Figure 2.5.** Model Boundary superimposed with HUC watersheds boundaries (Alberta Environment and Parks, 2014).

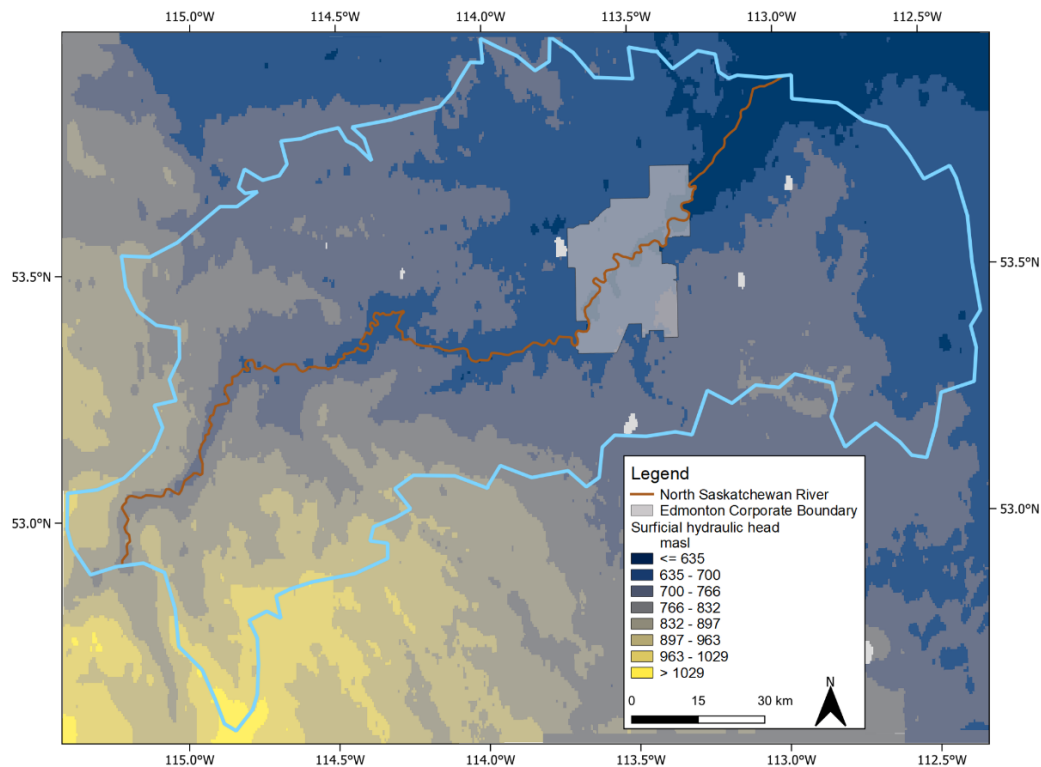


**Figure 2.6** Surficial Static water level map based off data from the AWWID database

(Government of Alberta, n.d.a).

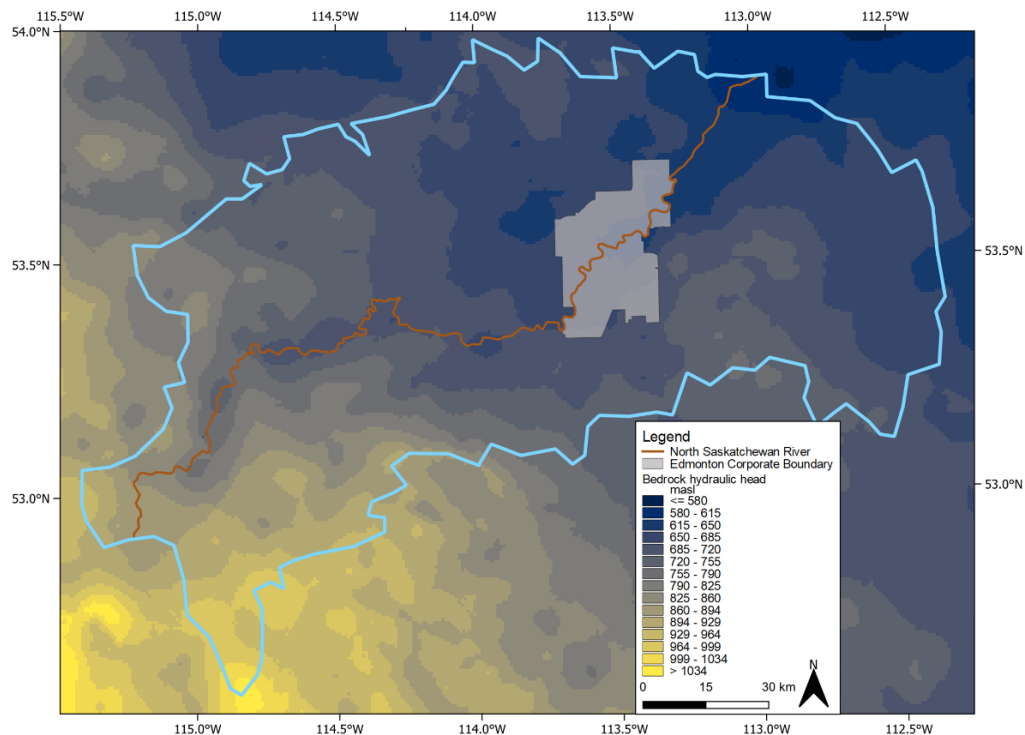


**Figure 2.7.** Bedrock static water level map based off data from the AWWID database

(Government of Alberta, n.d.a).

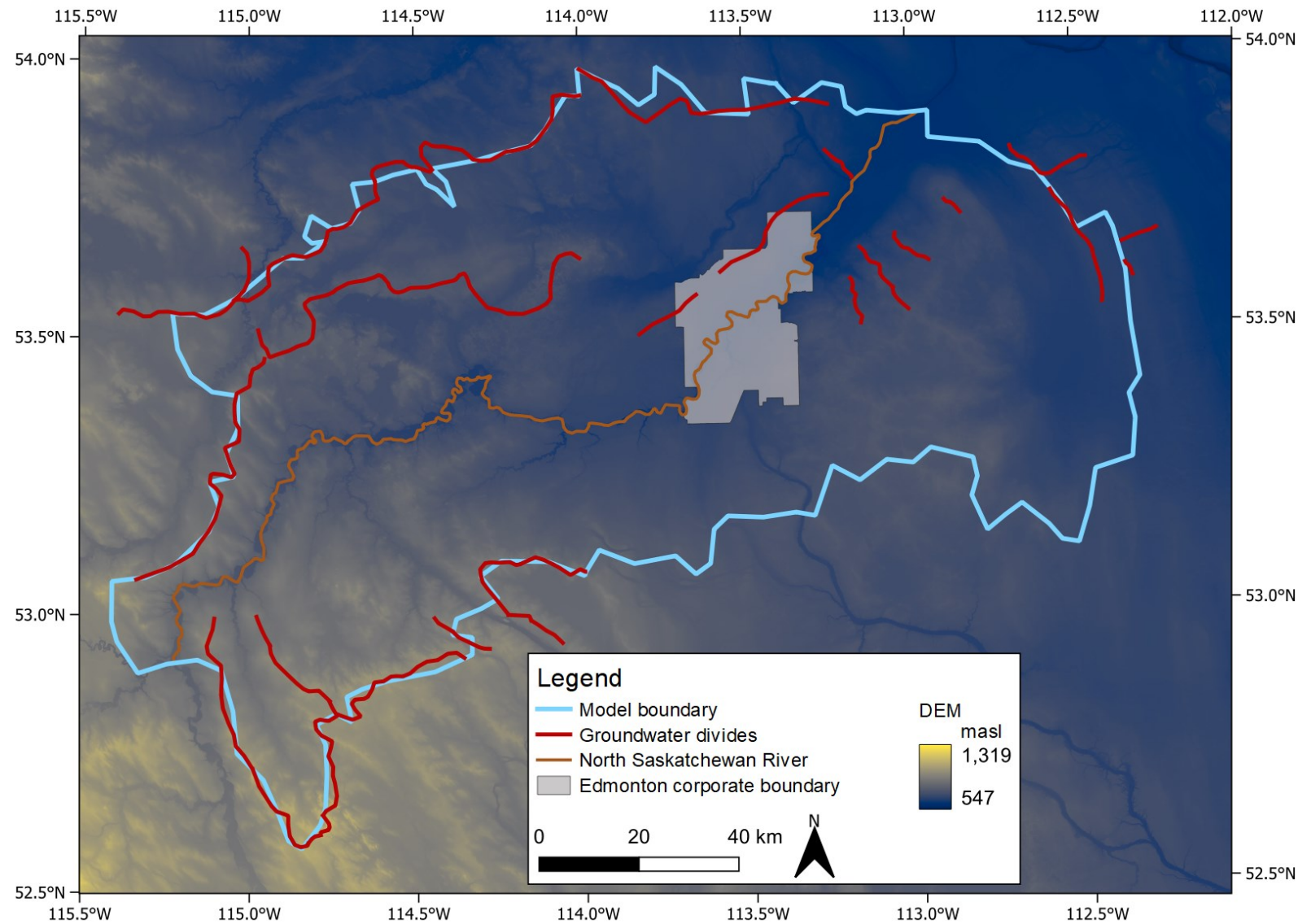


**Figure 2.8.** Model boundary with local groundwater divides modified from Bibby (1974b), Ceroici (1979b), Tokarsky (1971), Stein (1976b), and Stein & Carlson (1982) superimposed.

### **2.3.3 Grid Design**

Finite-difference model grid design involves discretizing the model domain into a series of 3-dimensional (3D) grid blocks. These grid blocks have  $\Delta x \times \Delta y$  dimensions in the horizontal plane, with the  $\Delta z$  dimension spanning the vertical plane. Horizontal discretization generally should follow the rule whereby no horizontal cell dimension shall vary by more than 1.5 times in size of its neighboring cell (Anderson et al., 2015). Keeping this in mind, horizontal grid spacing in the model was set uniformly at 100 m in the  $\Delta x$ - $y$  directions. This created 1660 rows by 2150 columns with 31,873,080 active cells when considering the 20 model layers spanning the  $z$  dimension. This was considered suitable in terms of scale and size as this is a regional groundwater model covering a 15,967 km<sup>2</sup> area intended to capture larger scale flow patterns.

Model discretization in the  $z$  dimension was defined by the number of model layers between explicitly defined surfaces. Ground surface topography, bedrock topography, and the constant elevation model bottom provided the explicitly define surfaces needed. Ground surface topography was defined by a 25 m provincial DEM from Alberta Environment and Parks (2017) with bedrock topography from the Alberta Geological Survey (AGS) (MacCormack et al., 2015). The model bottom was chosen at 500 metres above sea level (masl) to include the entirety of the dipping Paskapoo Formation and to avoid imposing no-flow conditions at too shallow of a depth.

Since MODFLOW can accommodate variations in vertical discretization, limitations in the vertical dimension are largely defined by resolutions required by model objectives (Harbaugh, 2005; Anderson et al., 2015). In the model, four layers were selected to represent the surficial deposits as this was needed to characterize areas with large vertical gradients, namely, the NSR valley. Sixteen layers were chosen to represent the bedrock to “down-step” each layer so that they remain in hydraulic connection while also creating the characteristic dipping of the WCSB (Figure 2.9). The thickness of surficial deposits can range from 0 to 120 metres as layers may pinch out. The mean thickness for layers 1 to 4 is 5.75 metres. For the bedrock, the mean thickness of the layers 5 to 13 is 12 m, layers 14 to 19 is 15.6 metres, and layer 20 is 31.2 metres.

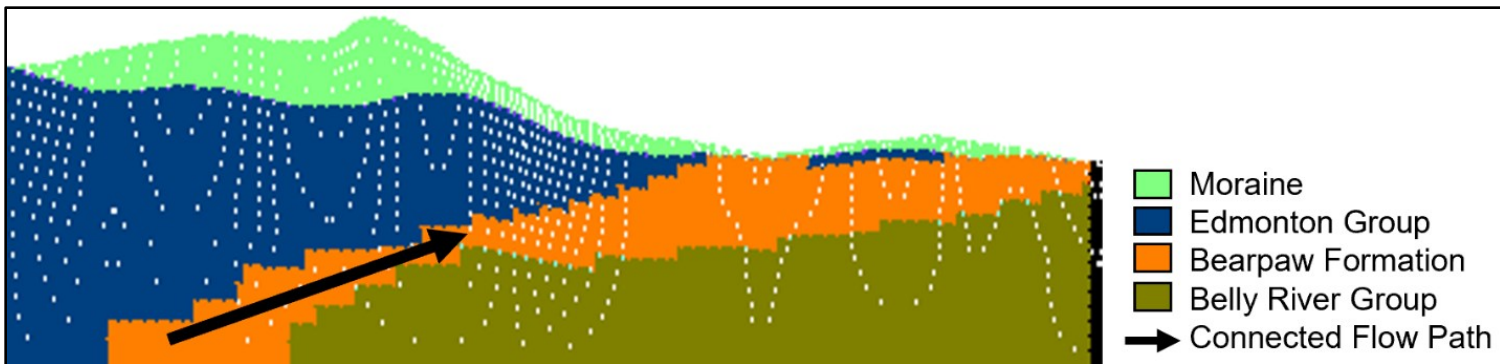


**Figure 2.9.** Example of discretizing dipping layers in finite difference grid.

### **2.3.4 Layer Types**

In MODFLOW-2005 there are layer types 0 to 3 (Harbaugh, 2005). Type 0 are for confined layers; these are for fully confined layers that have unchanging transmissivity. Type 1 is for unconfined layers; this layer type is restricted to the first layer of the model because transmissivities are recalculated at every iteration. Types 2 and 3 are confined/unconfined convertible layers, the difference being type 2 layers are limited convertible while type 3 are fully convertible. In this model, layer 1 is type 1, layers 2 to 6 are type 3 fully convertible, and layers 7 to 20 are type 0 confined.

### **2.3.5 Model Boundary Conditions**

#### **No-Flow, Constant head, and Lake boundaries**

As explained in section 2.3.3, the model is laterally bounded by no-flow boundaries that extend vertically downwards to the model bottom. The model is also bounded horizontally along the bottom by a no-flow boundary at 500 metres above sea level (masl). This was done to include the entirety of the dipping Paskapoo Formation, as it is often considered one of the most important groundwater resources in Alberta (Grasby et al., 2008). Additionally, 500 masl allows the model to equilibrate without imposing no-flow conditions at too shallow of a depth (Chunn et al., 2019). Several other boundary condition types were used to represent hydrologic features within the model area as described below.

Constant head boundaries were set at eight lakes in the model area, while for two additional lakes, a lake boundary was used (Table 2.1). Lake and constant head boundary water levels in the model were based off lake surface elevations. A lake boundary was chosen for Lac Ste Anne and Isle Lake because observed water levels were too high in the buried valleys when a constant head boundary was used for these lakes during initial modelling. The lake boundary contains a feature that enables the lakebed hydraulic conductivity to be set, allowing flow to be inhibited from the lakes if needed. Other lakes were represented with a constant head as it is assumed that lake levels remain constant through time. The lakes represented in the model were chosen based on their size, with lakes smaller than ~3 km in their largest dimension excluded. However, there are two exceptions with Big Lake and Astotin Lake. Big Lake was chosen to be represented because of its

known connection to groundwater (Von Hauff, 2004) and Astotin Lake was included due to its location in prominent wetlands in Elk Island National Park.

The NSR was the only river represented in model and was defined by the river boundary condition. The river was subdivided into four segments whereby each end of the polyline has a specified elevation and the elevation in between each end varied in a linear fashion.

A specified flux boundary is applied across the top of the model to simulate recharge (Figure 2.10). Recharge values were developed from observed initial modelling patterns and documented recharge distributions for the study area. Riddell et al. (2014), published a report including a map of minimum recharge in the study area that broadly shows a pattern of increasing recharge to higher elevations in the southwest. Klassen et al. (2018) found a similar trend of increasing recharge towards to southwest albeit with significantly lower recharge values. The range given by Klassen et al. (2018) has recharge varying between 6–10 mm/year and 31–35 mm/year in the study area. However, Riddell et al. (2014) estimates recharge at much higher values varying from around <100mm/year to almost 200 mm/year or more in the west and southwest of the study area. Figure 2.10 illustrates the recharge distribution that sufficiently reproduced observed water levels while also following general patterns observed in the previous studies.

Evapotranspiration (ET) was developed based on a map of average annual potential evapotranspiration (PET) in the study area (Riddell et al., 2014). ET is applied across the top of the model with an extinction depth of 1 metre so that ETs impact is constrained to areas where the water table is at a shallow depth (Figure 2.11). Since it is known that the recharge values chosen partially account for ET already, a lesser magnitude of ET than outlined in Riddell et al. (2014) was chosen.

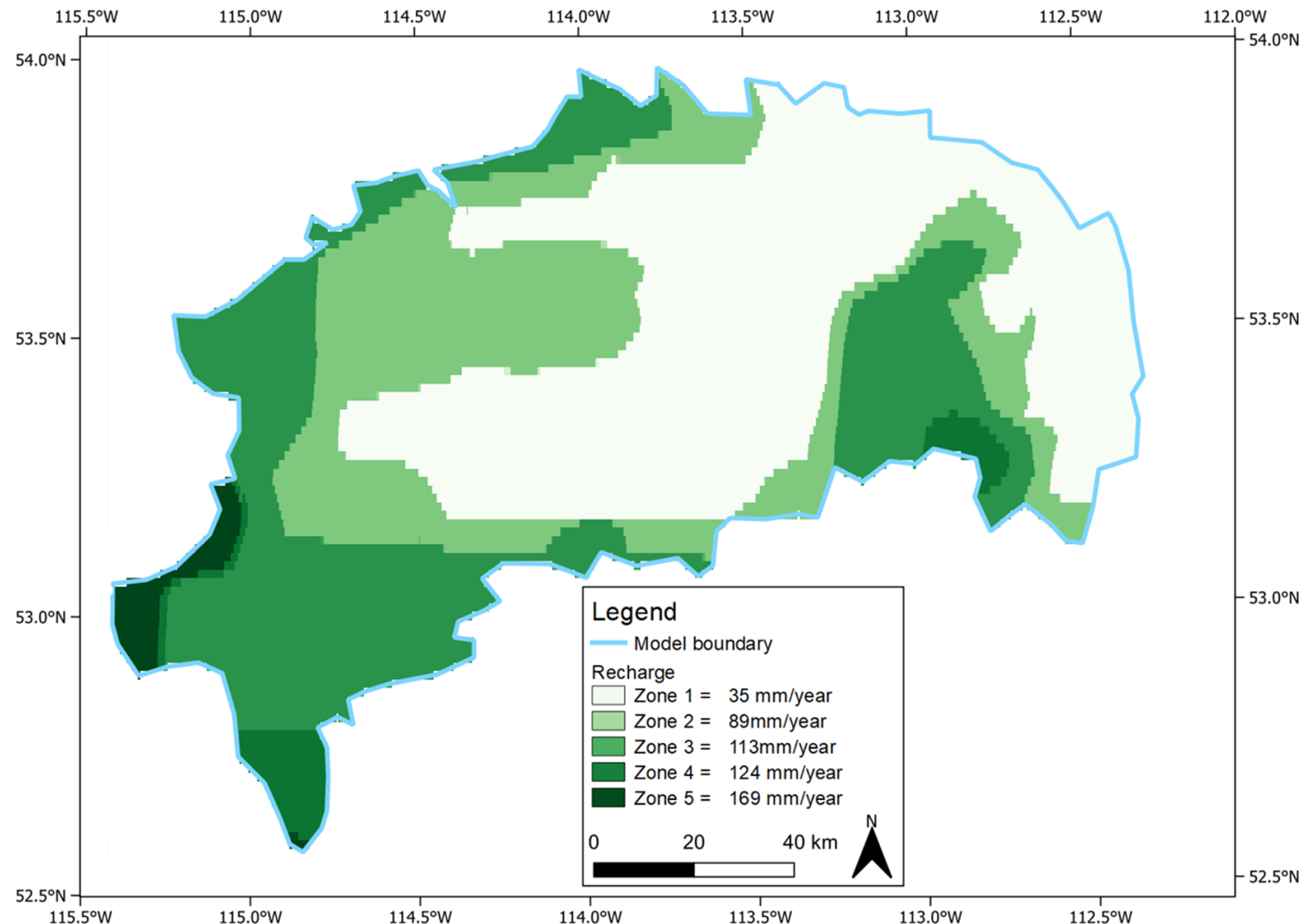


Figure 2.10. Recharge distribution in the model area.

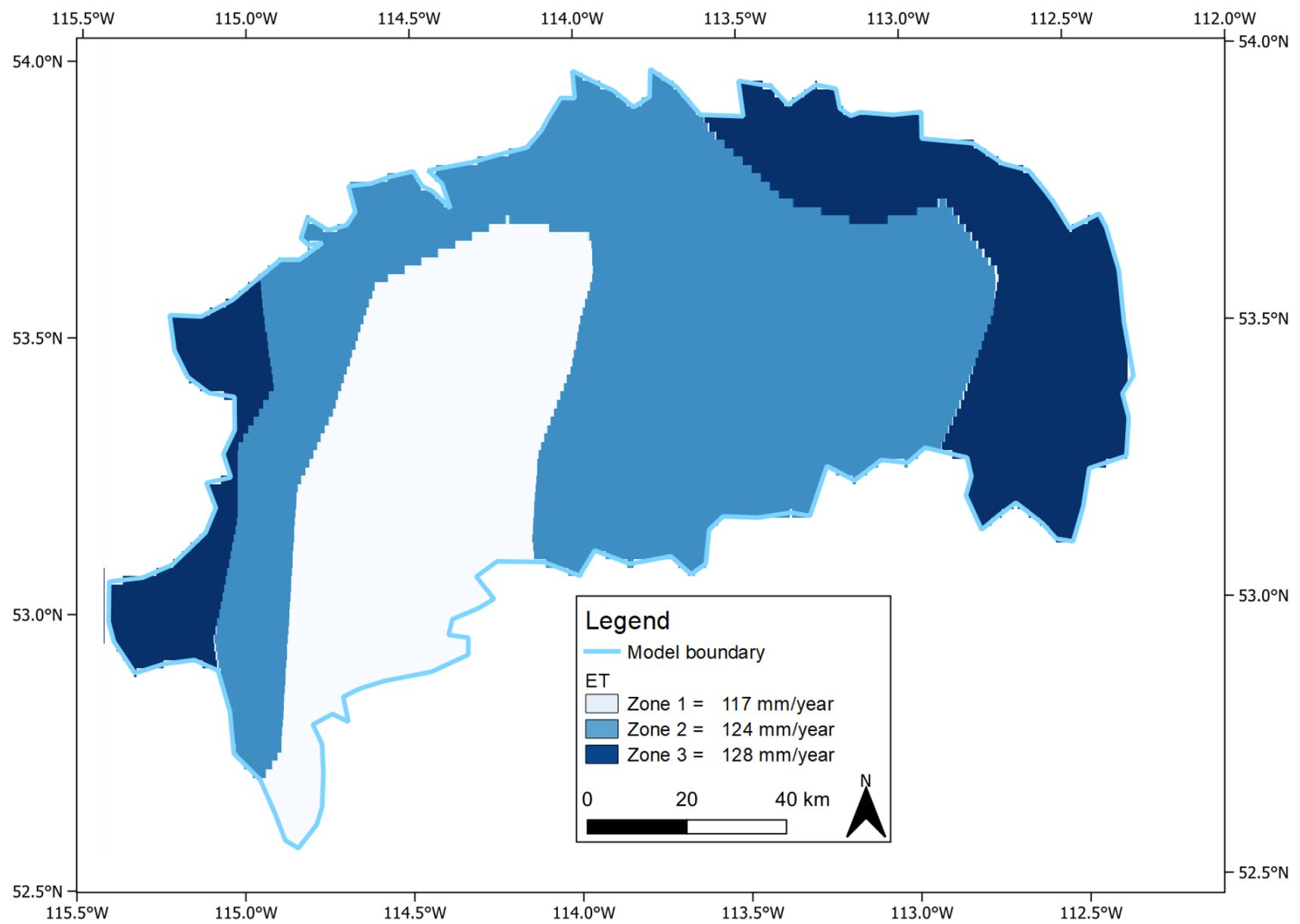


Figure 2.11. Evapotranspiration distribution in model area.

<b>Lake</b>	<b>Boundary Condition</b>	<b>Water Level (masl)</b>
Astotin Lake	Constant Head	709
Beaverhill Lake	Constant Head	669
Big Lake	Constant Head	652
Buck Lake	Constant Head	882
Cooking Lake	Constant Head	737
Hastings Lake	Constant Head	738
Isle Lake	Lake Boundary	725
Lac Ste Anne	Lake Boundary	720
Sandy Lake	Constant Head	697
Wabamun Lake	Constant Head	727

**Table 2.1.** Summary of boundary conditions to represent large lakes in the model area.

### **2.3.6. Parameterization**

Geologic units in the study area were combined into 11 hydrostratigraphic units based on their ability to be mapped, similarity, and scale of the model. Ability to be mapped was based on whether the geologic units were large enough to be mapped on regional surficial and bedrock geology maps (Andriashuk et al., 1979; Bayrock, 1972; Fenton et al., 2013; Prior et al., 2013). Similarity was decided based on how lithologically and hydrogeologically related rock units were with similar units being combined. With scale, nothing smaller than the grid size of 100 m in the x-y directions could be represented in the model. Together, these three criteria helped delineate appropriate hydrostratigraphic units for the model goals.

Bedrock units were based on the Bedrock Geology of Alberta Map (Prior et al., 2013). This map represented the scale of the geological detail required for the model so few modifications were made. One of the modifications that was made was beyond the southeast of the study area where the map by Prior et al. (2013) delineates the Dinosaur Park Formation, the Oldman Formation, and the Lower Belly River Group. These units, while subcropping outside of the study area, due to the dip of the bedrock, may enter the study area at depth. Despite this, these units are still all part of the Belly River Group and are lithologically similar. Hence, they were chosen to be amalgamated into the Belly River Group. A second modification worth noting is that the Horseshoe Canyon Formation was labelled the Edmonton Group as it may include the Battle Formation. The Scollard Formation and Bearpaw Formation, however, while part of the Edmonton Group were large enough to be mapped separately so they were included as a separate units.

Some surficial deposits were merged into equivalent hydrostratigraphic units due to lithological similarities and associations (Table 2.2). Glacial moraine in the model is the result of the amalgamation of several types of moraines from the Surficial Geology of Alberta Map (Fenton et al., 2013). The rationale for grouping is that the lithology of each moraine type is predominantly clay to silt till with small, locally present variations (discontinuous sand layers and geomorphological changes) distinguishing sub till types (Fenton et al., 2013). Since the bulk lithology is still predominately clay to silt, it is assumed that the till acts as a single hydrostratigraphic unit. Colluvial and alluvial sediments were also combined into a single hydrostratigraphic unit. This is due to their proximity and the fact that they are inseparable across many parts of the NSR, as the NSR crosses both deposits, frequently reworking sediments (Fenton

et al., 2013). The Empress Formation or buried valleys were chosen to be represented by two hydraulic conductivities, one for layer 3, and one for layer 4 due to the known variation in upper and lower buried valley properties (Hydrogeological Consultants Ltd., 1998b; Hydrogeological Consultants Ltd., 1998c; Kathol & McPherson, 1975). Overall, three of six surficial units included deviations from documented regional geologic maps.

Era	Period	Epoch	Hydrostratigraphic Unit	Layer (s)	Model Value	Literature Values	Source(s)
Cenozoic	Quaternary	Holocene	Alluvial/Colluvial	1 – 4	$K_{xy} = 7.4 \times 10^{-5}$ m/s; $K_z = 7.4 \times 10^{-6}$ m/s	Gravel - $10^{-2}$ m/s; Silt/Clay – $10^{-8}$ m/s	Kathol & McPherson, 1975
			Sand Dunes	1 – 4	$K_{xy} = 1.1 \times 10^{-4}$ m/s; $K_z = 1.2 \times 10^{-5}$ m/s	$10^{-4}$ m/s to $10^{-3}$ m/s	Kathol & McPherson, 1975
		Pleistocene	Glaciolacustrine	1 – 4	Silt/clay - $K_{xy} = 10^{-5}$ m/s; $K_z = 10^{-6}$ m/s; Sand – $k_{yz} = 2.3 \times 10^{-5}$ m/s	< $10^{-5}$ m/s	Kathol & McPherson, 1975
			Pitted Delta	1 – 4	$K_{xyz} = 3.5 \times 10^{-5}$ m/s	$10^{-4}$ m/s to $10^{-2}$ m/s	Kathol & McPherson, 1975
			Moraine	1 – 4	$K_{xy} = 5.8 \times 10^{-6}$ m/s; $K_z = 5.8 \times 10^{-7}$ m/s	< $10^{-5}$ m/s	Kathol & McPherson, 1975
			Empress Formation	3 – 4	Layer 3 - $K_{xy} = 1.1 \times 10^{-4}$ m/s; $K_z = 1.2 \times 10^{-5}$ m/s Layer 4 - $k_{xy} = 5.8 \times 10^{-4}$ m/s; $K_z = 5.8 \times 10^{-5}$ m/s	$10^{-4}$ m/s to $10^{-2}$ m/s	Kathol & McPherson, 1975
	Paleogene	Paleocene	Paskapoo Formation	5 - 20	$K_{xy} = 10^{-6}$ m/s; $K_z = 10^{-7}$ m/s	Siltstone/Mudstone - $10^{-10}$ m/s to $10^{-8}$ m/s; Sandstone – $2.5 \times 10^{-6}$ m/s to $10^{-3}$ m/s	Hughes et al., 2017
	Mesozoic		Scollard Formation	5 - 20	$K_{xy} = 10^{-7}$ m/s; $K_z = 10^{-8}$ m/s	$9.3 \times 10^{-10}$ m/s to $3.5 \times 10^{-6}$ m/s	Smerdon et al., 2017
			Edmonton Group	5 - 20	$K_{xy} = 10^{-8}$ m/s; $K_z = 10^{-9}$ m/s	$4.4 \times 10^{-10}$ m/s to $3.6 \times 10^{-6}$ m/s	Smerdon et al., 2017
			Bearpaw Formation	5 - 20	$K_{xy} = 10^{-9}$ m/s; $K_z = 10^{-10}$ m/s	$1 \times 10^{-11}$ m/s to $1 \times 10^{-14}$ m/s	Pétré et al., 2015
			Belly River Group	5 - 20	$K_{xy} = 10^{-7}$ m/s; $K_z = 10^{-8}$ m/s	$2.9 \times 10^{-8}$ m/s to $5.8 \times 10^{-6}$ m/s	Pétré et al., 2015; Stein, 1976b

**Table 2.2.** Model hydraulic conductivity compared with literature values.

## **2.4. Calibration**

### **2.4.1 Calibration Method**

Calibration head targets were chosen from the GOWN and the AWWID (Government of Alberta n.d.b; Government of Alberta n.d.a). GOWN wells in the study area were chosen if they were active. AWWID wells were chosen based on accuracy of location (surveyed or GPS located wells were preferred), whether a pumping test was preformed, and if lithology data was available.

Calibration was done by trial-and-error with hydraulic head targets. This involved visually inspecting hydraulic head targets and adjusting parameters accordingly to achieve the lowest residuals across the range of data as well as favorable calibration statistics. Parameters adjusted included hydraulic conductivity, recharge, and to a lesser extent ET.

Hydraulic conductivity was initially set to be anisotropic within a range of literature values (Table 2.2). It was then adjusted based on observed head target residuals with two hydrogeologic units being changed to isotropic, pitted delta deposits and sand lacustrine. These deposits were next to multiple major buried valley systems and in the case of pitted deltas deposits on a topographic slope. The net effect of the topographic slope and the high K buried valleys resulted in a high gradient across pitted delta sediments if they were anisotropic, causing anomalously low water levels. A similar effect was seen in sand lacustrine deposits to a lesser degree that necessitated their switch to isotropic K.

While recharge and ET were found partially through calibration, their values/distributions were informed by previous studies (section 2.3.6). Recharge was the main parameter adjusted during the calibration phase while ET was held constant after the appropriate ET values were selected. Given the broad range in recharge estimates (Klassen et al., 2018; Riddell et al., 2014), modelling efforts focused on testing by trial-and-error different recharge distributions and magnitudes while conforming to the bounds set by these previous studies.

ET applied to the model acts to take out excess water in key locations to compensate for the uncertainty in recharge estimates (Klassen et al., 2018; Riddell et al., 2014). Looking at where ET is applied in the model domain, it can be observed that ET is mainly applied at topographic lows, where we expect the water table to be close to the ground surface (Figure 2.12). This provides

evidence that the ET specified in the model is serving its intended purpose and only acting in key areas of excess water accumulation.

Lakebed K's were also set by trial and error and found to be significantly lower than surrounding glacial deposits in Lac Ste Anne and to a lesser extent, Isle Lake. Low lakebed K values inhibited flow from lakes into underlying channel deposits. Failure to include low K values would result in anomalously high hydraulic heads in the Onoway channel.

The final calibration chart is shown in Figure 2.13, illustrating that the model fit is consistent across the range of observed values. That is, model fit is not skewed to low or high elevations. The residual mean was 3.12 m with the residual standard deviation at 14.25 m; the absolute residual mean was 11.76 m. The final Root Mean Square (RMS) error was 14.59 m which gives a scaled RMS error of 3.1%. The absolute highest individual residual was 37.34 m. The global mass balance achieved was -0.53%.

The residual mean shows a slight skew to positive values indicating slightly low simulated water levels. The RMS error of 14.59 m is considered reasonable for a model of this scale, especially when considering the DEM error ranging from 5–8 m and the potential uncertainty in many calibration points. This is reinforced when considering the range of simulated head values from ~600–1000 m. These provide a scaled RMSE of 3.1%, below the commonly recommended target of 5–10% (Barnett et al., 2012). Global mass balance achieved was less than what is generally considered acceptable at 2% (Barnett et al., 2012). Given the model purpose, and the spatial distribution of residuals, this was deemed sufficient for recreating flow conditions on a regional scale.

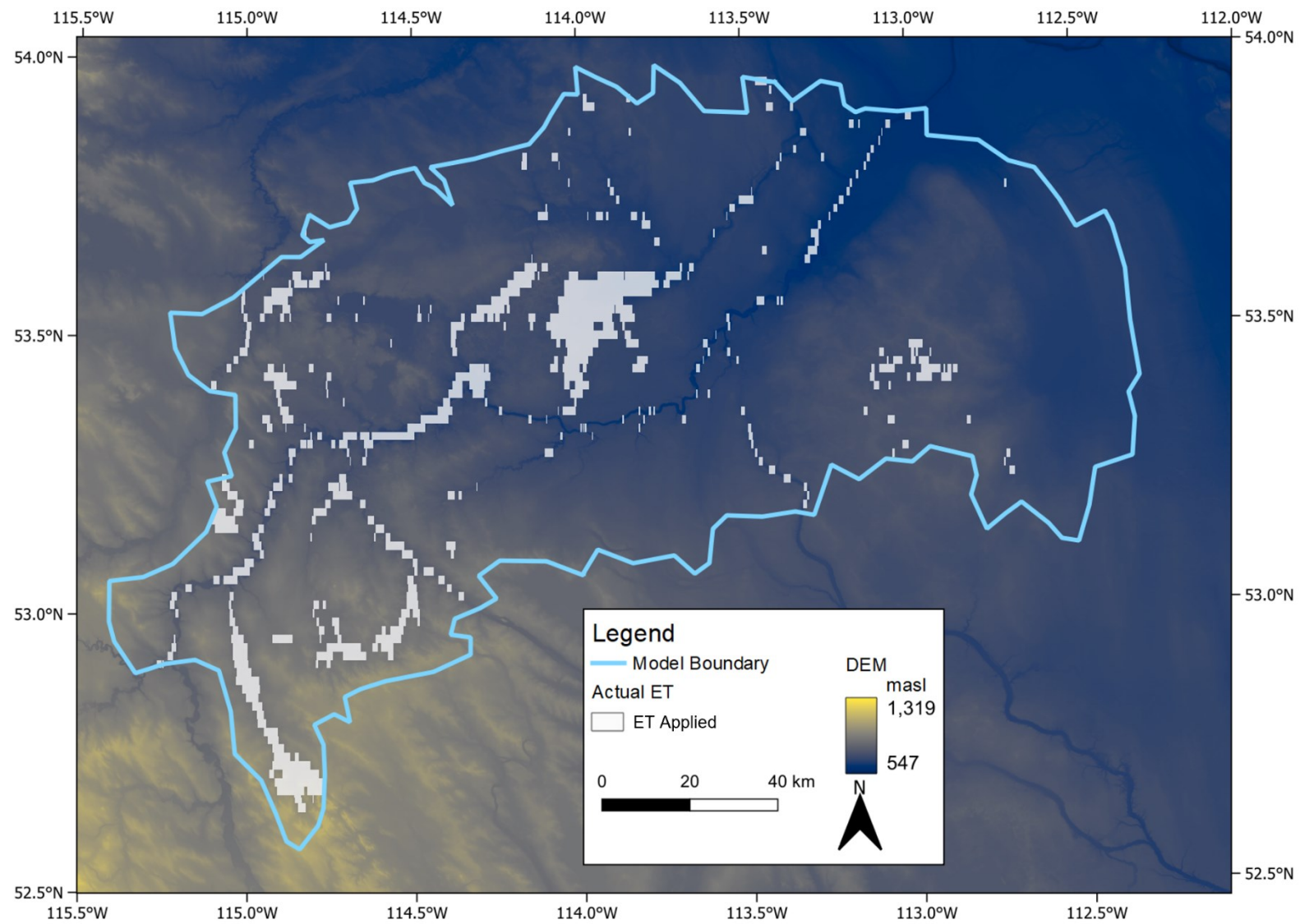


**Figure 2.12.** Digital Elevation Model (DEM) with locations of ET applied by model.

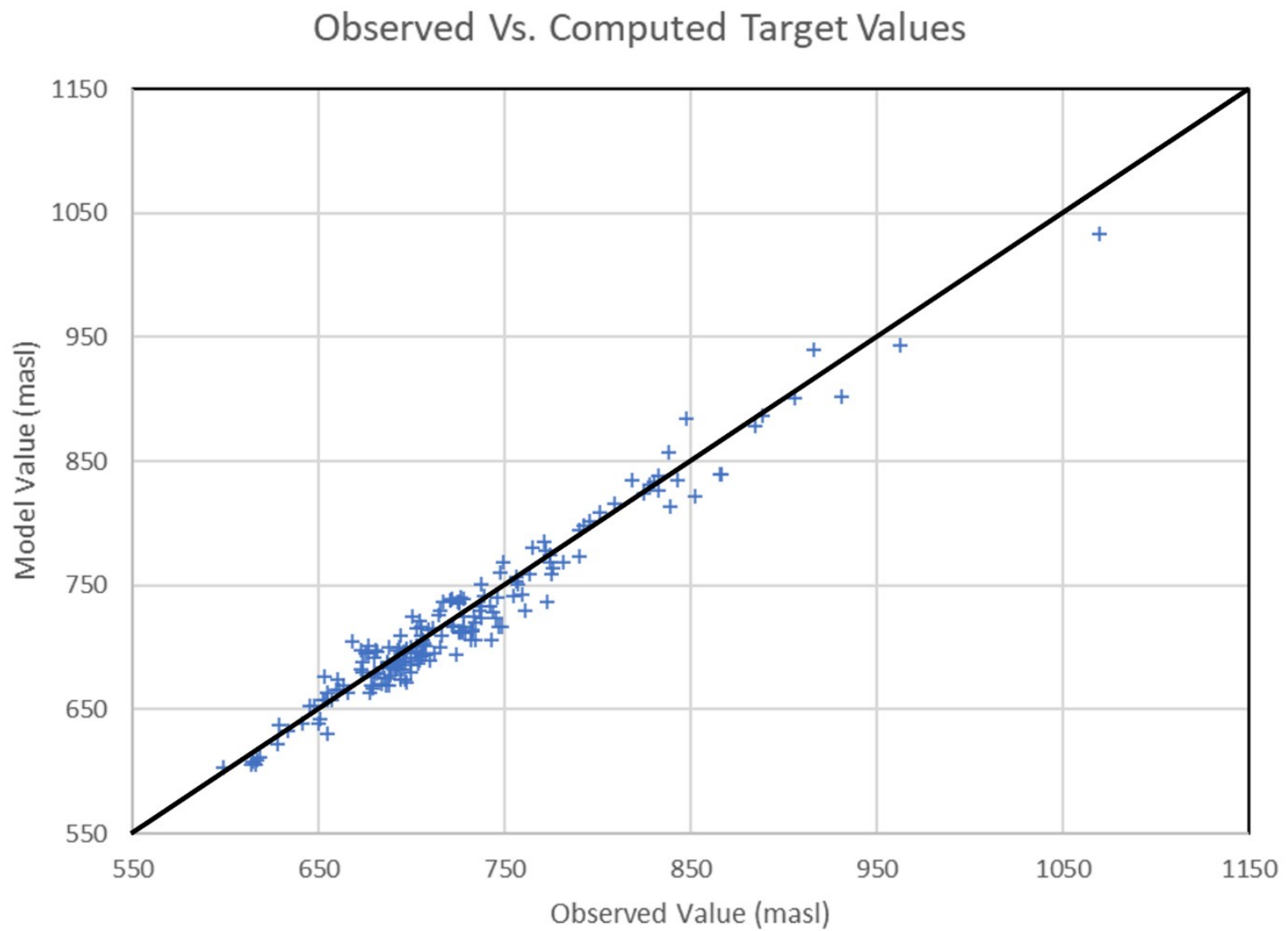


**Figure 2.13.** Calibration data with 1:1 line in black.

## **2.4.2 Sources of Error in Calibration Data**

For steady state calibration, simulated hydraulic head values were compared with observed hydraulic head values measured at groundwater wells in the study area. However, a significant source of error may be in the measured values themselves. Errors may arise from measurement, scaling, and time related effects. Therefore, it is important to contextualize potential sources of error when considering model applicability.

Measurement error is found in measurement equipment used, the DEM, screen length, and screen elevation among other sources. Since measurement error arising from water level measurement equipment is typically on the order of centimetres (Post & von Asmuth, 2013) it is not a major concern for a model of this scale. A larger source of error, on the order of  $<5$  to  $\sim 8$  metres is in the DEM used, with locations of rapid elevation change having larger error (Land Information Services Division, 1988). Since many groundwater levels were calculated relative to this DEM due to inaccurate or missing elevation data, they are subject to this relatively large error. Screen length can also contribute to uncertainties in measured water levels. Screen length can be on the order of several metres or more throughout the study area as most wells are drilled for water exploitation purposes. This means that head measurements may not be a point estimate. Rather, the hydraulic head would be the average of a potentially significant thickness in the screened material (Post & von Asmuth, 2013). To add to this, the screen may intersect multiple lithologies, further adding to the uncertainty. Lastly, well casing elevation may contribute to the error in surveyed wells as well drillers did not measure elevation at the top of the casing but rather the ground surface, a difference of approximately 1 metre.

Scaling error may arise as certain locally important hydrogeological units will fall below the extent of discretization and detail of parameterization in the model area. This may contribute to locally high residuals as many water wells may target sand lenses within surficial deposits and coal seams in bedrock. These heterogeneities are below the resolution of the model but can have significantly different material properties than the material they are surrounded by. This leads to the potential for local effects to be represented in the calibration data while the model utilizes bulk K values for hydrostratigraphic units. Nevertheless, this does not impact the models intended purpose as variations are typically below the accuracy of the model.

Time of groundwater level measurement in relation to seasonal and anomalous water level fluctuations can influence hydraulic head observations with varying degrees of uncertainty depending on data source. For piezometers in the GOWN, data are usually presented as time series (Government of Alberta, n.d.b), necessitating that an average value be used to compare with steady state simulated hydraulic heads. In addition to the GOWN data, water level data from the AWWID (Government of Alberta, n.d.a) were used. The AWWID data had static water levels reported as part of pumping tests at the time of well construction. With data spanning over six decades, these measurements are a point in time within normal seasonal groundwater fluctuations. This means they are subject to possible metre scale error as hydraulic head could be measured at a seasonally low or high point in a year. There is also the possibility that an external event has perturbed the system and caused the groundwater level to vary outside of its normal seasonal range. In this case, if the water level was measured prior to a long-term change, or immediately after a transient anomalous event, the calibration target would be less accurate. Since most water levels appear to be stable over time (Figure 2.4), this seems to be rare but should be documented along with seasonal variations in groundwater levels as potential error sources.

Additionally, a number of AWWID wells were included that did not have accurate location data in order to help create a better spatial distribution of calibration points. These wells only had their location known to a quarter section and elevation not measured accurately (or entirely absent). Therefore, there may be some additional error associated with location of calibration points, but this is acceptable when considering model goals and the level of discretization together with the parameterization scheme.

## **2.5 Model Results and Sensitivity Analysis**

### **2.5.1 Hydraulic Head Distribution**

Figure 2.14 shows the elevation of the simulated water table as a colour flood and with hydraulic head contours for reference. The highest hydraulic head values are found in the southwest and decrease gradually towards the northeast. The regional hydraulic head distribution also decreases towards the centre of the model area, both north and south of the northeast-southwest trending NSR. Superimposed on the regional hydraulic head distribution is series of local-intermediate scale hydraulic head patterns. These local-intermediate scale patterns are represented as refractions in equipotential contours or salients in the contours that deviate from regional hydraulic head

patterns. More prominent examples of this can be seen around lakes and constant head boundaries in the model domain. This results in distinct local-intermediate hydraulic head distributions superimposed on a regional hydraulic head pattern. The interpreted cause of these patterns is further discussed in section 2.6.

Figures 2.15a-d show hydraulic head results by layer. A general decrease in dry cells with increasing layer numbers is seen. However, no major changes from Figure 2.14 are noted in terms of regional/local hydraulic head distribution. Of note is Layer 4 (Figure 2.15b), which shows that groundwater flow is largely focused in the buried valley systems, whereas Figures 2.15c-d show bedrock with increasing depth, each layer illustrating a general congruence with the regional flow path.

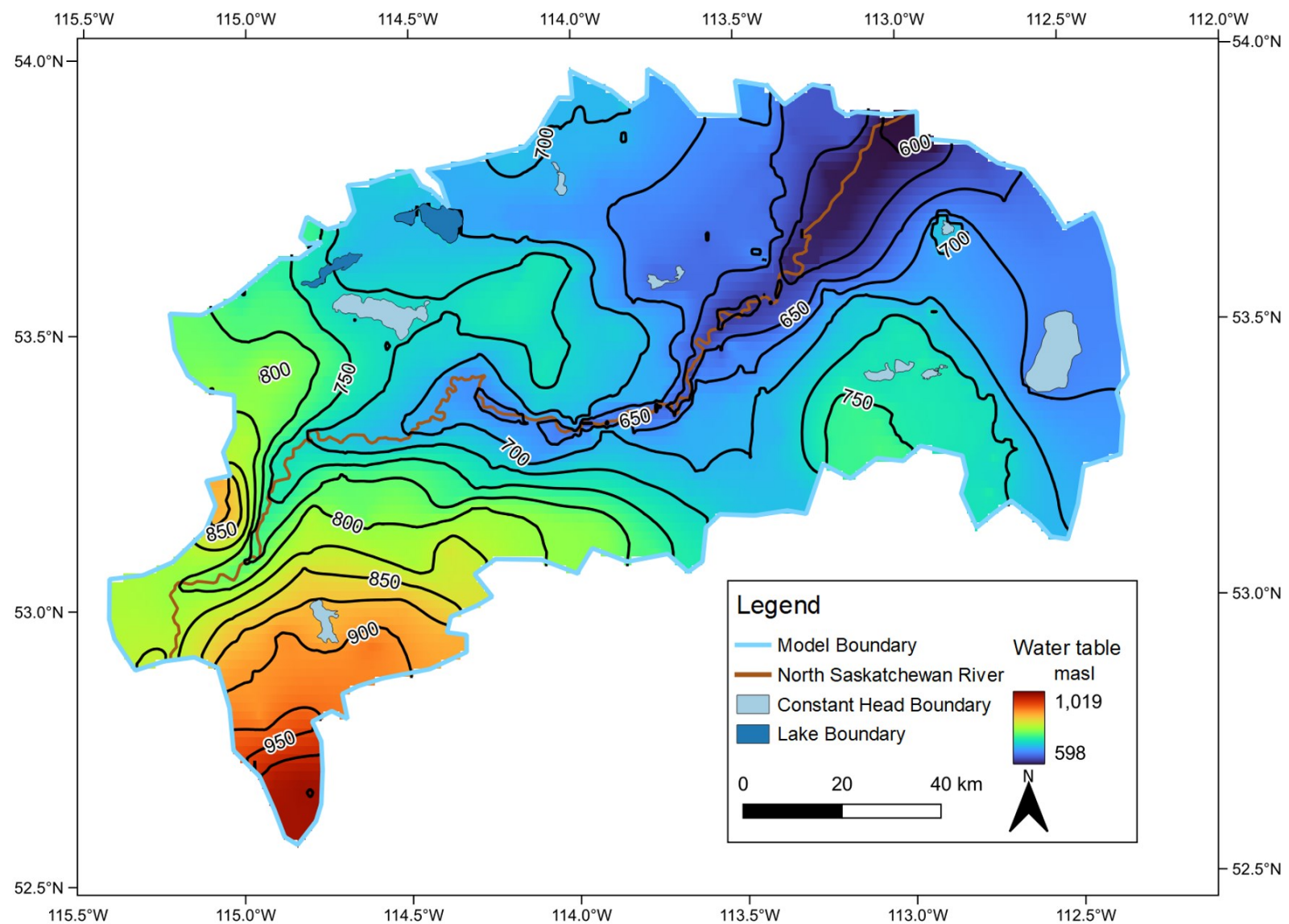


**Figure 2.14.** Simulated water table.

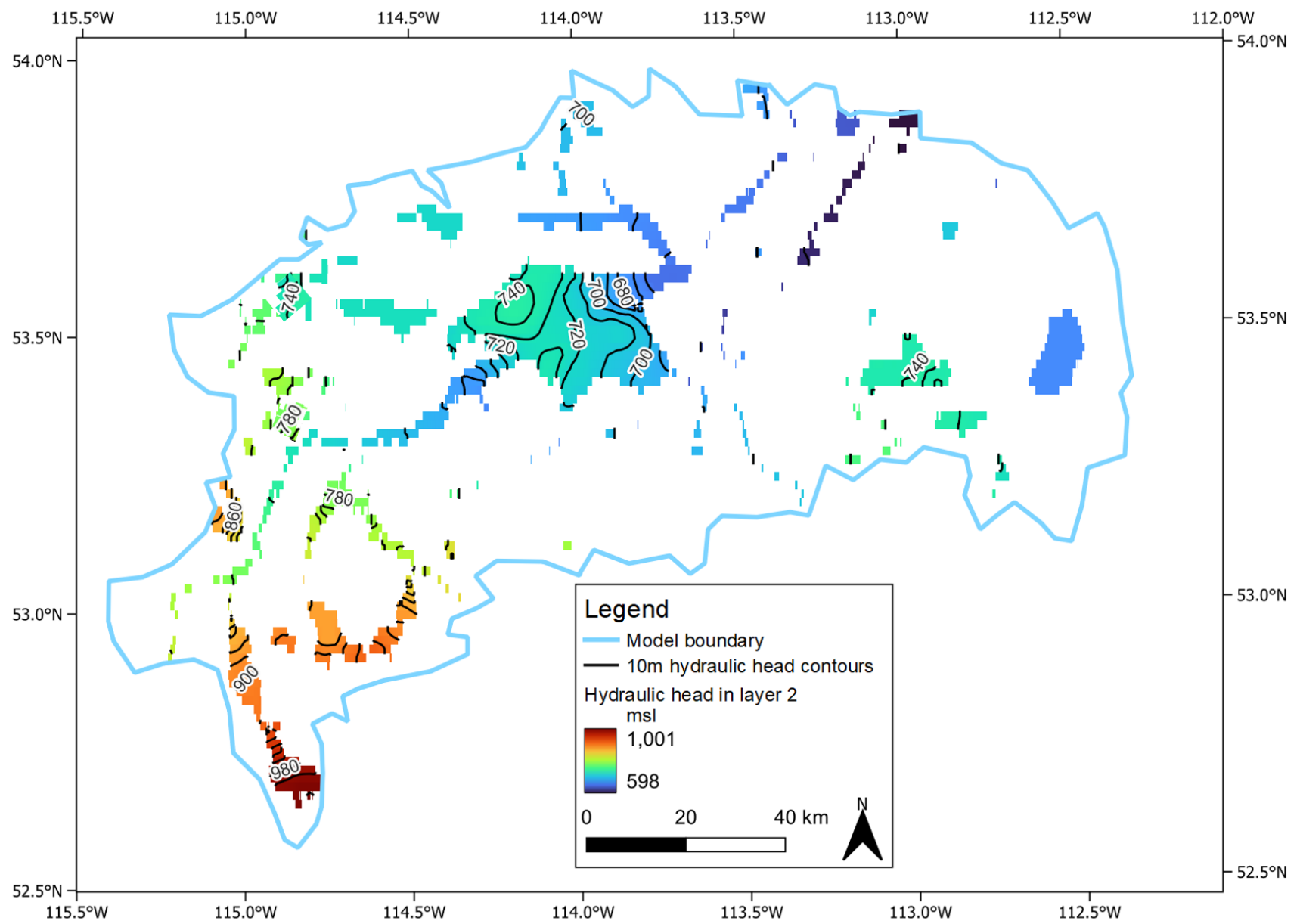


Figure 2.15a. Hydraulic head in layer 2 (surficial deposits without buried valleys).

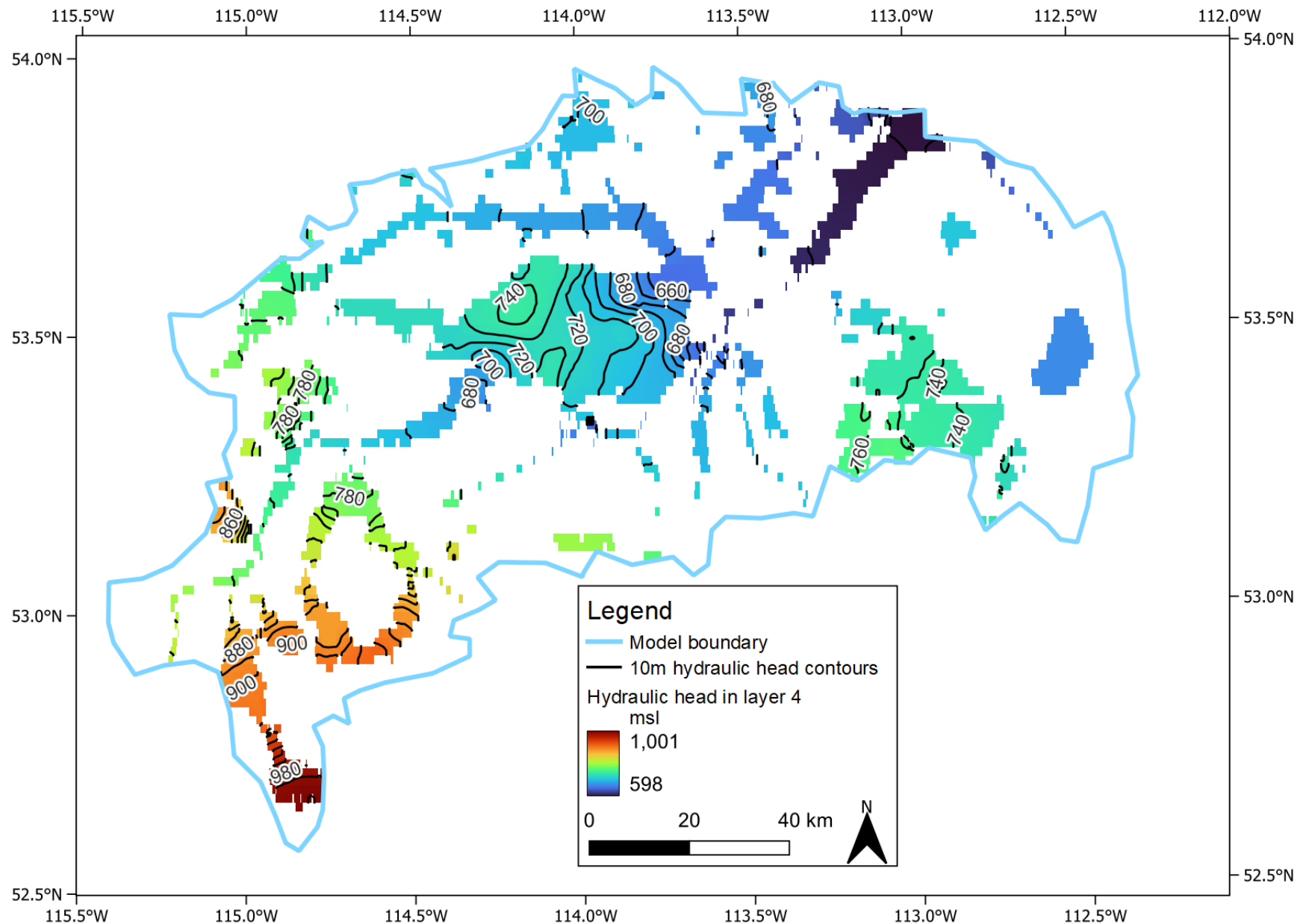


Figure 2.15b. Hydraulic head in layer 4 (surficial deposits including buried valleys).

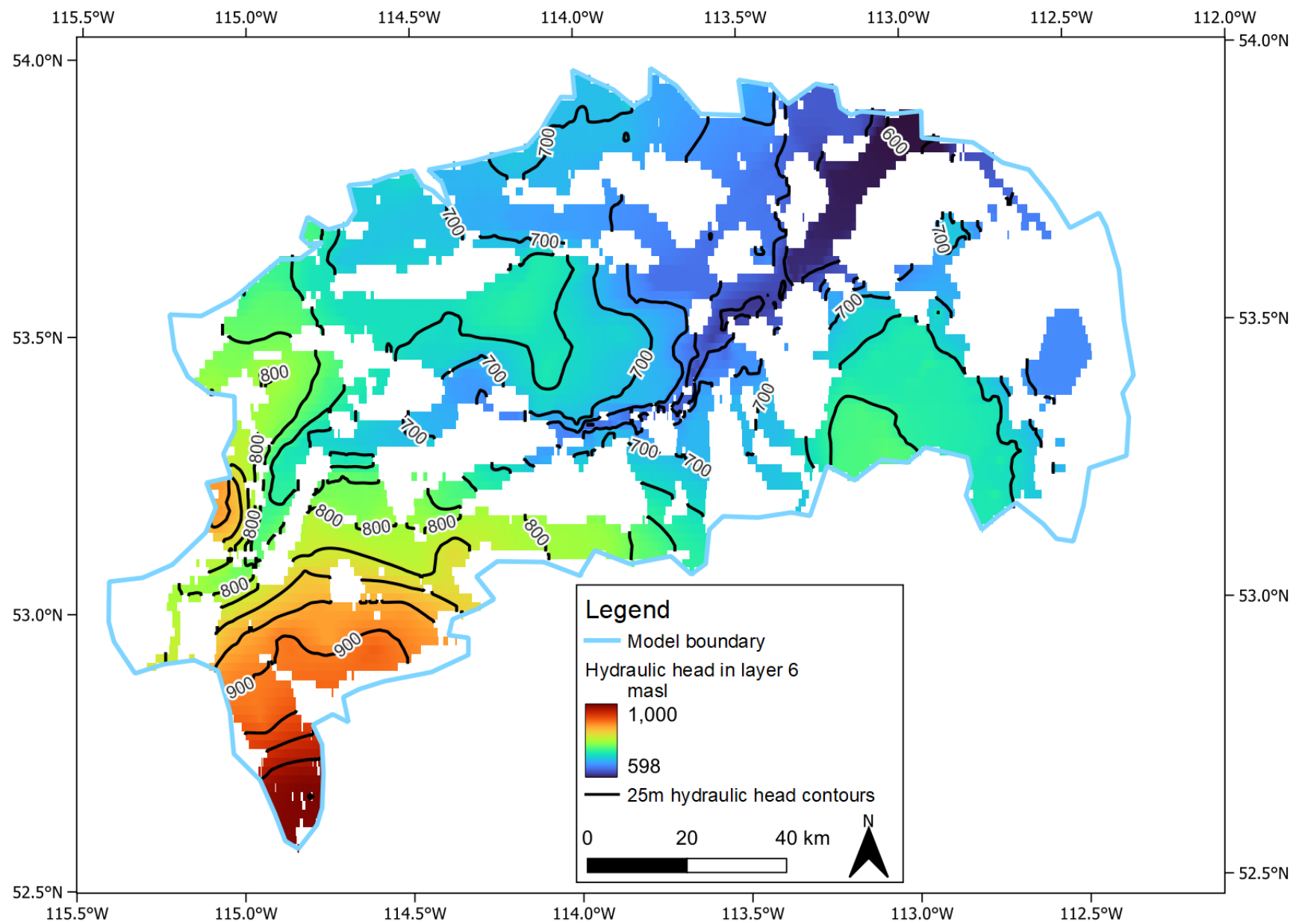


Figure 2.15c. Hydraulic head in layer 6 (shallow bedrock).

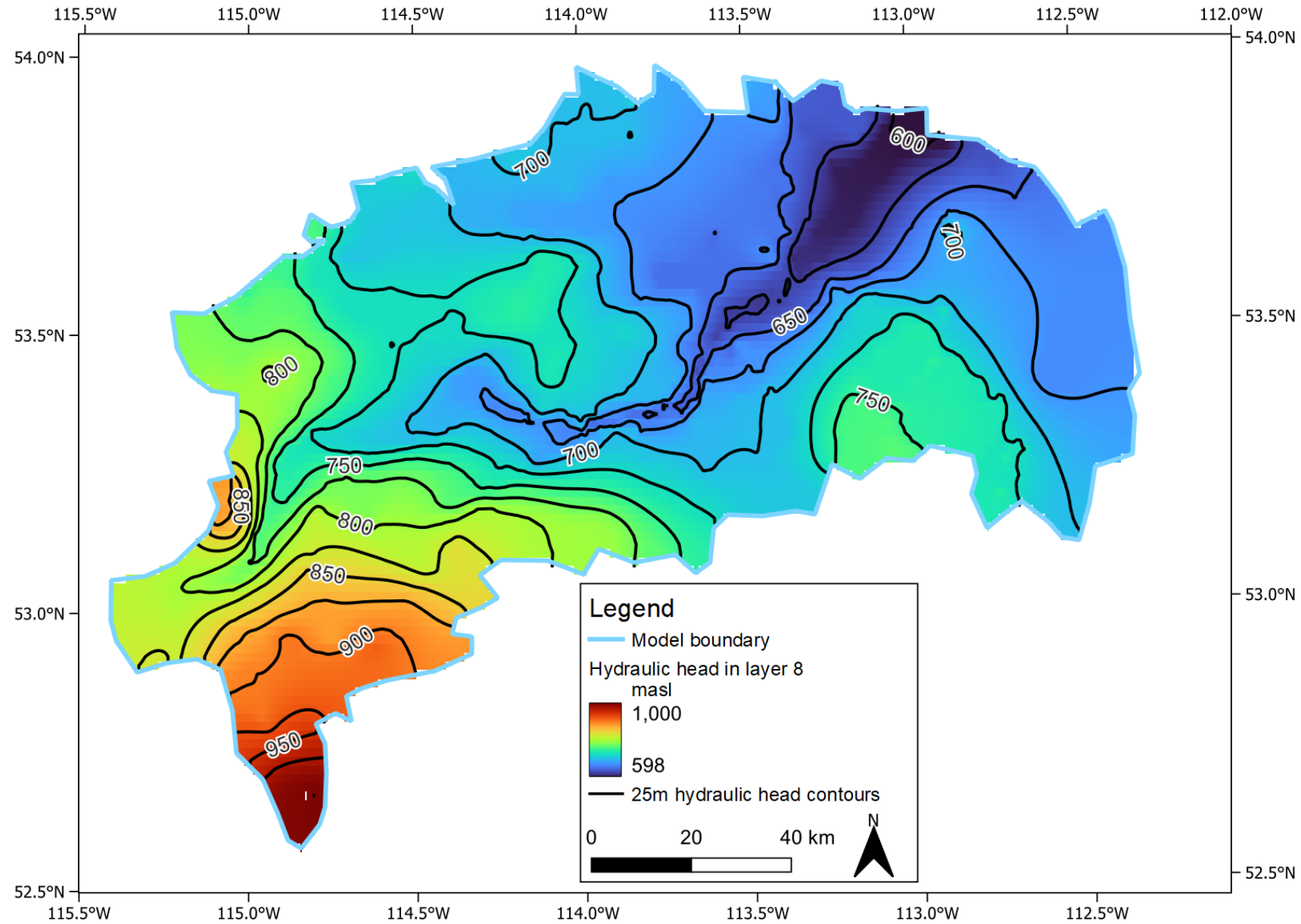


Figure 2.15d. Hydraulic head in layer 8 (deep bedrock).

## 2.5.2 Sensitivity Analysis

During model calibration, it was found that results depended most on the hydraulic conductivity in conjunction with recharge relative to ET. Since an increase in recharge has a similar effect as a proportional decrease in ET (Von Hauff, 2004), a sensitivity analysis was only preformed on the values of recharge and K. The details of the sensitivity analyses performed are described in more detail below.

Figure 2.16 shows the sensitivity analysis as percent change in RMS error for different surficial deposits. In terms of calibration statistics, a lower RMS error generally means a better model fit (Barnett et al., 2012). Within surficial deposits, till shows a large increase in the RMS error indicating that the model is most sensitive to lowered K for the till. Glaciolacustrine sand and lower buried valley deposits show the next largest impacts to increases in K by an order of magnitude. Meanwhile other surficial deposits appear to be less sensitive with alluvial/colluvial deposits providing better calibration statistics for an increase in K. However, this increase also results in less favorable calibration statistics in the pitted delta deposits, an important hydrogeologic unit and thus was not utilized.

The bedrock sensitivity analysis is provided in Figure 2.17 and follows the same statistical scheme as the surficial deposits. The model is most sensitive to changes in K in the Paskapoo Formation, with large changes in the percent error resulting from both increases and decreases in K. However, decreases in K in the Paskapoo appear to be most sensitive by almost an order of magnitude. Meanwhile, the other bedrock units show comparatively muted sensitivity. This reflects the relative importance of the Paskapoo Formation in groundwater flow across the southwestern portions of the model. That is, the Paskapoo Formation may serve a more active role in the near surface flow system compared to other bedrock present in the study area.

The recharge sensitivity analysis is shown in Figure 2.18 with the sum of squared residuals indicating model fit. The model is quite sensitive to recharge, with increases in recharge having over an order of magnitude greater impact than equivalent decreases in recharge. It should be noted that increases in recharge required forced convergence even at 1% global increase. This reflects the nature of recharge in the MODFLOW model and the need for ET. That is, excess recharge results in groundwater accumulation in topographic lows, that if not removed, causes anomalously high water levels and consequent ill-convergence.

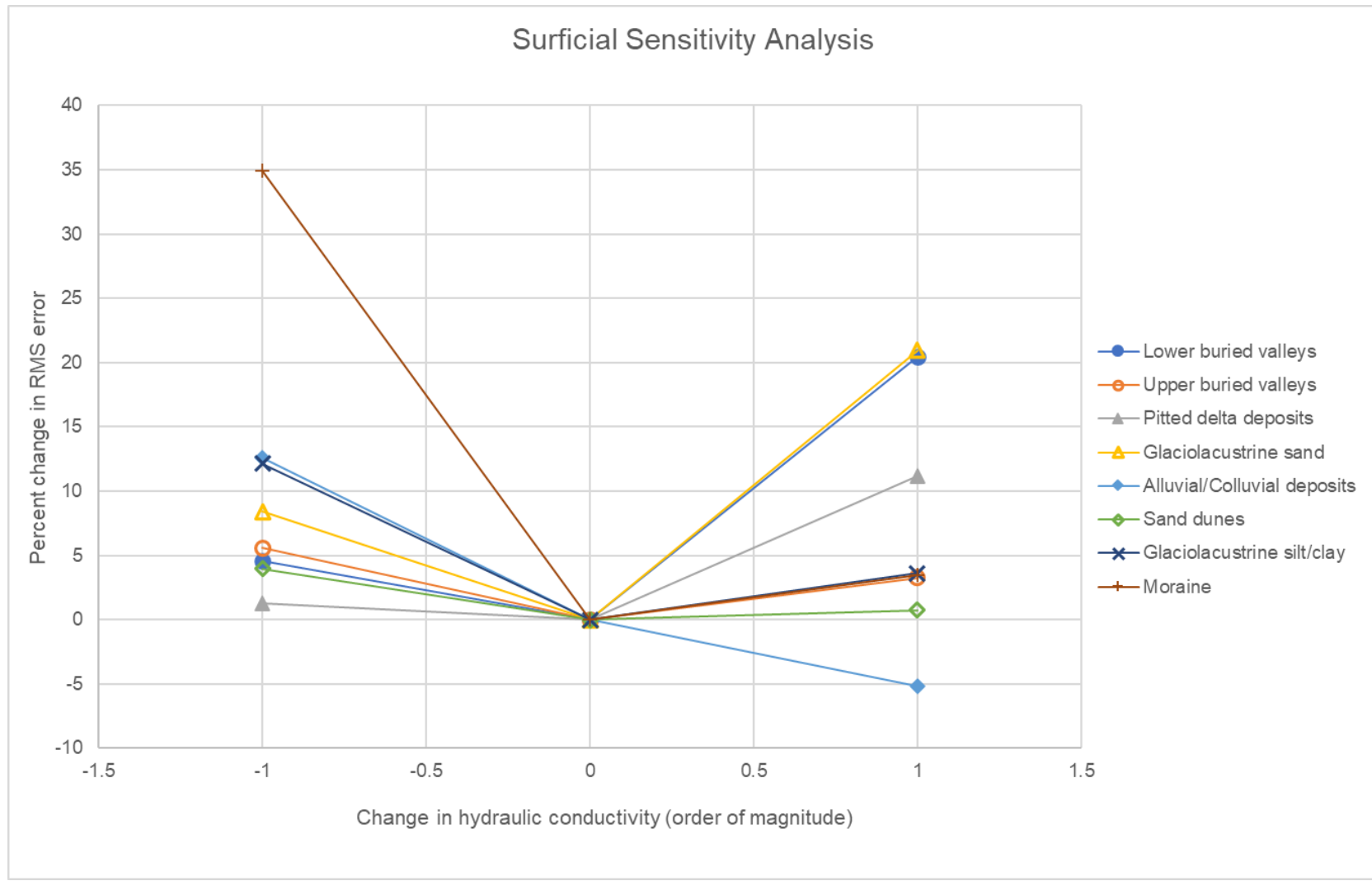


**Figure 2.16.** Percent change in RMS error for surficial sensitivity analysis.

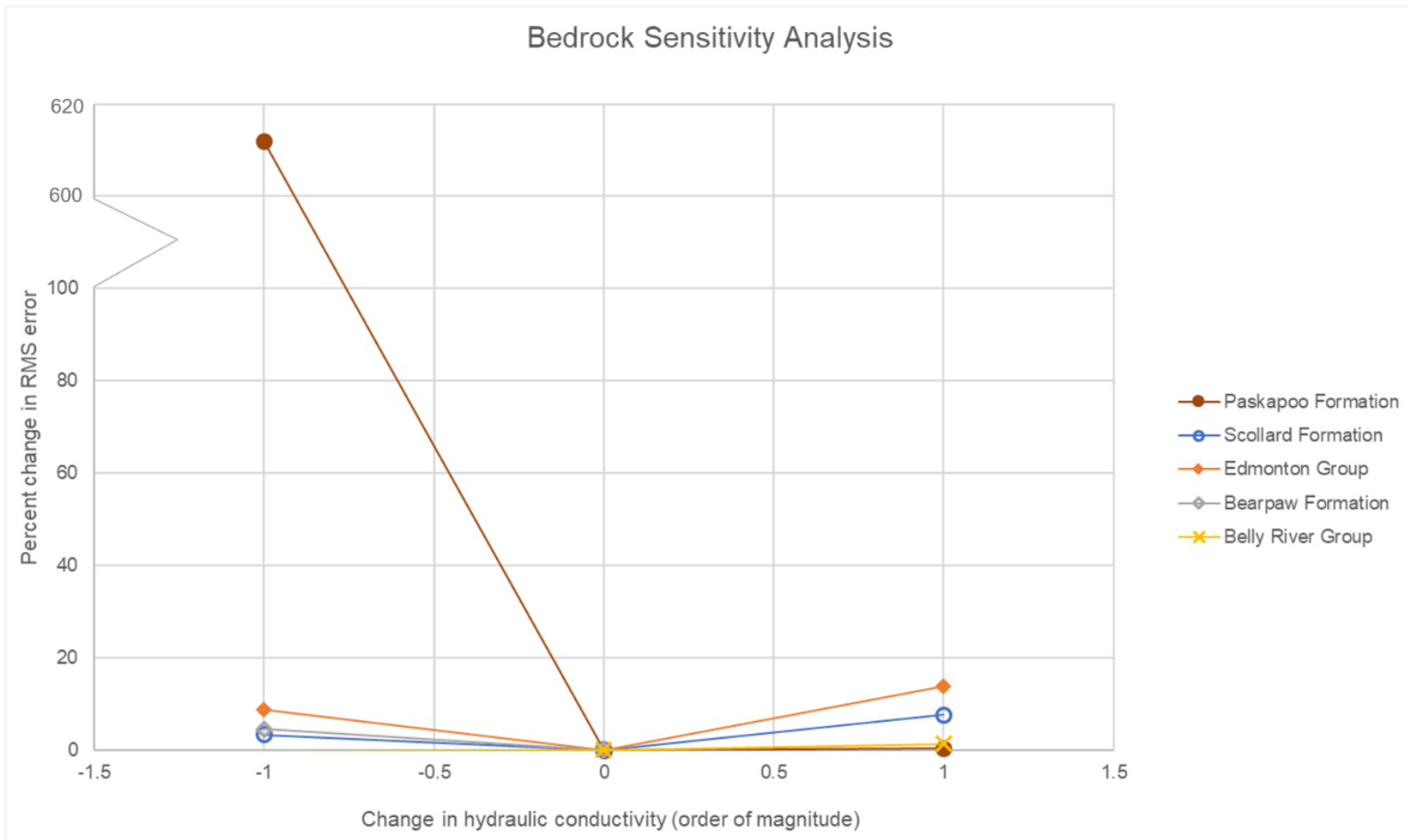


**Figure 2.17.** Percent change in RMS error for bedrock sensitivity analysis.

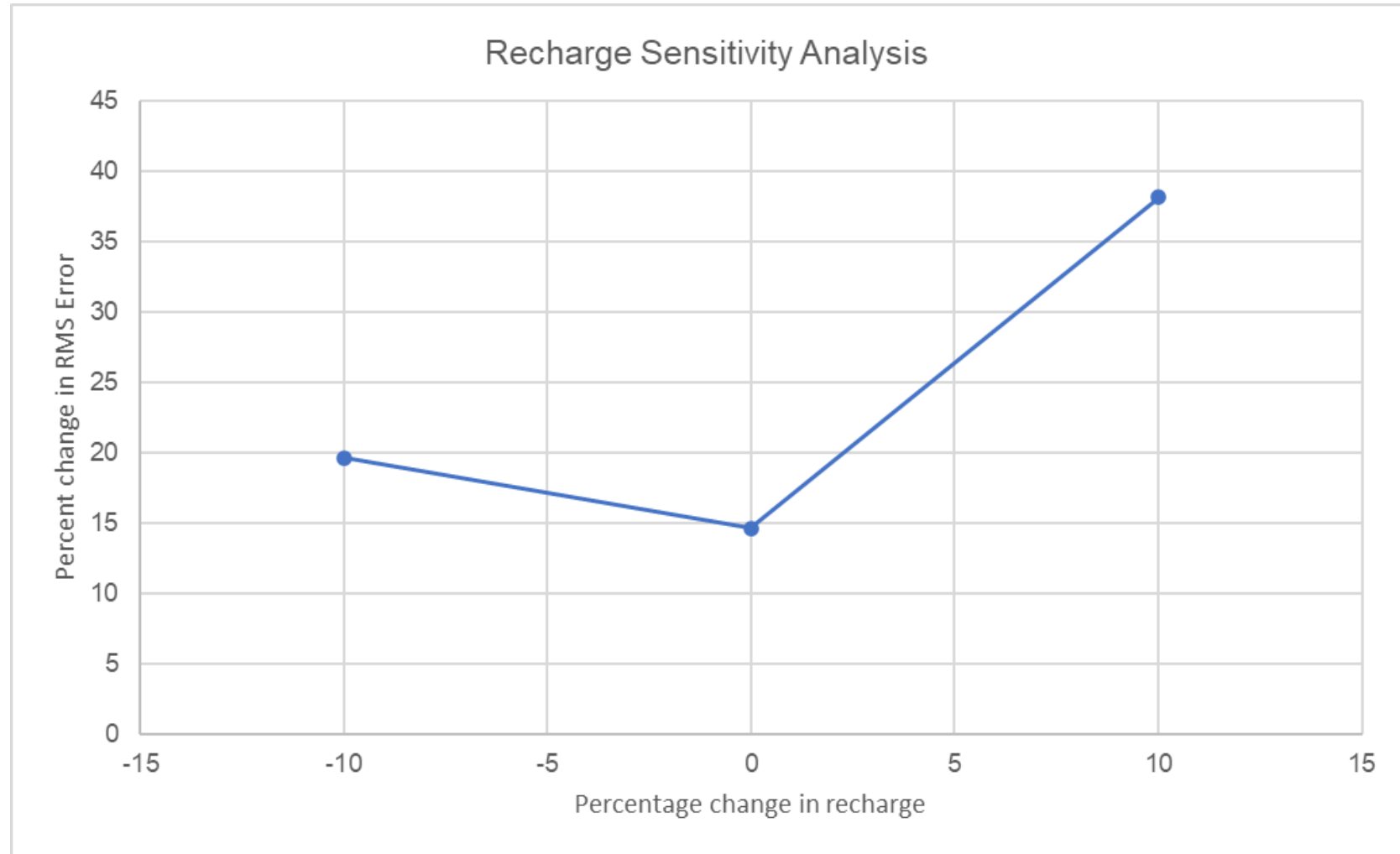


**Figure 2.18.** Percent change in RMS error for recharge sensitivity analysis.

## **2.6 Discussion**

### **2.6.1 Bedrock and Surficial hydraulic head distributions**

Since the model is designed with a regional conceptual framework, only larger scale trends in surficial hydraulic head may be visible. For instance, it is observed that surficial groundwater flow is largely focused within surficial aquifers (Figure 2.15 a-b; Figure 2.19). Additionally, surficial deposits become increasingly saturated with depth as the frequency of confined conditions increases with depth. Surficial aquifers include buried valleys, pitted deltas, aeolian dunes, glaciolacustrine sands, and fluvial deposits (Figure 2.2). Distributions of groundwater supply wells appear to support a regional restriction of groundwater to surficial aquifers. That is, few groundwater wells are completed in surficial deposits outside of large surficial aquifers (Hydrogeological Consultants Ltd., 1998a, 1998b, 1998c, 1999, 2001). However, while groundwater distributions within surficial deposits appear to be controlled by higher K geology there are some notable exceptions. Firstly, topographic lows where groundwater accumulates show increased groundwater saturation. This can be explained by the presence of upwards groundwater flow at these locations. Specifically, the effects of topography driven flow override that of geology in surficial deposits at topographic lows. Secondly, some eastern portions of the study area show groundwater more present in lower K till and glaciolacustrine deposits (Figure 2.19). However, increased, persistent recharge in lower K deposits in this area accounts for the increased saturation observed (Klassen et al., 2018; Riddell et al., 2014). Both trends appear to coincide with observational literature that indicates negligible groundwater yields outside of regional surficial aquifers and some eastern tills/glauciolacustrine deposits (Research Council of Alberta, 1978). This reflects both the minimal groundwater present outside of surficial aquifers as well as the regional design of the model. Large scale water resources are confined to surficial aquifers, but topography driven flow and recharge in relation to geology produce regionally noticeable deviations from this trend.

As with surficial deposits, only regional trends in bedrock hydraulic head distribution may be visible due to model conceptualization. Bedrock hydraulic head distributions become increasingly saturated with depth until layer eight where fully confined flow occurs (Figure 2.15 c-d). Unlike surficial deposits however, bedrock deposits do not appear to show any obvious trends in hydraulic head distribution related to bedrock geology. This is because bedrock has more homogeneous and

lower K values in the model, whereas surficial deposits contain regionally extensive, high K aquifers that create large K contrasts to direct groundwater flow. Instead, bedrock hydraulic head distributions are primarily related to topography and depth. As bedrock depth increases, progressively uninterrupted topography driven flow patterns are observed (Figure 2.15d). Conversely, near surface bedrock mimics surficial water level saturation and distribution, but to a greater spatial extent (Figure 2.15b-c). Hydraulic head distribution within the bedrock is controlled by topography but shallow bedrock may follow unsaturated trends mirroring surficial deposits.

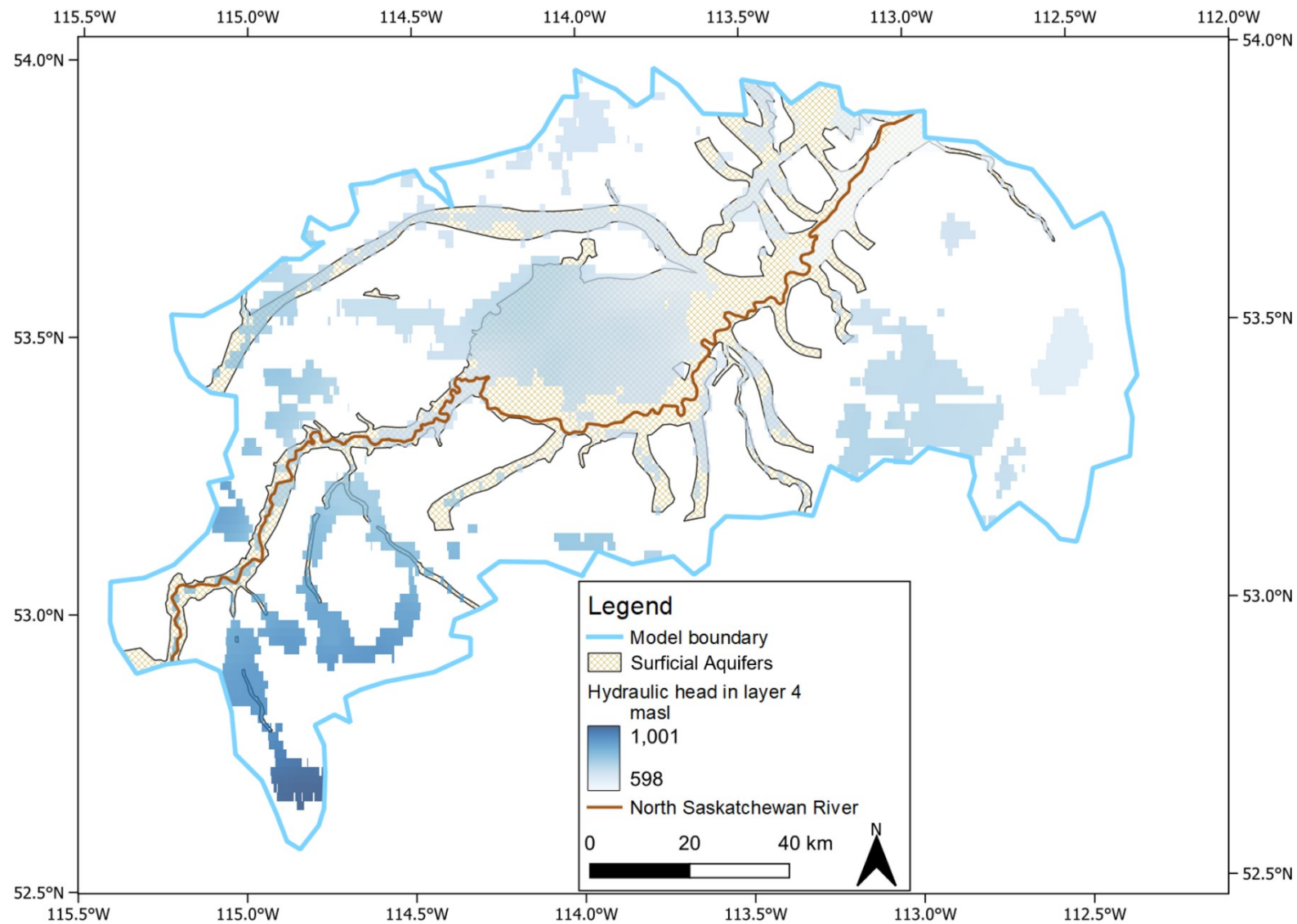


**Figure 2.19.** Surficial aquifers superimposed on Layer 4 hydraulic head distribution.

## 2.6.2 Groundwater flow patterns and directions

The NSR splits the model in half, providing a linear topographic low as it trends SW to NE across the study area (Figure 2.0; Figure 2.14). The water table is expected to be a subdued replica of topography and the NSR occupies the lowest point in the immediate and regional landscape (Figure 2.20; Hubbert, 1940). On either side of the NSR, broad potentiometric patterns indicate groundwater flow is directed towards to the NSR across its entire length (Figure 2.20). This is because the NSR is surrounded by regional and local topographic highs. The NSR provides a regional topographic low and a destination for regional groundwater flow within the model.

While regional flow distances span from the edge of the model area to the NSR, local-intermediate flow distances span shorter distances, with larger topographic variation causing larger local-intermediate flow systems to be developed. Local-intermediate flow patterns focus groundwater that has recharged at local to intermediate topographic highs into similar scale depressions and valleys. Indications of these flow patterns are manifested through small-scale deflections in water table contours at breaks in topography (Figure 2.14; Figure 2.20). Local-intermediate flow patterns do not penetrate as deeply into the model as regional groundwater flow, the depth of impact is commensurate with the size of topographic variation (Freeze & Witherspoon, 1967). More specifically, regional flow patterns travel to greater depths along longer flow paths and local-intermediate flow patterns follow shorter, shallower flow paths. Flow systems of different flow direction, flow path length, and depth across the model are caused variably scaled topography.

Buried valleys provide large K contrasts with surrounding materials that cause local to intermediate scale deflections in water table contours. They are also frequently present in topographic lows as recent valleys tend to follow paleo valley trends. This causes them to receive groundwater input from two mechanisms: (i) relatively high transmissivities, and (ii) the presence in topographic lows. This can be seen as large deflections in water table contours in the vicinity of buried valleys (Figure 2.20). Additionally, due to the K contrast, once groundwater enters the buried valley aquifers, appreciable quantities of groundwater will reside in them until they are exposed, subcrop, or dry out (Freeze & Witherspoon, 1967). This means groundwater may enter buried valleys on a local to intermediate scale but once groundwater is in buried valleys it is unlikely to exit provided hydrogeologic conditions persist. This highlights the regional importance of buried valleys in the groundwater flow system. Buried valleys act as a possible meso-scale

conduit that water flows into on a local to intermediate scale but may transport groundwater on a regional scale given the right hydrogeologic conditions.

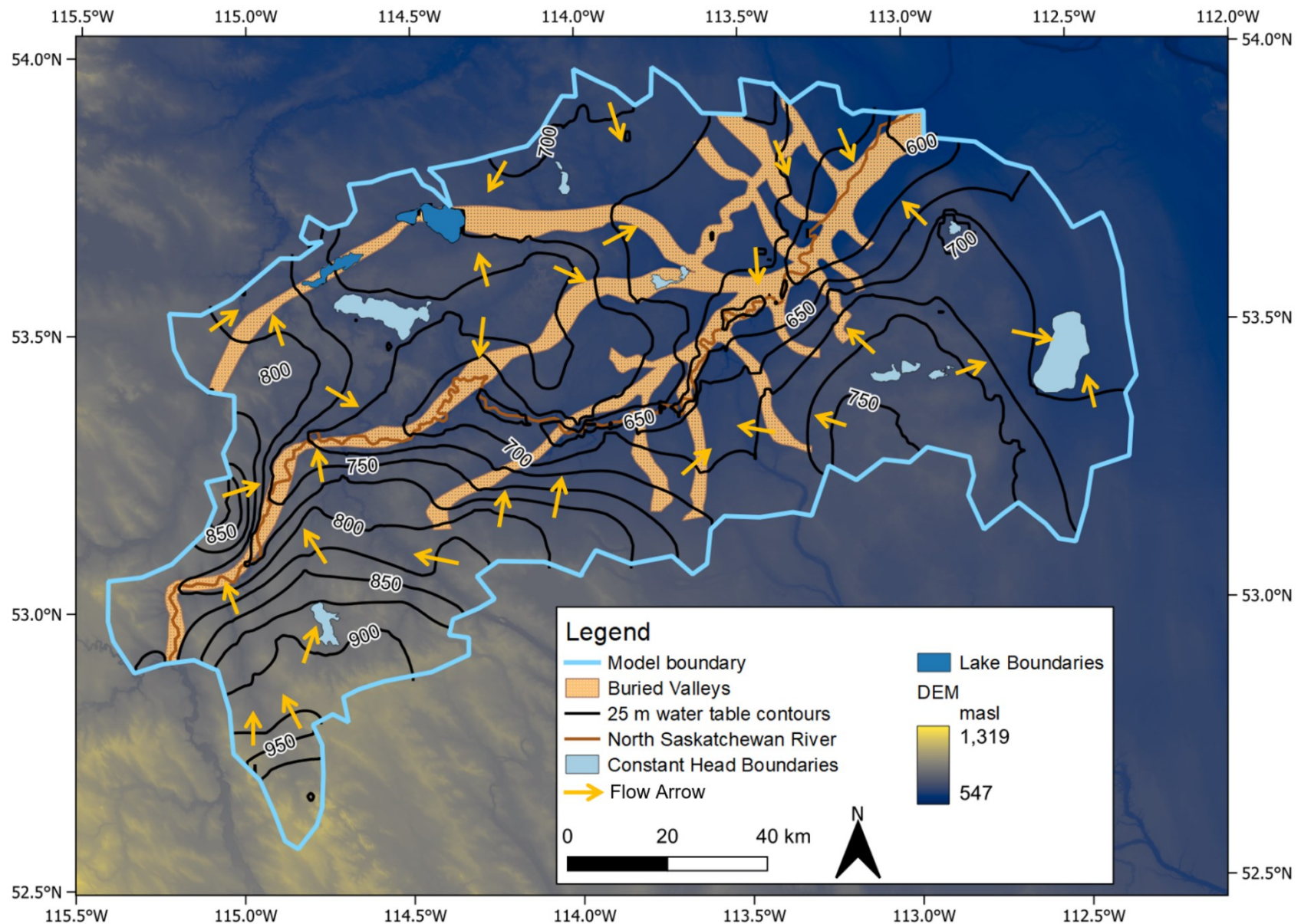


**Figure 2.20.** Water table contours superimposed on topography with interpreted flow arrows.

### **2.6.3 Groundwater Discharge Areas**

A groundwater discharge area occurs where net saturated flow is directed towards the ground surface (Tóth, 1962). Flowing wells and springs are common features of groundwater discharge areas since the water table is close to or above the ground surface at these locations (Freeze & Cherry, 1979; Tóth, 1962). Examination of model potentiometric patterns (Figure 2.20), indicate that regional groundwater flow is broadly directed towards the NSR. Likewise, local to intermediate scale flow is directed towards local to intermediate topographic lows. As expected, many topographic lows across the model area have springs and flowing wells present (Figure 2.21a-b; Freeze & Cherry, 1979; Tóth, 1962). When compared with model results, upwards groundwater flow also occurs at many lows in topography across the model area that are correlated with springs/flowing wells (Figure 2.21a-b). The distribution of applied ET indicates the water table is close to ( $<1$  m) or above the ground surface at these locations as well (Figure 2.12). Thus, groundwater discharge areas can be interpreted based on potentiometric patterns, upwards groundwater flow, the presence of springs/flowing wells, and applied ET correlated with topographic lows (Figure 2.21c).

Some notable groundwater discharge areas in Figure 2.21c are along the buried valleys. Buried valleys coincide with both regional and local to intermediate discharge areas. As priorly indicated, this is partly due to their high K nature and position in low lying valleys. This causes groundwater to be directed towards buried valleys from surrounding sediments and develops a favorable vertical gradient for upwards groundwater flow at these locations.

Lakes also appear to be frequent locations of groundwater discharge (Figure 2.21c). This is because lakes frequently occupy low lying areas. Lakes surrounded by topographic highs see discharge surrounding the entire lake. Conversely, lakes in a local topographic low along a sloping surface may only experience discharge in a portion of the lake (Winter, 1976). However, Isle Lake, and Lac Ste Anne do not appear to be groundwater discharge locations. Instead, Lac Ste Anne and Isle Lake leak water into the underlying channels. The location of buried valleys beneath them suggests that buried valleys may change the nature of the GW-SW interactions in some lakes along their length. A possible explanation for this is that high K sediments do not maintain a hydraulic gradient well, resulting in lower hydraulic heads and the induction of flow towards high K deposits (Freeze & Cherry, 1979). Dependent on the hydrologic/hydrogeologic setting, the presence of high K

deposits such as buried valleys may have an influence on whether a losing lake (loses water to groundwater system) is observed. Because of buried valleys potential influence on overlying lakes, buried valleys should be accounted for in future groundwater and surface water studies as well as models regarding Isle Lake and Lac Ste Anne.

#### **2.6.4 Buried valleys and the North Saskatchewan River**

Upwards groundwater flow varies along the length of the NSR. Increased upwards groundwater flow is correlated with buried valleys (Figure 2.21a-c). The NSR follows paleo valleys (buried valleys) for the southwestern and northeastern portions of the model but diverges in the central portion of the NSR in the model (Figure 2.20; Rubin, 2022). In the central portion of the NSR in the model that diverges from paleo valleys, groundwater is still directed towards the NSR horizontally within model layers, but very little groundwater flow is directed upwards towards the NSR across underlying model layers. This suggests buried valley sediments may play a role in directing groundwater upwards from the bedrock towards the NSR, facilitating increased hydraulic communication.

To further examine this result, the river has been divided into three segments with relative baseflow calculated for each segment (Figure 2.21d). This was done by recording the input flux into each of the three defined segments of the river boundary condition, then normalizing to remove the effect of the different segment lengths. This provides average baseflow per metre of river in each segment. The pattern observed is that relative baseflow is the highest in the southwest portion of the NSR, lowest in the middle, and of moderate magnitude in the northeastern portions (Figure 2.21d). Interestingly, the southwest, and northeast portions coincide to the buried valley sediments while the middle deviates from them. The expected trend would be for baseflow to decrease to the northeast due to decreases in recharge and gradient to the northeast. Instead, baseflow is observed to increase where buried valley sediments are present and decreasing where absent. Because of this, the presence of buried valleys sediments is interpreted to be correlated with increased relative baseflow.

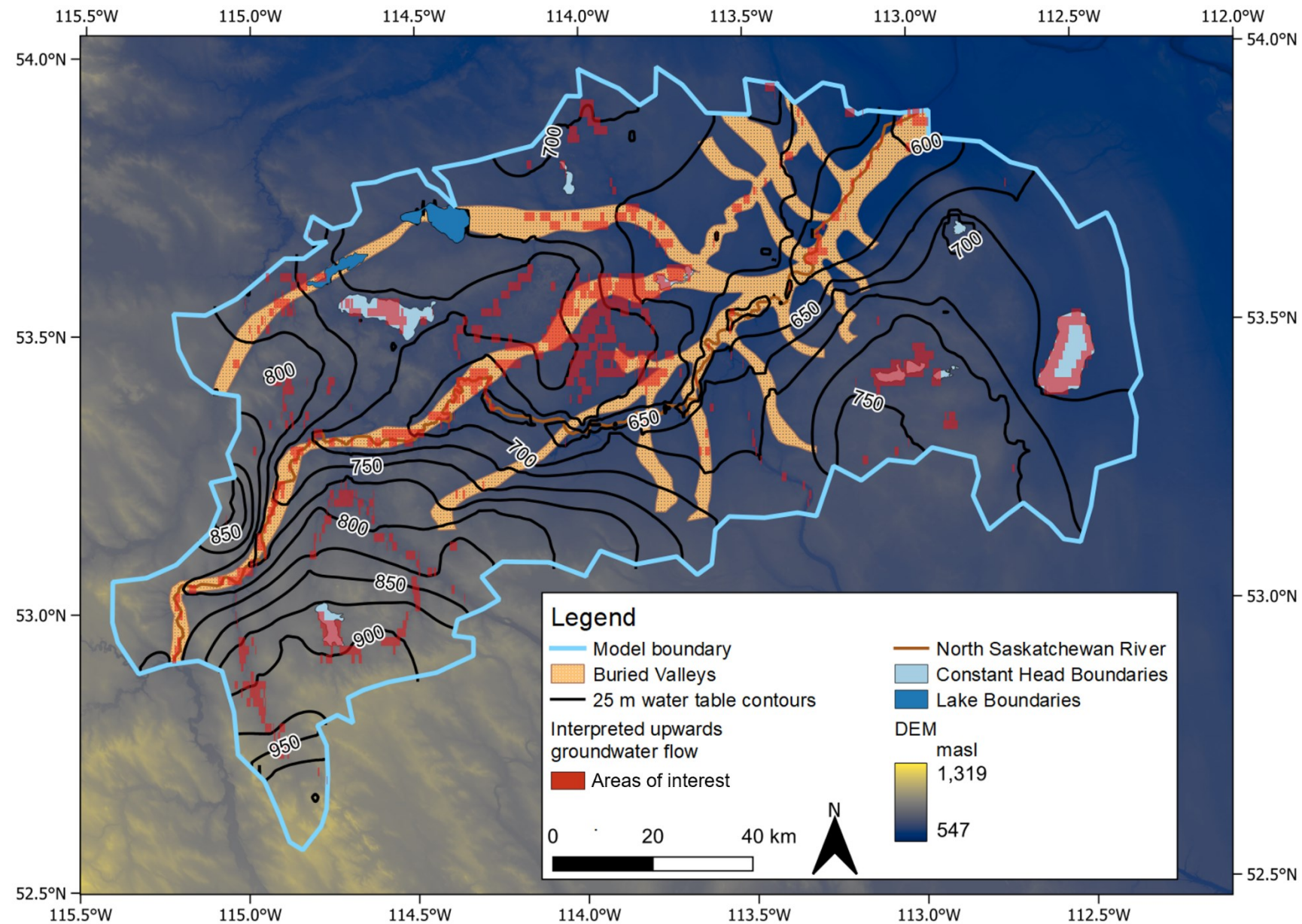


**Figure 2.21a.** Areas with a favourable head gradient for upwards groundwater flow.

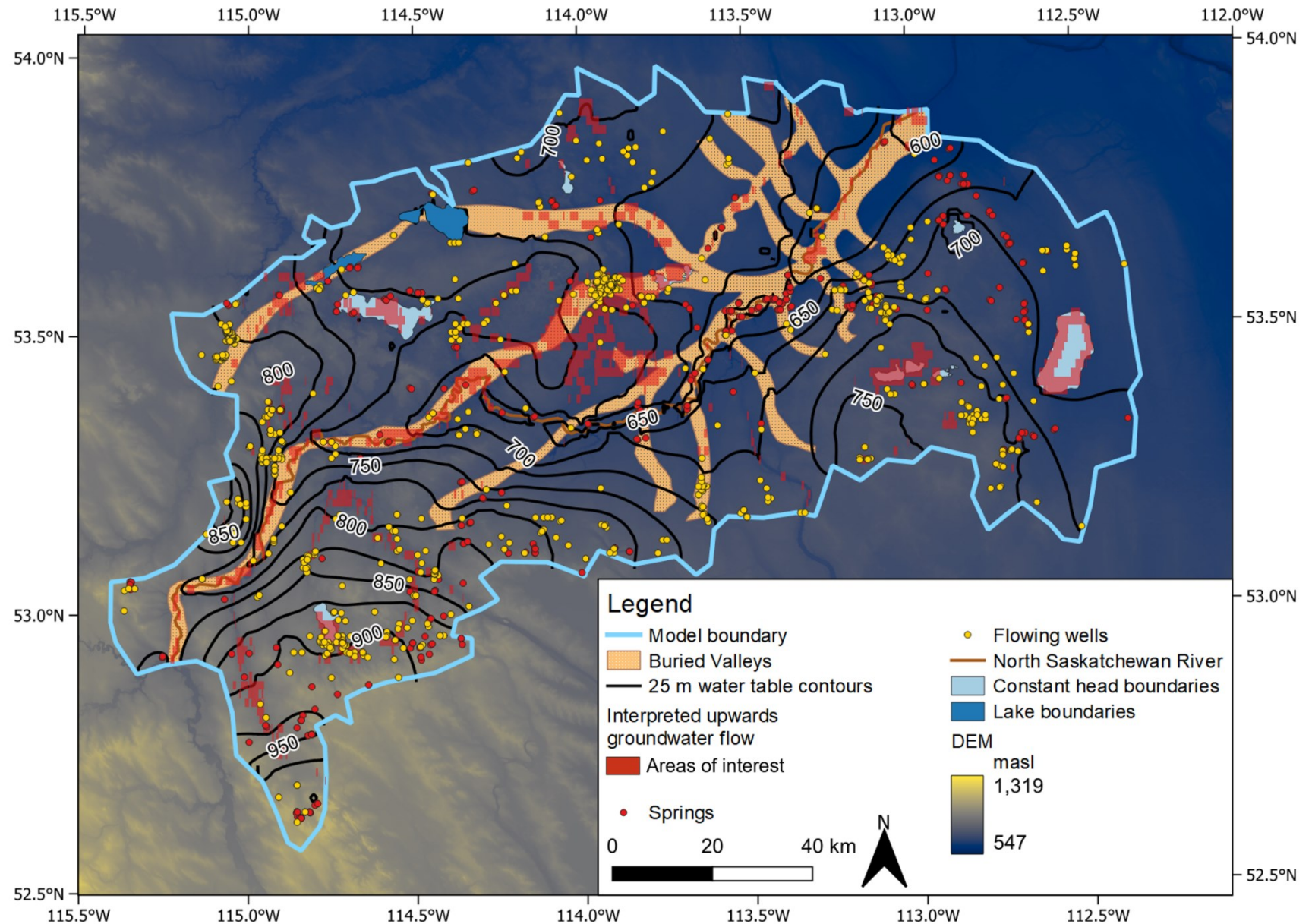


**Figure 2.21b.** Areas with a favourable head gradient for upwards groundwater flow with observed spring and flowing wells.

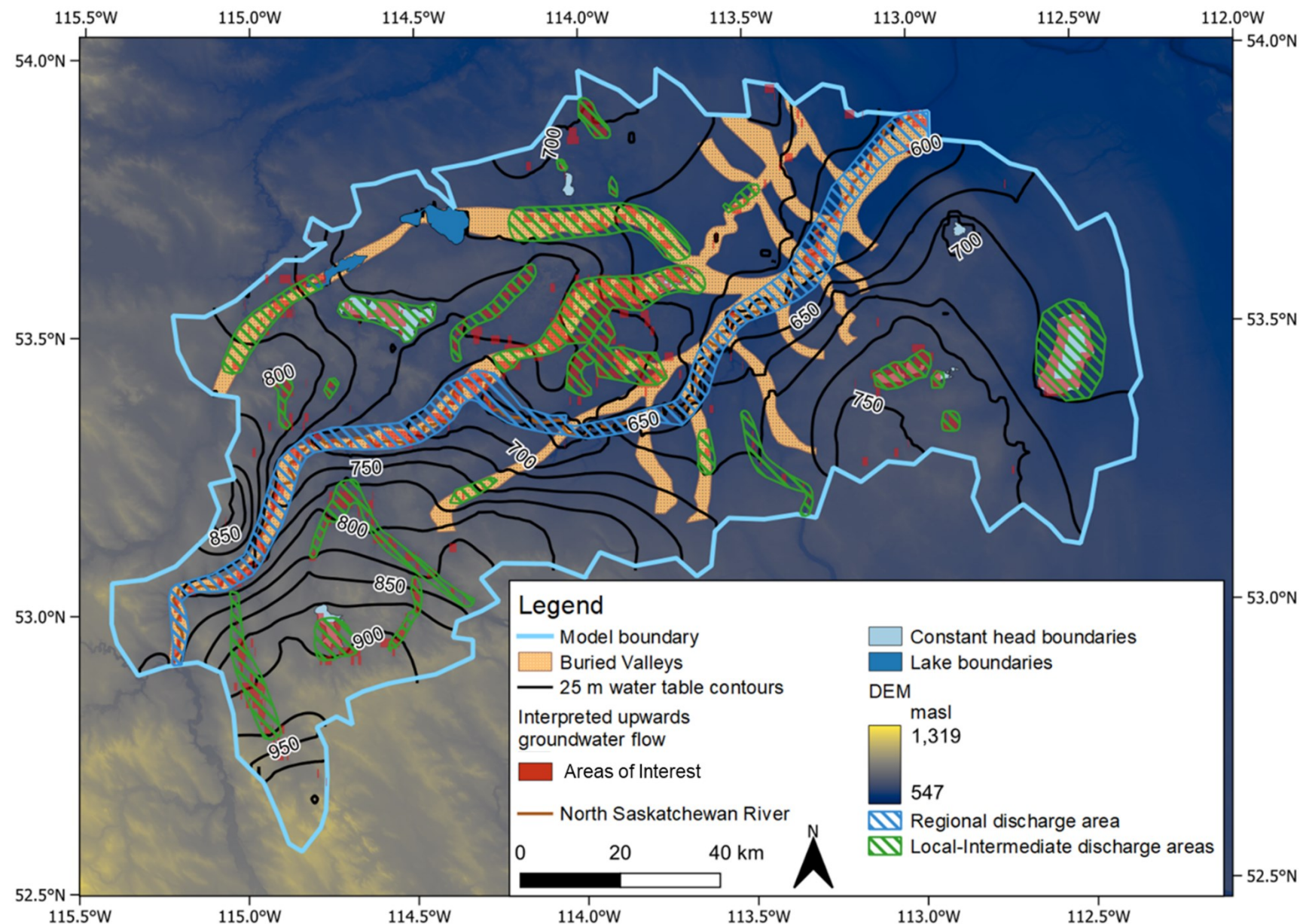


**Figure 2.21c.** Areas with a favourable head gradient for upwards GW with interpreted GW discharge areas.

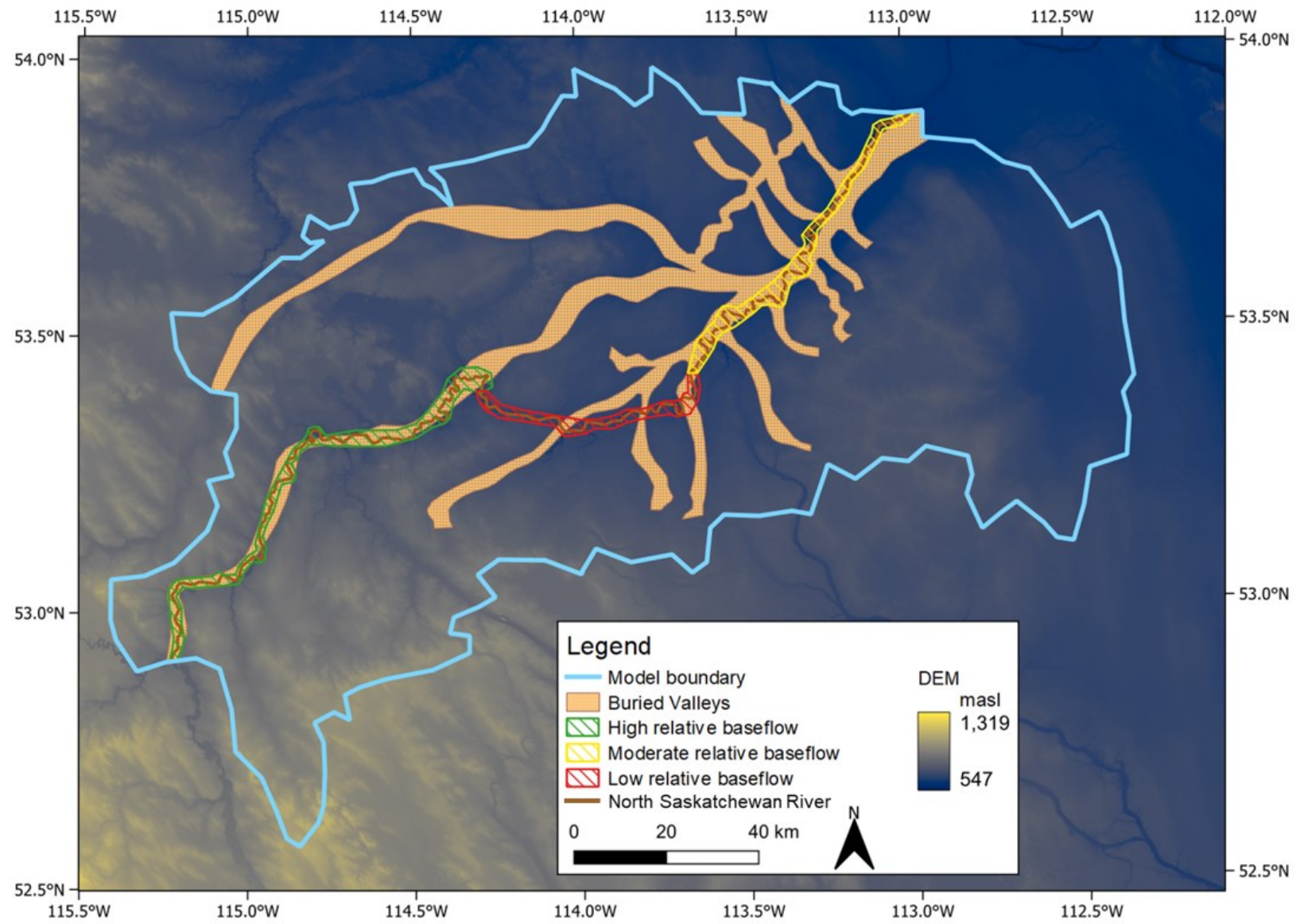


**Figure 2.21d.** Relative baseflow variation across the NSR.

## **2.7 Conclusions and recommendations**

Regional and local-intermediate groundwater flow patterns are observed in the model area. However, buried valleys function as an intersection between the two distinct categories of flow systems. Buried valleys appear to have groundwater flow directed towards them on local-intermediate scale, or in their vicinity. Yet, once groundwater resides in buried valleys, it will stay there until hydrogeologic conditions change along the flow path. Therefore, buried valleys act as a meso-scale conduit linking local-intermediate scale flow distances with regional flow distances.

Buried valleys may also impact GW-SW interactions through discharge areas. Buried valleys sediments frequently produce gradients that favour upwards flow from underlying sediments. These areas are commonly correlated with interpreted discharge areas, suggesting the presence of buried valleys influences the locations of discharge areas.

Both Lac Ste Anne and Isle Lake leak (lose) groundwater down into underlying buried valley deposits, while other lakes in the model appear to receive groundwater from below. This suggests buried valleys may play a role in creating losing lakes by providing a gradient favourable for drainage.

Buried valleys change the amount of baseflow along the length of the NSR in the study area. Where the river coincides with buried valleys in the southwestern and northeastern segments, baseflow is higher. When the river diverts from the buried valleys in the central portion, relatively little baseflow is observed. This suggests buried valleys may facilitate the increased relative quantity of baseflow where the NSR coincides with paleo-valleys.

### **Recommendations for future research**

Future work should focus on improved representation of buried valleys. In the model buried valleys are represented with two bulk K values, however, they can include significant heterogeneity. Heterogeneity may be present within and between channels. Heterogeneity within channels may be more suitably represented in a local-intermediate scale model, whereas heterogeneity between channels may be able to be included in a regional model if the differences in K were significant. Improved representation of buried valleys may also include enhanced vertical discretization to better represent the actual thickness of the buried valleys. However, this

has a downside in excess cells. The model grid design would most likely have to be reformulated to include less grid cells if this was attempted.

Additional rivers and lakes could be included in the model to better constrain water table elevations. Larger tributaries to the NSR would be the most logical place to start. For lakes, areas of interest might be area of the model lacking constant head boundaries. Still, it is not clear that this would significantly improve predictions.

In general, more data would be required to coincide with increased model discretization and finer scale representation of hydrogeological or hydraulic features. This may take the form of more pumping test data, borehole data, improved DEM data as well as ERT measurements. Pumping test data may be used to improve estimates of K or interpreted channel boundaries. Borehole data and ERT measurements may be used to better delineate channel extents, other hydrogeological unit boundaries, and heterogeneities within deposits. DEM data could be used to more closely represent the ground surface in areas of high topographic relief or buried valleys. Each of these data types in conjunction with one another may provide the necessary scale of data to justify a finer discretization scheme.

Despite these methods to improve the current model formulation, an alternate use of time might be to utilize a fully coupled GW-SW model. A similar conceptual model could be used but the surface processes may be simulated as well. This model may also require enhanced, finer scale data depending on the scale. In general, improved buried valleys representation may involve local-intermediate scale models while improvements to river and surface water could be implemented in the current groundwater model but may be better represented in a fully coupled GW-SW model. Another benefit may be the increased certainty in recharge and ET parameters. However, the increased certainty of a fully coupled model in simulating recharge and ET may be offset by a decreased certainty in other parameters used to simulate unsaturated soil moisture curves, which are largely unknown across the study area. Therefore, model type used is dependent on the problem the model is attempting to address.

## 2.8 References

- Alberta Environment and Parks. (2014). *HUC Watersheds of Alberta*. [Shapefile].
- Alberta Environment and Parks. (2017, March 1). *Alberta Provincial 25 Metre Raster*. [DEM].  
<https://open.alberta.ca/opendata/gda-c16469a2-5541-455c-bba0-63a24c0ff08a#summary>
- Anderson, M. P., Woessner, W. W., & Hunt, R. J. (2015). *Applied groundwater modeling: Simulation of flow and Advective Transport*. Elsevier, Academic Press.
- Andriashuk, D. L. (1988). *Quaternary Stratigraphy of the Edmonton Map Area, NTS 83H*. (Open File Report 198804). Edmonton, AB: Natural Resources Division, Alberta Research Council.
- Andriashuk, D. L. (2019). *Thalwegs of Bedrock Valleys, Alberta, Version 2 (GIS data, line features) Edition: v.2*. [Data file] Alberta Energy Regulator/Alberta Geological Survey. Retrieved from [http://ags.aer.ca/document/DIG/DIG\\_2018\\_0001.zip](http://ags.aer.ca/document/DIG/DIG_2018_0001.zip).
- Andriashuk, L. D., Fenton, M. M., Root, J. D. (1979). *Surficial Geology Wabamun Lake, Alberta (NTS 83G)*. (Map 149). Edmonton, AB: Alberta Geological Survey. Retrieved from <https://ags.aer.ca/publication/map-149>.
- Barnett, B., Townley, L. R., Post, V., Evans, R. E., Hunt, R. J., Peeters, L., Richardson, S., Werner, A. D., et al. (2012). (Waterlines Report Series 82.). *Australian groundwater modelling guidelines*. Canberra: National Water Commission.
- Barker, A.A., Riddell, J.T.F., Slattery, S.R., Andriashuk, L.D., Moktan, H., Wallace, S., Lyster, S., Jean, G., et al. (2011). *Edmonton-Calgary Corridor groundwater atlas* (ERCB/AGS Information Series 140, 98 p). Edmonton, AB: Energy Resources Conservation Board.
- Bayrock, L. A. (1972). *Surficial Geology Edmonton (83H)*. (Map 143). Edmonton, AB: Alberta Research Council.
- Bayrock, L.A. & Hughes, G.M. (1962). *Surficial geology of the Edmonton district, Alberta; Research Council of Alberta*. (RCA/AGS Earth Sciences Report 1962-06). Edmonton, AB, Alberta Research Council.

Bibby, R. (1974a). *Hydrogeology of the Edmonton area (northwest segment), Alberta*. (ARC/AGS Earth Sciences Report 1974-10). Edmonton, AB: Alberta Research Council.

Bibby, R. (1974b). *Hydrogeological map of the Edmonton area, northwest segment, Alberta, NTS 83H (part)*. (Map 108). Edmonton AB: Alberta Geological Survey.

Bibby, R. (1974c). *Regional chemistry and water level distribution of the near-surface groundwaters of the Edmonton area (northwest segment) Alberta*. (ARC/AGS Earth Sciences Report 1974-06). Edmonton AB, Alberta Research Council.

Brown, C. M., Evans, D. C., Ryan, M. J., & Russell, A. P. (2013). New data on the diversity and abundance of small-bodied ornithopods (Dinosauria, ornithischia) from the Belly River Group (campanian) of Alberta. *Journal of Vertebrate Paleontology*, 33(3), 495–520. <https://doi.org/10.1080/02724634.2013.746229>

Burns, E. R., Bentley, L. R., Hayashi, M., Grasby, S. E., Hamblin, A. P., Smith, D. G., & Wozniak, P. R. (2010). Hydrogeological implications of Paleo-fluvial architecture for the Paskapoo Formation, SW Alberta, Canada: A Stochastic analysis. *Hydrogeology Journal*, 18(6), 1375–1390. <https://doi.org/10.1007/s10040-010-0608-y>

Ceroici, W.J. (1979a). *Hydrogeology of the southwest segment, Edmonton, Alberta*. (ARC/AGS Earth Sciences Report 1978-05). Edmonton AB: Alberta Research Council.

Ceroici, W. J. (1979b). *Hydrogeological map of the Edmonton area (southwest segment), Alberta, NTS 83H (part)*. (Map 117). Edmonton AB: Alberta Geological Survey.

Chunn, D., Faramarzi, M., Smerdon, B., & Alessi, D. (2019). Application of an integrated SWAT-MODFLOW model to evaluate potential impacts of climate change and water withdrawals on groundwater–surface water interactions in west-central Alberta. *Water*, 11(1), 110. <https://doi.org/10.3390/w11010110>

Cummings, D. I., Russell, H. A., & Sharpe, D. R. (2012). *Buried valleys and till in the Canadian Prairies: Geology, hydrogeology, and origin*. (Current research - Geological Survey of Canada). Ottawa, ON: Natural Resources Canada.

Demchuk, T. D., & Hills, L. V. (1991). A Re-examination of the Paskapoo Formation in the Central Alberta Plains: The Designation of Three New Members. *Bulletin of Canadian Petroleum Geology*, 39(3), 270–282.

Enviroatlas. (n.d.). *Hydrologic Unit Codes: HUC 4, HUC 8, and HUC 12*. Washington, DC: United States Environmental Protection Agency. Retrieved from <https://enviroatlas.epa.gov/enviroatlas/datafactsheets/pdf/Supplemental/HUC.pdf>

Environment and Climate Change Canada. (2022, March 2). *Canadian Climate Normals 1981-2010 Station Data*. Retrieved from [https://www.climate.weather.gc.ca/climate\\_normals/results\\_1981\\_2010\\_e.html?stnID=2402&dispBack=0](https://www.climate.weather.gc.ca/climate_normals/results_1981_2010_e.html?stnID=2402&dispBack=0)

Feltham, K. (1993). Quaternary sediments in central Edmonton, Alberta, Canada: Stratigraphy, distribution and Geotechnical Implications. *Quaternary International*, 20, 13-26. doi:10.1016/1040-6182(93)90033-c

Fenton, M. M., Waters E. J., Pawley, S. M., Atkinson, N., Utting E. J., & Mckay, K. (2013). *Surficial Geology of Alberta, 1:1,000,000 scale (GIS data, polygon features)*. [Data File]. Alberta Geological Survey. Retrieved from [http://www.agi.gov.ab.ca/publications/DIG/ZIP/DIG\\_2013\\_0002.zip](http://www.agi.gov.ab.ca/publications/DIG/ZIP/DIG_2013_0002.zip)

Freeze, R. A., & Cherry, J. A. (1979). *Groundwater*. Prentice-Hall.

Freeze, R. A., & Witherspoon, P. A. (1967). Theoretical analysis of regional groundwater flow: 2. effect of water-table configuration and subsurface permeability variation. *Water Resources Research*, 3(2), 623–634. <https://doi.org/10.1029/wr003i002p00623>

Glombick, P. (2010). *Top of the Belly River Group in the Alberta Plains: Subsurface Stratigraphic Picks and Modelled Surface*. (ERCB/AGS Open File Report No. 2010-10). Edmonton, AB: Energy Resources Conservation Board, Alberta Geological Survey.

Godfrey, J. D. (2001). *Edmonton beneath our feet: A guide to the geology of the Edmonton Region*. Edmonton, AB: Edmonton Geological Society.

Government of Alberta. (n.d.a) *Alberta Water Well Information Database (or Baseline Water Well Test Database)*. [Database]. Retrieved from <http://groundwater.alberta.ca/WaterWells/d/>

Government of Alberta. (n.d.b). *Groundwater Observation Well Network*. [Database]. Retrieved April 5, 2021, from <https://www.alberta.ca/lookup/groundwater-observation-well-network.aspx>

Grasby, S. E., Chen, Z., Hamblin, A. P., Wozniak, P. R. J., & Sweet, A. R. (2008). Regional characterization of the Paskapoo Bedrock Aquifer System, Southern Alberta. Geological Survey of Canada Contribution 2008-0479. *Canadian Journal of Earth Sciences*, 45(12), 1501–1516. <https://doi.org/10.1139/e08-069>

Harbaugh, A. W. (2005). MODFLOW-2005, The U.S. Geological Survey Modular Ground-Water Model—the Ground-Water Flow Process. In *Modeling Techniques*. U.S. Geological Survey.

Harbaugh, A.W., Langevin, C.D., Hughes, J.D., Niswonger, R.N., and Konikow, L. F., (2017), MODFLOW-2005, the U.S. Geological Survey modular groundwater model: U.S. Geological Survey Software Release (Version 1.12.00) [Software]. U.S. Geological Survey. <http://dx.doi.org/10.5066/F7RF5S7G>

Hubbert, M. K. (1940). The theory of ground-water motion. *Transactions, American Geophysical Union*, 21(2), 648. <https://doi.org/10.1029/tr021i002p00648-1>

Hughes, A. T., Smerdon, B. D., & Alessi, D. S. (2017). Hydraulic properties of the Paskapoo Formation in west-central Alberta. *Canadian Journal of Earth Sciences*, 54(8), 883–892. <https://doi.org/10.1139/cjes-2016-0164>

Hydrogeological Consultants Ltd. (1998a). *County of Lamont No. 30 Part of the North Saskatchewan River Basin Parts of Tp 051 to 058, R 15 to 20, W4M Regional Groundwater Assessment*. (Report No. 97-100). Agriculture and Agri-Food Canada, Prairie Farm Rehabilitation.

Hydrogeological Consultants Ltd. (1998b). *Lac Ste. Anne County Parts of the North Saskatchewan and Athabasca River Basins Parts of Tp 053 to 059, R 01 to 09, W5M Regional*

*Groundwater Assessment*. (Report No. 97-112). Agriculture and Agri-Food Canada, Prairie Farm Rehabilitation.

Hydrogeological Consultants Ltd. (1998c). *Parkland County Part of the North Saskatchewan and Athabasca River Basins Parts of Tp 050 to 054, R 25, W4M to R 08, W5M Regional Groundwater Assessment*. (Report No. 97-202). Agriculture and Agri-Food Canada, Prairie Farm Rehabilitation.

Hydrogeological Consultants Ltd. (1999). *Leduc County Part of the North Saskatchewan River Basin Parts of Tp 047 to 051, R 21 to 28, W4M and R 01 to 04, W5M Regional Groundwater Assessment*. (Report No. 98-130). Agriculture and Agri-Food Canada, Prairie Farm Rehabilitation.

Hydrogeological Consultants Ltd. (2001). *Sturgeon County Part of the North Saskatchewan River Basin Parts of Tp 053 to 058, R 20 to 28, W4M & Tp 054 to 057, R 01, W5M Regional Groundwater Assessment*. (Report No. 01-100). Agriculture and Agri-Food Canada, Prairie Farm Rehabilitation.

Irish, E J W; Havard, C J. (1968). *Whitemud and Battle Formations, Kneehills Tuff Zone, a Stratigraphic Marker*. (Paper 67-63). Ottawa, ON: Geological Survey of Canada. <https://doi.org/10.4095/101442>

Kathol, C. P., & McPherson, R. A. (1975). *Urban geology of Edmonton*. (ARC/AGS Bulletin 32, 91 p). Edmonton, AB: Alberta Research Council.

Khidir, A., & Catuneanu, O. (2010). Reservoir characterization of scollard-age fluvial sandstones, Alberta Foredeep. *Marine and Petroleum Geology*, 27(9), 2037–2050. <https://doi.org/10.1016/j.marpetgeo.2010.05.001>

Klassen, J., Liggett, J.E., Pavlovskii, I. and Abdurakhimova, P. (2018). *First-order groundwater availability assessment for southern Alberta* (AER/AGS Open File Report No. 2018-09). Alberta Energy Regulator/Alberta Geological Survey.

Land Information Services Division. (1988). *Specifications and Procedures Manual*. Alberta Forestry, Lands, and Wildlife.

- MacCormack, K. E., Atkinson, N., & Lyster, S. (2015). *Bedrock Topography of Alberta* (Map 602). Edmonton, AB: Alberta Geological Survey.
- Mossop, G. D., Shetsen, I., Dawson, F. M., Evans, C. G., Marsh, R., Richardson, R., Power, B., Sweet, A. R., et al. (1994). Chapter 24 - Uppermost Cretaceous and Tertiary Strata of the Western Canada Sedimentary Basin. In *Geological atlas of the western canada sedimentary basin*. Calgary, AB: Canadian Society of Petroleum Geologists.
- Ozoray, G.F. (1972). *Hydrogeology of the Wabamun Lake area, Alberta* (RCA/AGS Earth Sciences Report 1972-08). Edmonton, AB, Research Council of Alberta.
- Pétré, M.-A., Rivera, A., & Lefebvre, R. (2015). Three-dimensional unified geological model of the Milk River Transboundary Aquifer (Alberta, Canada – Montana, USA). *Canadian Journal of Earth Sciences*, 52(2), 96–111. <https://doi.org/10.1139/cjes-2014-0079>
- Post, V. E., & von Asmuth, J. R. (2013). Review: Hydraulic head measurements—new technologies, Classic Pitfalls. *Hydrogeology Journal*, 21(4), 737–750. <https://doi.org/10.1007/s10040-013-0969-0>
- Prior, G. J., Hathway, B., Glombick, P. M., Pana D. I., Banks C. J., Hay, D. C., Schneider C. L., Grobe, M., et al. (2013). *Bedrock Geology of Alberta (GIS data, polygon features)*. [Data File]. Edmonton, AB: Alberta Geological Survey. Retrieved from [http://www.agc.gov.ab.ca/publications/DIG/ZIP/DIG\\_2013\\_0018.zip](http://www.agc.gov.ab.ca/publications/DIG/ZIP/DIG_2013_0018.zip)
- Research Council of Alberta (1978). *Edmonton Regional Utilities Study* (Vol. IV Groundwater). Edmonton, AB: Alberta Environment and RPA Consultant Limited.
- Riddell, J.T.F., Moktan, H. and Jean, G. (2014). *Regional hydrology of the Edmonton–Calgary Corridor, Alberta* (AER/AGS Open File Report No. 2014-02). Edmonton, AB: Alberta Energy Regulator. Retrieved from <https://ags.aer.ca/publication/ofr-2014-02>
- Rubin, A. D. (2022). *Pre-Laurentide and Deglacial History of the Edmonton Region, Alberta, Canada* (master's thesis). Edmonton, AB: University of Alberta.
- Seaber, R, P., Kapinos, F, P., & Knapp, L, G. (1987). *Hydrologic Unit Maps*. [Water-Supply Paper 2294]. U.S. Geological Survey. [https://pubs.usgs.gov/wsp/wsp2294/pdf/wsp\\_2294.pdf](https://pubs.usgs.gov/wsp/wsp2294/pdf/wsp_2294.pdf)

- Smerdon, B.D., Hughes, A.T. and Jean, G. (2017). Permeability measurements of Upper Cretaceous and Paleogene bedrock cores made from 2004-2015 (tabular data, tab-delimited format, to accompany Open File Report 2016-03) (AER/AGS Digital Data 2016-0042). Edmonton, AB: Alberta Energy Regulator.
- Stein, R. (1976a). *Hydrogeology of the Edmonton area, (northeast segment), Alberta* (ARC/AGS Earth Sciences Report 1976-01). Edmonton, AB, Alberta Energy and Utilities Board.
- Stein, R. (1976b). *Hydrogeological map of the Edmonton area (northeast segment), Alberta, NTS 83H* (Map 112). Edmonton, AB: Alberta Energy and Utilities Board.
- Stein, R. (1982). *Hydrogeology of the Edmonton area (southeast segment), Alberta* (ARC/AGS Earth Sciences Report 1979-06). Edmonton, AB, Alberta Research Council.
- Stein, R., Carlson, V. A., (1982). *Hydrogeological map of the Edmonton area (southeast segment), Alberta, NTS 83H* (Map 152). Edmonton, AB: Alberta Energy and Utilities Board.
- Tokarsky, O., (1971). *Hydrogeological map of the Rocky Mountain House area, Alberta, NTS 83B* (Map 099). Edmonton, AB: Alberta Geological Survey. Retrieved from <https://ags.ars.ca/publication/map-099>
- Tóth, J. (1962). A theory of groundwater motion in small drainage basins in central Alberta, Canada. *Journal of Geophysical Research*, 67(11), 4375–4388. <https://doi.org/10.1029/jz067i011p04375>
- Tóth, J. (1963). A theoretical analysis of groundwater flow in small drainage basins. *Journal of Geophysical Research*, 68(16), 4795–4812. <https://doi.org/10.1029/jz068i016p04795>
- Tóth, J. (1970). A conceptual model of the groundwater regime and the hydrogeologic environment. *Journal of Hydrology*, 10(2), 164–176. [https://doi.org/10.1016/0022-1694\(70\)90186-1](https://doi.org/10.1016/0022-1694(70)90186-1)
- Von Hauff, H. M. (2004). *Three-dimensional numerical modelling of the Wagner Natural Area Groundwater Flow System* (master's thesis). Edmonton, AB: University of Alberta.
- Winter, T. C. (1976). Numerical simulation analysis of the interaction of lakes and Ground Water. *Professional Paper*. <https://doi.org/10.3133/pp1001>

WorleyParsons. (2009). *North Saskatchewan River Basin Overview of Groundwater Conditions, Issues, and Challenges* (Report No. E00088100). Edmonton, AB, North Saskatchewan Watershed Alliance.

## **Chapter 3: Transient Model**

### **3.1 Introduction**

Water security, the access to an adequate quantity of water of an acceptable quality, faces a dual threat in populated regions of anthropogenic contamination and climate change. Ongoing contamination of water can be a byproduct of population centres and industry alike (Akhtar et al., 2021). Countries such as Canada, fare better than others as Canada has the second highest Environmental Protection Index (EPI) for water in the world (Environment and Climate Change Canada, 2017). Despite this, 18% of monitored water in Canadian rivers is rated marginal to poor quality due to contamination (Environment and Climate Change Canada, 2021). Climate change is expected to impact water resources around the world through changes in temperature, snow cover, and precipitation (European Environmental Agency, 2020). Within Canada, climate change is expected put strain on surface water resources in the prairies of Western Canada and Southeastern British Columbia as the frequency and duration of drought increases (Cathcart et al., 2008; Natural Resources Canada, 2020; Timoney & Lee, 2009). Alberta's water security is especially vulnerable due to its location in the prairies, where drought is expected to be worst, and its major industries of agriculture and oil and gas can lead to anthropogenic contamination (Natural Resources Canada, 2020). Runoff from agricultural production frequently seeps into rivers, providing a yearly contaminant flux occurring contemporaneously with the spring melting events (Kaushal et al., 2014). Meanwhile, oil and gas may generate contamination in the form of sudden catastrophic events such as from pipeline breaks and long-term releases from legacy sites (Timoney & Lee, 2009; Yang et al., 2020). This provides a dual threat from both climate change and contamination in Alberta.

In Alberta, the North Saskatchewan River (NSR) is a river of special concern. This is primarily due to its importance for the city of Edmonton, which relies on the NSR as its sole water source (Edmonton Power Corporation (EPCOR), 2020). Lack of alternative water supplies means that the city is vulnerable to water scarcity should the NSR be adversely impacted. Climate change is a possible scenario where drought may become more frequent, threatening surface water supplies (Environment Alberta, 2008; Natural Resources Canada, 2020). For the NSR, climate change is expected to yield an overall increase in flow due to earlier spring melt and runoff; however, lower

natural flows in the summer are also expected that could lead to prolonged drought (Anis & Sauchyn, 2021). Alternatively, a more sudden, short-term issue that could arise is contamination from upstream sources such as agriculture or oil and gas pipelines. For example, a sudden pipeline rupture in 2016, resulted in 90 m<sup>3</sup> of heavy crude spilling into the NSR (Yang et al., 2020). However, this was downstream (Saskatchewan) of city of Edmonton water intakes. Upstream contamination in a similar scenario could lead to reduction or cessation of water withdrawal from the NSR for an indefinite period. Whether from climate change or contamination, water supply from the NSR may be greatly reduced or even stopped completely, highlighting the fragility of water security and need for alternative water supplies.

Groundwater could be a more reliable water supply, or a reserve source because the risk from contamination or drought differs from surface water (U.S. Geological Survey, n.d.). Understanding groundwater resources in the Edmonton area is important should climatological or catastrophic disasters occur. In the Edmonton area, buried valley aquifers or buried channels (used interchangeably throughout this chapter) provide a source of groundwater (Research Council of Alberta, 1978). For a large city such as Edmonton, the proximity of the buried valleys coupled with their dimensions and sediment type make them a potential option for large scale water resource needs. Therefore, it is crucial to understand groundwater flow within and around buried valley aquifers should they become a target for large scale groundwater exploitation.

Buried valley aquifers can be hydrogeologically investigated through desktop investigations, field investigations, and groundwater modelling. Desktop analyses typically focus on examination of historical pumping records for wells completed in buried valley aquifers, or application of analytical solutions (Shaver & Pusc, 1992; van der Kamp & Maathuis, 2011). Meanwhile field investigations may involve pumping tests or geophysical investigations (Shaver & Pusc, 1992; Steelman et al., 2018). However, each of these methods often yield results at a local scale or in the case of geophysics a lack of information regarding extractable water. Conversely, groundwater modelling allows for the examination of regional scale trends where data may be sparse and field/geophysical investigation not feasible (Chapter 2; Melnik, 2018; Morgan et al., 2019; Sheets, 2007). In addition, groundwater modelling also allows for subsequent investigation of extractable water volumes (Melnik, 2018; Riddle, 2021), the focus of this chapter.

In chapter two a steady state model of the groundwater flow system was created and tested using MODFLOW-2005 (Harbaugh, 2005) for Edmonton and the surrounding area. The model spans a 15,967 km<sup>2</sup> area, contains 20 layers down to a depth of 500 m above sea level (masl), and includes buried valley extents previously mapped by Rubin (2022) (Figure 3.0). The model includes surficial geologic deposits and regional dipping bedrock geology (Figure 3.1; Figure 3.2; Figure 3.3). This model provided a regional representation of groundwater flow in the context of buried valleys to serve as a starting point for transient simulations.

The purpose of this chapter is to determine maximum achievable extraction rates from buried valley aquifers in the Edmonton area using transient simulations under idealized conditions. Several pumping scenarios were developed to provide a first order regional scale estimate of achievable water withdrawal rates for buried valleys aquifers in the Edmonton area. Unique patterns in maximum areal extent of the drawdown cone and maximum drawdown value were related to pumping time, initial conditions, saturated thickness, and overlying material. Hierarchization and potential factors driving differences between regional scale maximum water withdrawal rates in buried valleys in the Edmonton region are established.

## **3.2 Methods**

### **3.2.1 Model Area**

The model area includes the City of Edmonton (Figure 3.0) and was chosen using three criteria: Hydrologic Unit Code (HUC) watersheds (Alberta Environment and Parks, 2014), groundwater divides from regional analyses (Bibby, 1974b; Ceroici, 1979b; Stein, 1976b; Stein & Carlson, 1982; Tokarsky, 1971), and the extent of buried valleys mapped by Rubin (2022). HUC watersheds were chosen as a starting point for the model boundary as these provided a basis to capture surface water extents. However, it should be noted that HUC watersheds do not always align with groundwater flow boundaries (Enviroatlas, n.d.; Seaber et al., 1987). Therefore, the model boundary was verified to confirm that it largely aligned with groundwater divides which justified no-flow conditions at the model boundary. This is explained in more detail in chapter 2 of this thesis. Lastly, the model area was chosen to be large enough to include newly mapped buried valley extents by Rubin (2022) since the buried valleys are the focus on this study.

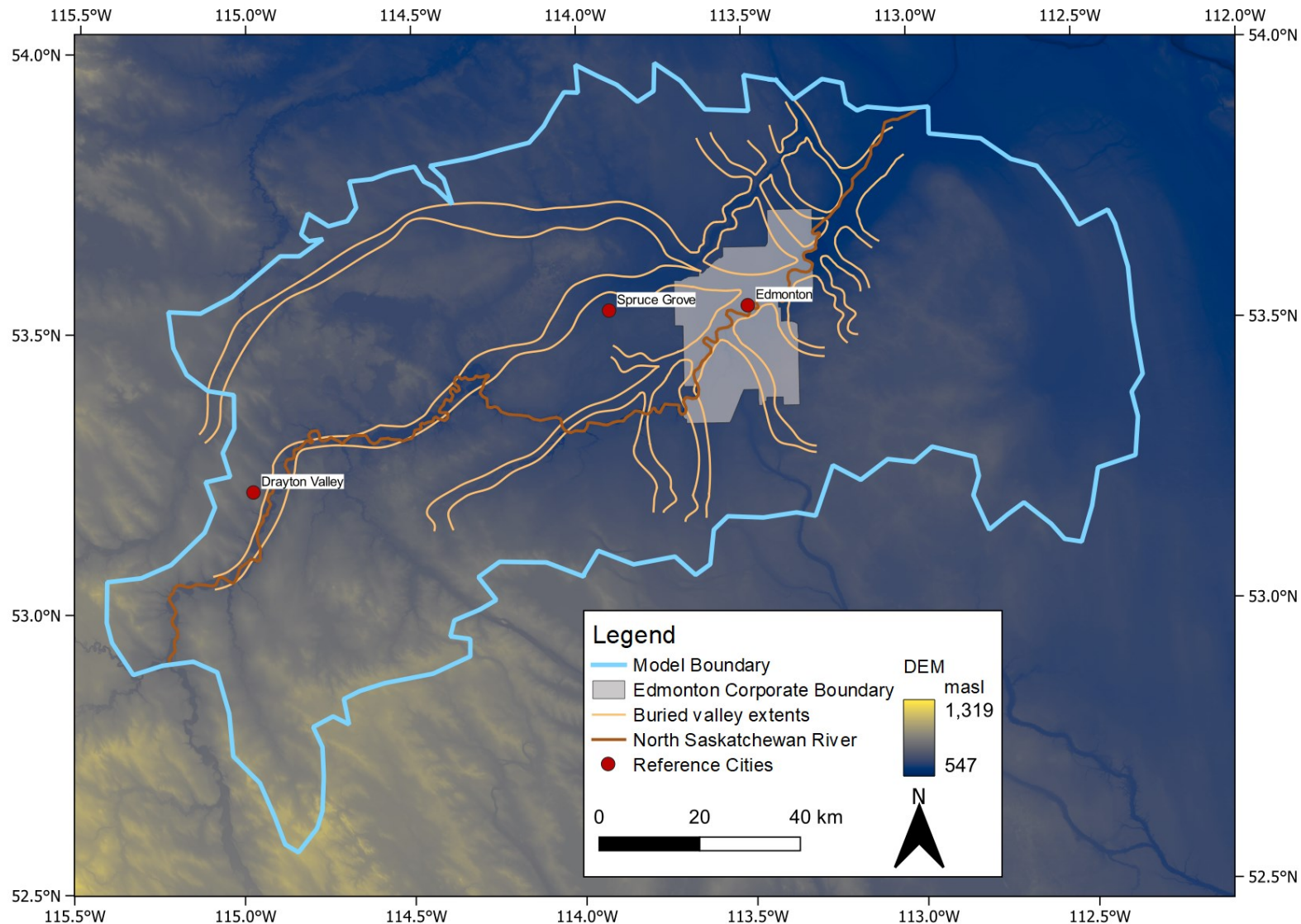


**Figure 3.0.** Study area map with reference cities and digital elevation model (DEM) (Alberta Environment and Parks, 2017). Buried valley extents from Rubin (2022).

### **3.2.2 Geology**

Geology within the study area can be divided into bedrock and surficial deposits. Bedrock deposits are represented in layers 5-20 in the model and include the Belly River Group, the Bearpaw Formation, the Edmonton Group, the Scollard Formation, and the Paskapoo Formation (Figure 3.1; Table 3.0). Surficial deposits represented are in layers 1-4 in the model include the Empress formation (buried valleys) (only represented in layers 3-4), glaciolacustrine sediments, glacial moraine, pitted deltas, sand dunes, and recent alluvial/colluvial deposits (Figure 3.2; Figure 3.3; Table 3.0). Since buried valleys are the primarily focus on this chapter, only their geology is summarized in detail below. More detailed geological background can be found for all (other) geological units in chapter 2.

Buried valleys or channels were first recognized in the late 19<sup>th</sup> century; since then, much work has been done to understand their origin and delineate their boundaries (McConnell, 1885; Tyrrell, 1887). These preglacial channels are the remnants of elaborate Quaternary River systems originating from the Rocky Mountains to the west and extending east across much of Alberta (Andriashuk, 2019; Cummings, et al., 2012). They are often incised into the bedrock and composed of characteristic quartzite sands and gravels colloquially referred to as the “Saskatchewan sands and gravels” (Cummings, et al., 2012). Subsequent glacial advance and retreat has covered these ancient river systems with metres to 10s of metres of glacial deposits, usually in the form of low permeability diamicton (Cummings, et al., 2012). Single channels can be hundreds of kilometres (km) in length, kilometres wide, and may contain up to 75 metres (m) of high hydraulic conductivity (K) sand and gravel sediments (Andriashuk, 2019; Cummings, et al., 2012; Rubin, 2022). For the central Alberta area, several major SW-NE trending buried valley systems converge in the Edmonton region (Andriashuk, 2019; Rubin, 2022). Major buried valleys of interest in the region include the Onoway, Beverly, and Drayton valleys (Andriashuk, 2019; Rubin, 2022). These are often connected to smaller tributary valleys such as the Sturgeon, Stony, and Warburg among others (Andriashuk, 2019; Rubin, 2022).

### **3.2.3 Hydrogeology**

Hydrostratigraphy and material properties are represented in Table 3.0 and Table 3.1. Table 3.0 shows bulk K values for each hydrostratigraphic unit. Likewise, each hydrostratigraphic unit has

unique storage values utilized in transient simulations (Table 3.1). Further background information for hydrostratigraphy and material properties is described in chapter 2.

Groundwater flow in bedrock and surficial deposits in the study area are both driven by topography and influenced by geology (Bibby, 1974a; Ceroici, 1979a; Stein, 1976a; Stein, 1982, WorleyParsons, 2009). In either deposit, the regional groundwater flow direction is towards the NSR as the NSR occupies a regional topographic low in the landscape (Bibby, 1974a; Ceroici, 1979a; Stein, 1976a; Stein, 1982, WorleyParsons, 2009). In addition to this, local-intermediate flow systems are superimposed on the regional flow path according to local-intermediate topographic variations (Bibby, 1974a; Ceroici, 1979a; Stein, 1976a; Stein, 1982). This produces topography driven nested flow systems across the study area.

Geology modifies flow paths induced by topography. In bedrock deposits, geological variation often has a noticeable role on groundwater flow in localized small scale studies (Bibby, 1974a; Ceroici, 1979a; Stein, 1976a; Stein, 1982). However, it does not have a noticeable impact on groundwater flow directions at a regional level (scale of the model) (Bibby, 1974a; Ceroici, 1979a; Stein, 1976a; Stein, 1982). Conversely, in surficial deposits, geology has a clear impact on groundwater flow directions at a regional scale. Specifically, buried valleys cause groundwater to flow into them from surrounding surficial and bedrock deposits due to their high K sand and gravel composition (Bibby, 1974a; Ceroici, 1979a; Research Council of Alberta, 1978; Stein, 1976a; Stein, 1982). Due to this, the buried valley aquifers provide regional pathways for intermediate-regional scale groundwater flow (Chapter 2). Further detail and hydrogeological background is provided in chapter 2.

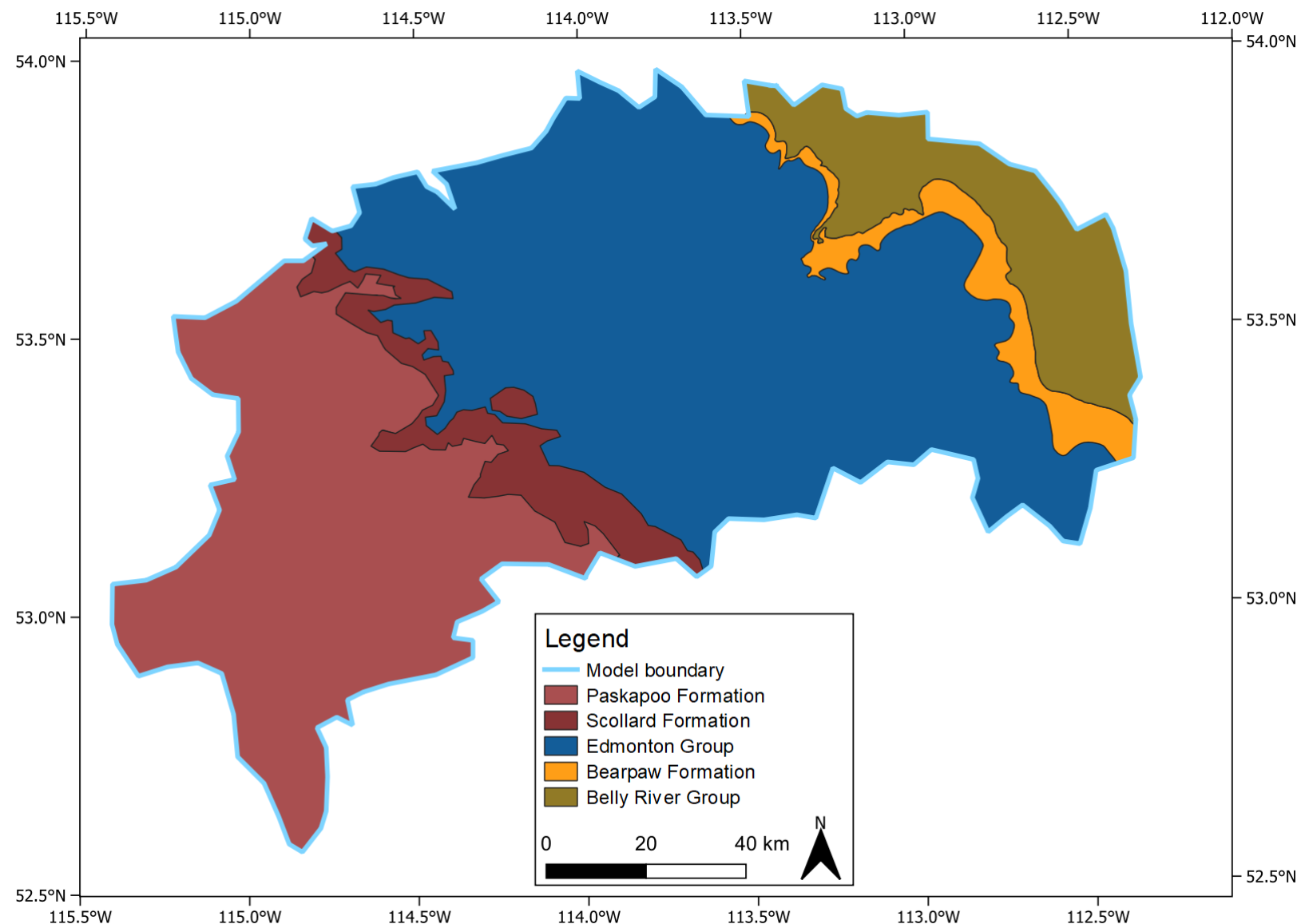


**Figure 3.1.** Bedrock geology in layers 5 to 20 of model, modified from Prior et al. (2013).

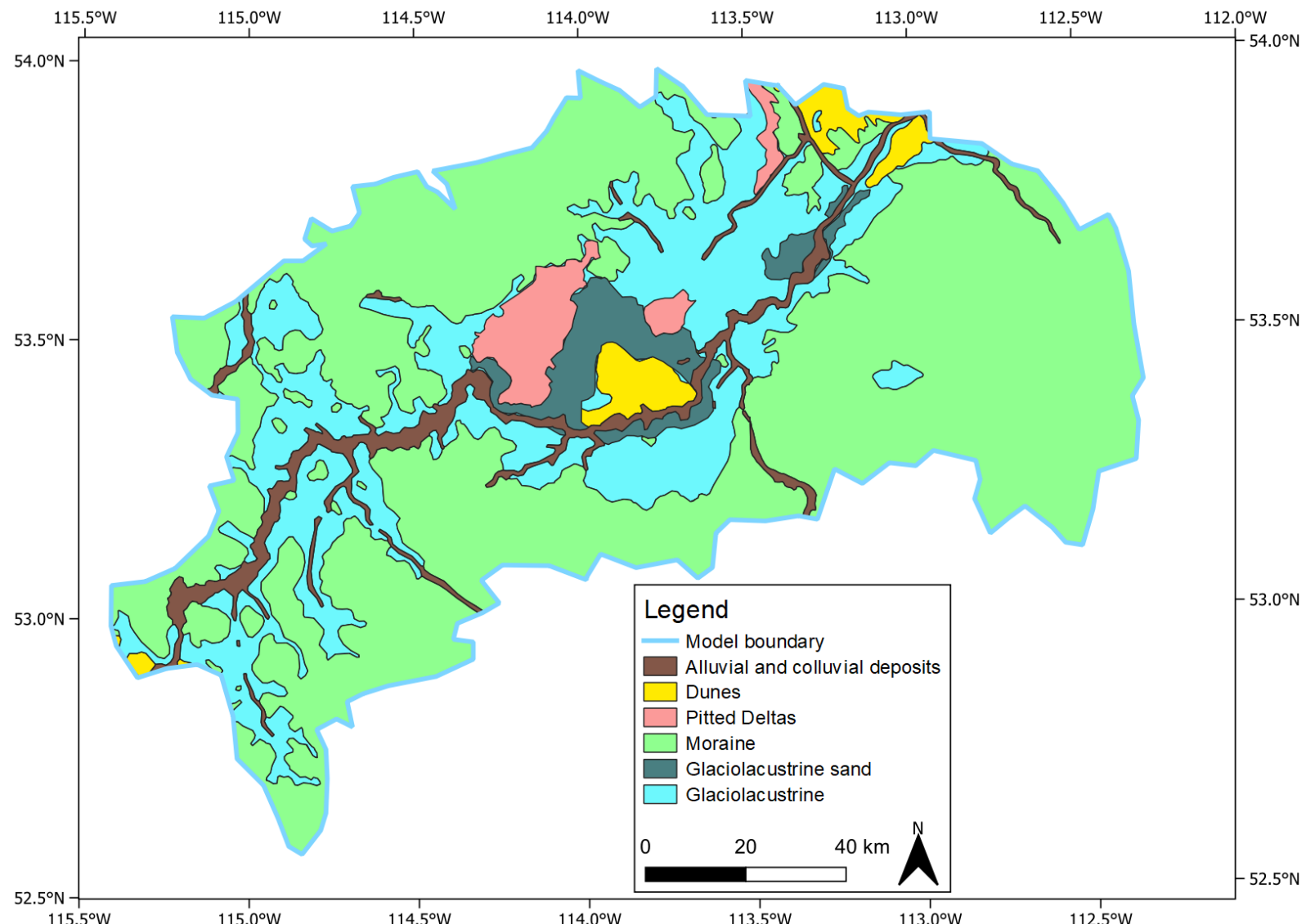


**Figure 3.2.** Surficial geology in layers 1 and 2 of model, modified from Andriashuk et al., (1979), Bayrock (1972), and Fenton et al. (2013).

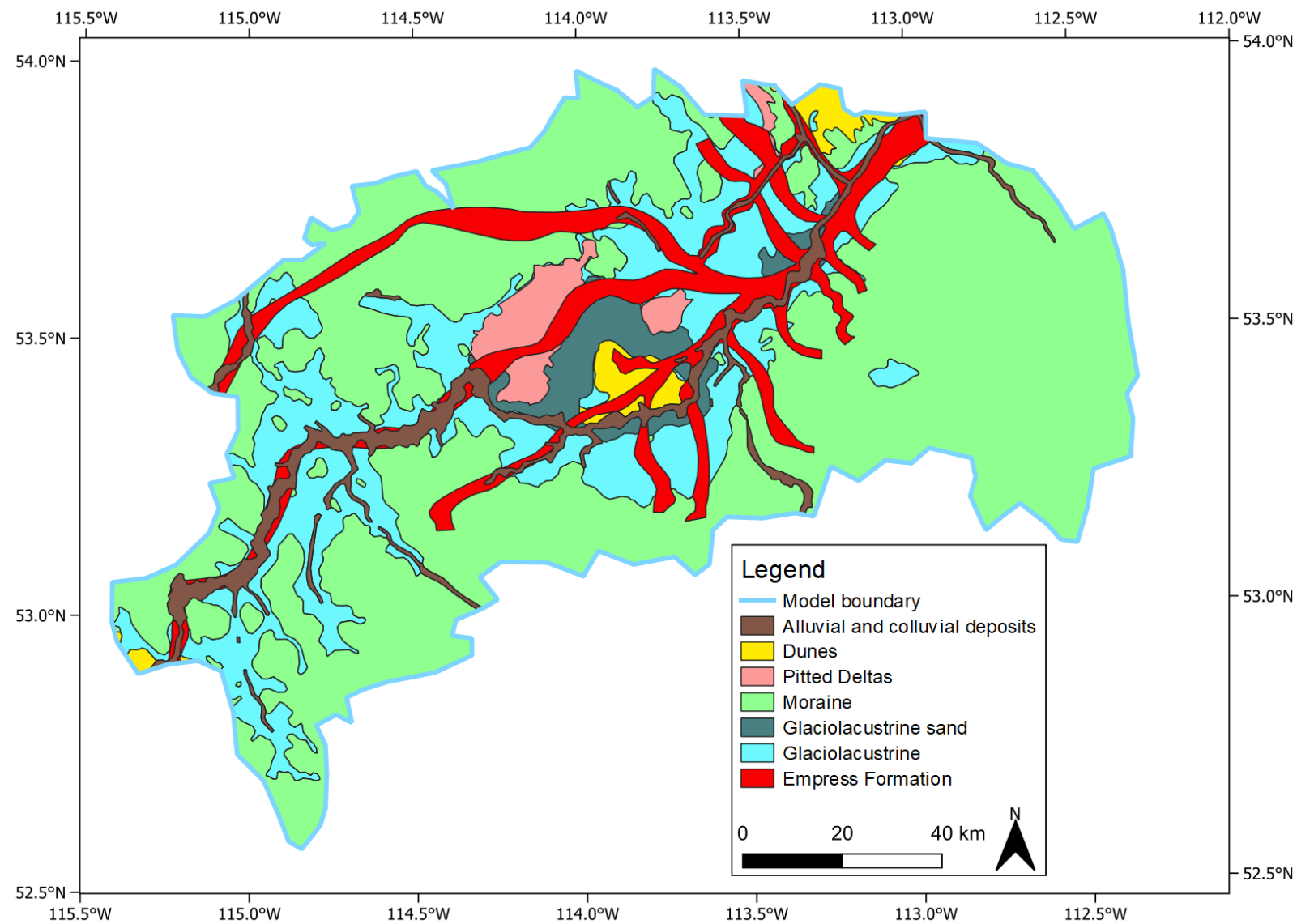


**Figure 3.3.** Surficial geology in layers 3 and 4 of model, modified from Andriashek et al., (1979), Bayrock (1972), Fenton et al. (2013), and Rubin (2022).

Era	Period	Epoch	Hydrostratigraphic Unit	Layer (s)	Model Value	Literature Values	Source(s)
Cenozoic	Quaternary	Holocene	Alluvial/Colluvial	1 – 4	$K_{xy} = 7.4 \times 10^{-5}$ m/s; $K_z = 7.4 \times 10^{-6}$ m/s	Gravel - $10^{-2}$ m/s; Silt/Clay – $10^{-8}$ m/s	Kathol & McPherson, 1975
			Sand Dunes	1 – 4	$K_{xy} = 1.1 \times 10^{-4}$ m/s; $K_z = 1.2 \times 10^{-5}$ m/s	$10^{-4}$ m/s to $10^{-3}$ m/s	Kathol & McPherson, 1975
		Pleistocene	Glaciolacustrine	1 – 4	Silt/clay - $K_{xy} = 10^{-5}$ m/s; $K_z = 10^{-6}$ m/s; Sand – $k_{yz} = 2.3 \times 10^{-5}$ m/s	< $10^{-5}$ m/s	Kathol & McPherson, 1975
			Pitted Delta	1 – 4	$K_{xyz} = 3.5 \times 10^{-5}$ m/s	$10^{-4}$ m/s to $10^{-2}$ m/s	Kathol & McPherson, 1975
			Moraine	1 – 4	$K_{xy} = 5.8 \times 10^{-6}$ m/s; $K_z = 5.8 \times 10^{-7}$ m/s	< $10^{-5}$ m/s	Kathol & McPherson, 1975
			Empress Formation	3 – 4	Layer 3 - $K_{xy} = 1.1 \times 10^{-4}$ m/s; $K_z = 1.2 \times 10^{-5}$ m/s Layer 4 - $k_{xy} = 5.8 \times 10^{-4}$ m/s; $K_z = 5.8 \times 10^{-5}$ m/s	$10^{-4}$ m/s to $10^{-2}$ m/s	Kathol & McPherson, 1975
	Paleogene	Paleocene	Paskapoo Formation	5 - 20	$K_{xy} = 10^{-6}$ m/s; $K_z = 10^{-7}$ m/s	Siltstone/Mudstone - $10^{-10}$ m/s to $10^{-8}$ m/s; Sandstone – $2.5 \times 10^{-6}$ m/s to $10^{-3}$ m/s	Hughes et al., 2017
	Mesozoic		Scollard Formation	5 - 20	$K_{xy} = 10^{-7}$ m/s; $K_z = 10^{-8}$ m/s	$9.3 \times 10^{-10}$ m/s to $3.5 \times 10^{-6}$ m/s	Smerdon et al., 2017
			Edmonton Group	5 - 20	$K_{xy} = 10^{-8}$ m/s; $K_z = 10^{-9}$ m/s	$4.4 \times 10^{-10}$ m/s to $3.6 \times 10^{-6}$ m/s	Smerdon et al., 2017
			Bearpaw Formation	5 - 20	$K_{xy} = 10^{-9}$ m/s; $K_z = 10^{-10}$ m/s	$1 \times 10^{-11}$ m/s to $1 \times 10^{-14}$ m/s	Pétré et al., 2015
			Belly River Group	5 - 20	$K_{xy} = 10^{-7}$ m/s; $K_z = 10^{-8}$ m/s	$2.9 \times 10^{-8}$ m/s to $5.8 \times 10^{-6}$ m/s	Pétré et al., 2015; Stein, 1976b

**Table 3.0.** Hydraulic conductivity model values compared literature reported values.

Era	Period	Epoch	Hydrostratigraphic Unit	Layer (s)	Model Value	Literature Values	Source(s)
Cenozoic	Quaternary	Holocene	Alluvial/Colluvial	1 – 4	Ss = $3.6 \times 10^{-5} \text{ m}^{-1}$ Sy = 0.16	Ss = $5.0 \times 10^{-5} \text{ m}^{-1} – 1.0 \times 10^{-4} \text{ m}^{-1}$ Sy = 0.19-.33	Domenico & Mifflin, 1965; Heath, 1983; Morris & Johnson, 1967
			Sand Dunes	1 – 4	Ss = $1.7 \times 10^{-4} \text{ m}^{-1}$ Sy = 0.28	Ss = $5.0 \times 10^{-5} \text{ m}^{-1} – 1.0 \times 10^{-4} \text{ m}^{-1}$ Sy = 0.22-.33	Domenico & Mifflin, 1965; Heath, 1983; Morris & Johnson, 1967
		Pleistocene	Glaciolacustrine	1 – 4	Silt/clay - Ss = $2.4 \times 10^{-2} \text{ m}^{-1}$ ; Sy = 0.18 Sand - Ss = $2.4 \times 10^{-2} \text{ m}^{-1}$ ; Sy = 0.20	Ss = $1.3 \times 10^{-3} \text{ m}^{-1} – 2.4 \times 10^{-2} \text{ m}^{-1}$ Sy = 0.06-.33	Domenico & Mifflin, 1965; Grisak & Cherry, 1975; Heath, 1983; Morris & Johnson, 1967
			Pitted Delta	1 – 4	Ss = $1.7 \times 10^{-4} \text{ m}^{-1}$ Sy = 0.28	Ss = $5.0 \times 10^{-5} \text{ m}^{-1} – 1.0 \times 10^{-4} \text{ m}^{-1}$ Sy = 0.19-.33	Domenico & Mifflin, 1965; Heath, 1983; Morris & Johnson, 1967
			Moraine	1 – 4	Ss = $1.0 \times 10^{-2} \text{ m}^{-1}$ Sy = 0.15	Ss = $2.0 \times 10^{-3} \text{ m}^{-1} – 1.9 \times 10^{-2} \text{ m}^{-1}$ Sy = 0.06-.33	Grisak & Cherry, 1975; Heath, 1983; Morris & Johnson, 1967
			Empress Formation	3 – 4	Ss = $7.5 \times 10^{-5} \text{ m}^{-1}$ Sy = 0.22	Ss = $5.0 \times 10^{-5} \text{ m}^{-1} – 1.0 \times 10^{-4} \text{ m}^{-1}$ Sy = 0.19-.33	Domenico & Mifflin, 1965; Heath, 1983; Morris & Johnson, 1967; Smerdon et al., 2005
	Paleogene	Paleocene	Paskapoo Formation	5 - 20	Ss = $3.6 \times 10^{-5} \text{ m}^{-1}$ Sy = 0.16	Ss = $8.3 \times 10^{-7} \text{ m}^{-1} – 1.7 \times 10^{-5} \text{ m}^{-1}$ Sy = 0.06-.33	Augustine, 2015; Heath, 1983; Morris & Johnson, 1967
Mesozoic	Cretaceous		Scollard Formation	5 - 20	Ss = $3.6 \times 10^{-5} \text{ m}^{-1}$ Sy = 0.16	Ss = $<1.0 \times 10^{-6} \text{ m}^{-1} – 2.1 \times 10^{-5} \text{ m}^{-1}$ ; Sy = 0.06-.33	Domenico & Mifflin, 1965; Heath, 1983; Morris & Johnson, 1967
			Edmonton Group	5 - 20	Ss = $2.75 \times 10^{-6} \text{ m}^{-1}$ Sy = 0.15	Ss = $<1.0 \times 10^{-6} \text{ m}^{-1} – 2.1 \times 10^{-5} \text{ m}^{-1}$ ; Sy = 0.06-.33	Domenico & Mifflin, 1965; Heath, 1983; Morris & Johnson, 1967
		Bearpaw Formation		5 - 20	Ss = $3.3 \times 10^{-6} \text{ m}^{-1}$ Sy = 0.12	Ss = $<1.0 \times 10^{-6} \text{ m}^{-1} – 2.1 \times 10^{-5} \text{ m}^{-1}$ ; Sy = 0.06-.12	Domenico & Mifflin, 1965; Heath, 1983; Morris & Johnson, 1967
		Belly River Group		5 - 20	Ss = $3.6 \times 10^{-5} \text{ m}^{-1}$ Sy = 0.16	Ss = $<1.0 \times 10^{-6} \text{ m}^{-1} – 2.1 \times 10^{-5} \text{ m}^{-1}$ ; Sy = 0.06-.33	Domenico & Mifflin, 1965; Heath, 1983; Morris & Johnson, 1967

**Table 3.1.** Storage parameters compared literature reported values.

### **3.2.4 Numerical model Set-Up**

For the model area (Figure 3.0), steady state groundwater conditions were simulated as the initial condition for the transient simulations that evaluated pumping scenarios. The model utilized a finite-difference discretization scheme with grid spacing at 100 m in the horizontal (x-y) dimensions and variable grid thickness in the vertical (z) dimension (Chapter 2).

A total of 20 model layers were utilized, 4 layers for surficial geology, and 16 layers for dipping bedrock geology (Chapter 2). Surficial geology represented in the model is shown in Figures 3 and 4. Bedrock geology represented in the model is shown in Figure 3.1. The model parameterization, including literature values for reference, can be found in Table 3.0, with Table 3.1 showing storage parameters for the transient model.

Calibration data for steady state were derived from the Alberta Water Well Database (AWWID) and the Groundwater Observation Well Network (GOWN) (Government of Alberta, n.d.a; Government of Alberta, n.d.b.). A trial-and-error calibration approach was followed to slightly adjust some of the model parameters (hydraulic conductivity, recharge, and ET) to match simulated hydraulic heads with observed hydraulic head values measured at groundwater wells in the study area (Chapter 2). The final calibration chart is shown Figure 3.4; an RMSE of 14.59 m was achieved which yielded a nRMSE of 3.1%. When considering the inherent error in the calibration data set and in the DEM at 5-8 m (Alberta Environment and Parks, 2017), a RMSE of 14.59 m was considered reasonable as the DEM could account for half of the model error in some cases (Chapter 2). Additionally, an nRMSE of 3.1% aligns with other published models/modelling guidelines for the regional scale model as an initial condition for transient simulation (Barnett et al., 2012; Melnik, 2018).

### **Boundary Conditions**

Boundary conditions consisted of no-flow, specified flux, river, lake, and constant head boundaries, with additional well boundaries for transient simulations. No-flow boundaries are applied along the model boundary to coincide with groundwater divides (section 3.2.1), and the bottom of the model (chapter 2). As in section 3.2.1, this was mostly based on published or inferred groundwater divides. Across the top of the model, specified flux boundaries are applied as recharge and evapotranspiration (ET) (chapter 2).

Recharge values in published works varied significantly from <100mm/year to over 200 mm/year for Riddell et al., (2014) and ~6 – 35 mm/year for Klassen et al., (2018). Therefore, values were adjusted in the steady state model calibration phase while conforming to previous studies (Klassen et al., 2018; Riddell et al., 2014). Actual ET values also followed published spatial distributions with literature values ranging from 320 – 360 mm/year (Riddell et al., 2014). However, model values used were significantly lower at ~117 – 128 mm/year (Riddell et al., 2014) because the recharge values already partially account for ET (chapter 2). Moreover, ET was only active at topographic lows based on shallow water table depth (<1 m) rather than across the entire model.

A river boundary was utilized to represent the NSR across the model area based on segments and linear topographic gradient. River boundaries in MODFLOW-2005 are defined by a constant head and a riverbed K term that allow for the computation of conductance between the river system and the groundwater system (Harbaugh, 2005).

Additionally, eight lakes are represented as constant head boundaries and another 2 lakes as lake boundaries (chapter 2). Lake boundaries were chosen at two locations due to their position above the channel and the need for more pronounced vertical hydraulic head gradient at these locations (chapter 2).

Wells were represented as analytical elements and added along buried valley thalwegs, screened across the thickness of buried valleys sediments in layers 3 and 4. This was done for three buried valleys, the Onoway, the Beverly, and the Stony, to examine different pumping locations. Pumping was completed using several rates and time periods (detailed in subsequent section) with time divided into five equal timesteps in each case.

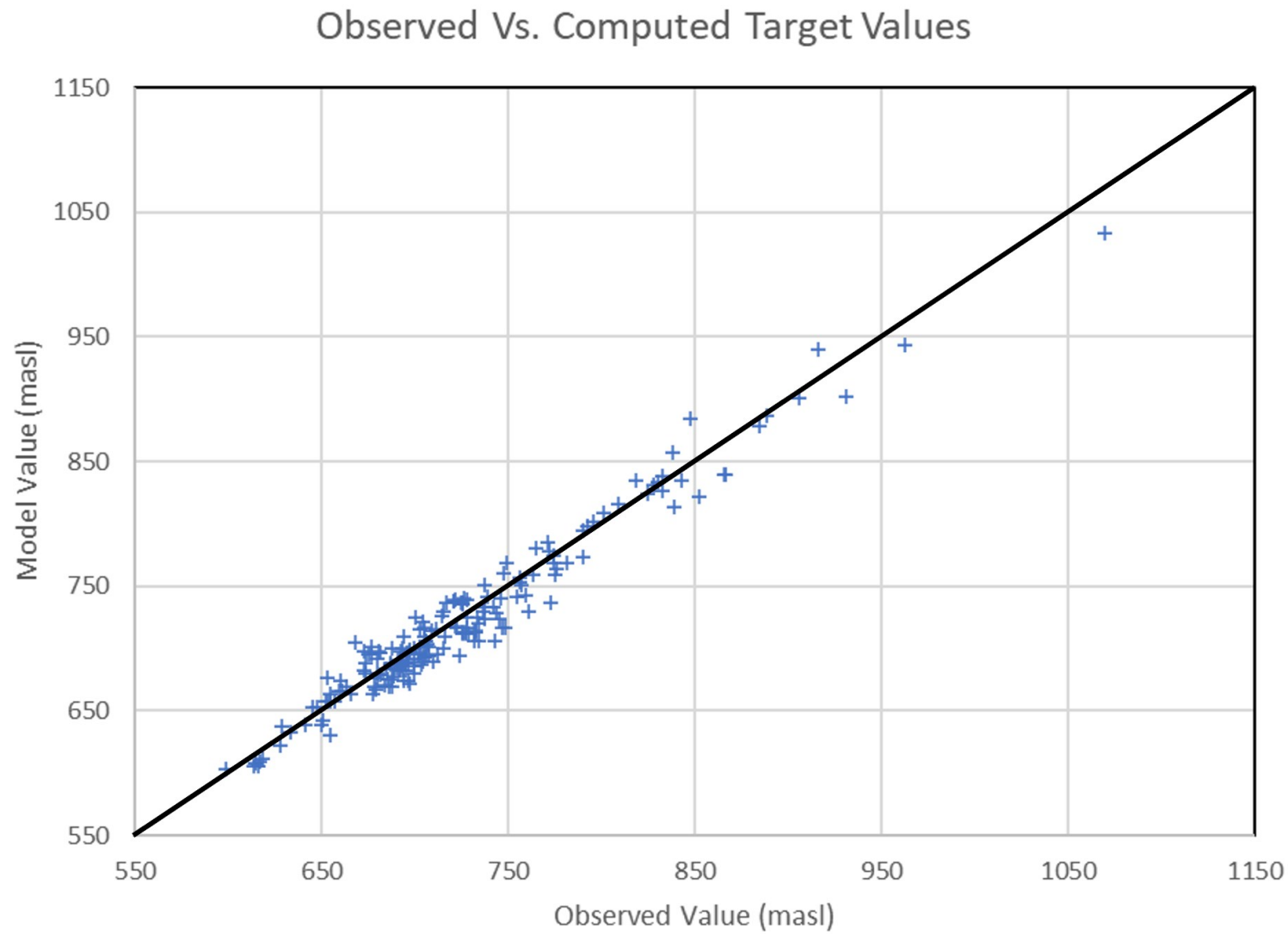


**Figure 3.4.** Calibration chart for steady state model with 1:1 line in black.

### **3.2.5 Pumping Scenarios**

Transient simulations were completed to investigate the response of hydraulic heads to pumping scenarios. Other transient processes such as time-varying river and lake levels or groundwater recharge were not considered to constrain/isolate the response of pumping, which would cause significant changes in hydraulic head compared to other time-varying drivers. Seasonal variations in water level could not be represented in the accurately and were not included in the model conceptualization (Chapter 2). Pumping rates and durations required by the city of Edmonton were made in consultation with EPCOR Utilities, Inc., the main water provider (H. Zarski, personal communication, March 25<sup>th</sup>, 2022).

Three pumping rates were defined: 375ML/day, 190ML/day, and 10ML/day. Current daily demand is 375 ML/d, which is the ideal volume of water for EPCOR as it would result in no changes to service. A pumping rate of 190 ML/d is the next target water extraction rate and would provide a water source in a force majeure emergency such as widespread river contamination. However, at the 190ML/day rate, service would be reduced to approximately half capacity to residential customers with no commercial water use available. 10 ML/d is the emergency scenario. This rate would be enough to supply customers of EPCOR with only the necessary water for survival while other facilities such as hospitals and correctional facilities could function with business as usual.

Additional pumping scenarios were added outside of the recommended 10 ML/day, 190 ML/day, 375 ML/day scenarios as intermediate reference scenarios. These reference scenarios were added because of the large gaps in extraction rates between 10 ML/day, 190ML/day, and 375 ML/day. They functioned to provide insights into what other intermediate extraction rates may be possible in the current well configurations. This included adding a 20 ML/day simulation that was done following the same well configuration as the 10 ML/day scenario. A 95 ML/day scenario was also added for the Onoway and Beverly valleys as it was found during testing that the Stony could not support this extraction rate. Results from reference scenarios are not explicitly provided unless relevant to understanding and interpretation. Overall, two additional extraction scenarios were added outside of three target extraction rates to examine the impact of a wider range of pumping rates.

Each scenario was tested for 3, 30, and 365 days, a variation by roughly an order of magnitude between each pumping time. These timeframes were considered because an alternate groundwater supply would only be expected to provide a short-term temporary resource. Replacement of NSR water that is expected at low-flow conditions would be seasonal, and contamination would be remediated or solved in a short time period.

Required extraction rates in relation to known infrastructure and potential well yields influenced the number and location of wells in transient simulations (Figure 3.5). Pumping wells were placed based in proximity to known infrastructure and areas where it was suspected large scale water extraction could be achieved (Figure 3.5). Within the Stony valley, groundwater wells were placed close to the city of Edmonton, ~3.5 km south-west of the E.L. Smith water treatment plant (Figure 3.6; Figure 3.7). For the Beverly valley, well locations were initially chosen to be close to the town of Stony Plain due to proximity to known infrastructure. Subsequent wells extended both North and South along the valley thalweg at 1 km intervals. The Onoway Valley's initial well location was chosen based on the distance to the city of Edmonton and where the well yield was sufficient. Subsequent refinement of well placement was necessary when rates greater than 20 ML/day were introduced. This involved placing wells eastward in an East-West trending line at 1 km intervals along the valley thalweg as this is where valley sediments are expected to be thickest, and water yields the highest.

The total number of wells used for trial simulations varied between buried valleys and with pumping rates/times (Table 3.2). Only one well was needed for the 3- and 30-day pumping scenarios in the Stony channel (Table 3.2; Figure 3.6). However, a second well, placed 1 km to the southwest along the valley thalweg, was required for the 365-day pumping scenario (Table 3.2; Figure 3.7). For the Beverly and Onoway valleys, only one well was needed in all time scenarios for the 10 and 20 ML/day cases. In the 95ML/day, 190ML/day, and 375 ML/day cases, 7 wells were required for 3-days while 13 wells were utilized for 30- and 365- days (Table 3.2; Figure 3.8; Figure 3.9).

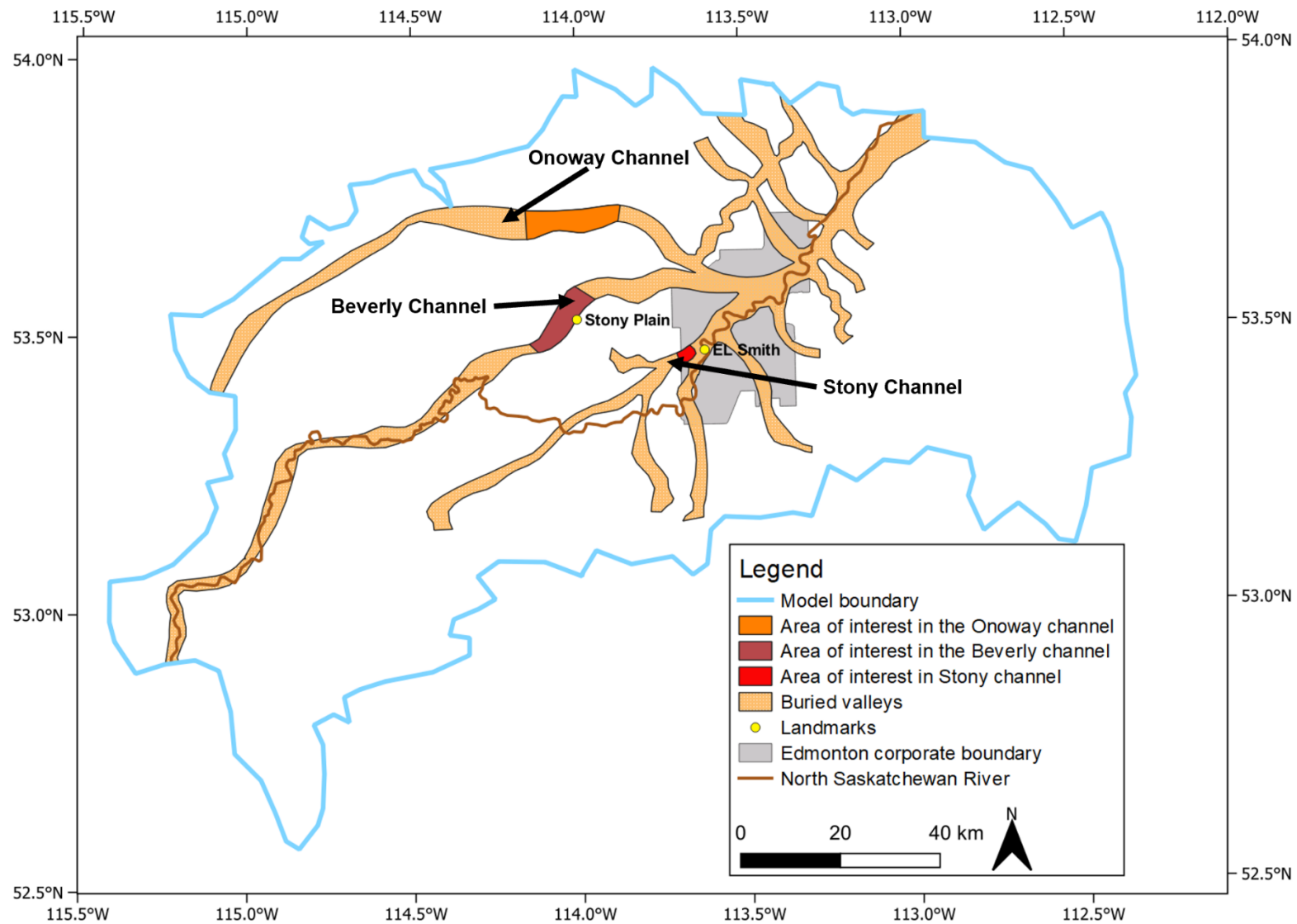


**Figure 3.5.** Areas of interest within chosen channels.

Time	3 days					30 days					365 days					
	Volume/day	10 ML	20 ML	95 ML	190 ML	375 ML	10 ML	20ML	95 ML	190 ML	375 ML	10 ML	20ML	95ML	190 ML	375 ML
Onoway Channel	w = 1	w = 1	w = 7	w = 7	w = 7	w = 7	w = 1	w = 1	w = 13	w = 13	w = 13	w = 1	w = 1	w = 13	w = 13	w = 13
Beverly Channel	w = 1	w = 1	w = 7	w = 7	w = 7	w = 7	w = 1	w = 1	w = 13	w = 13	w = 13	w = 1	w = 1	w = 13	w = 13	w = 13
Stony Channel	w = 1	w = 1	w = 7	w = 7	w = 7	w = 7	w = 1	w = 1	w = 13	w = 13	w = 13	w = 2	w = 1	w = 13	w = 13	w = 13

w = # of wells used in model

**Table 3.2.** Number and location of wells used the in each model pumping scenario.

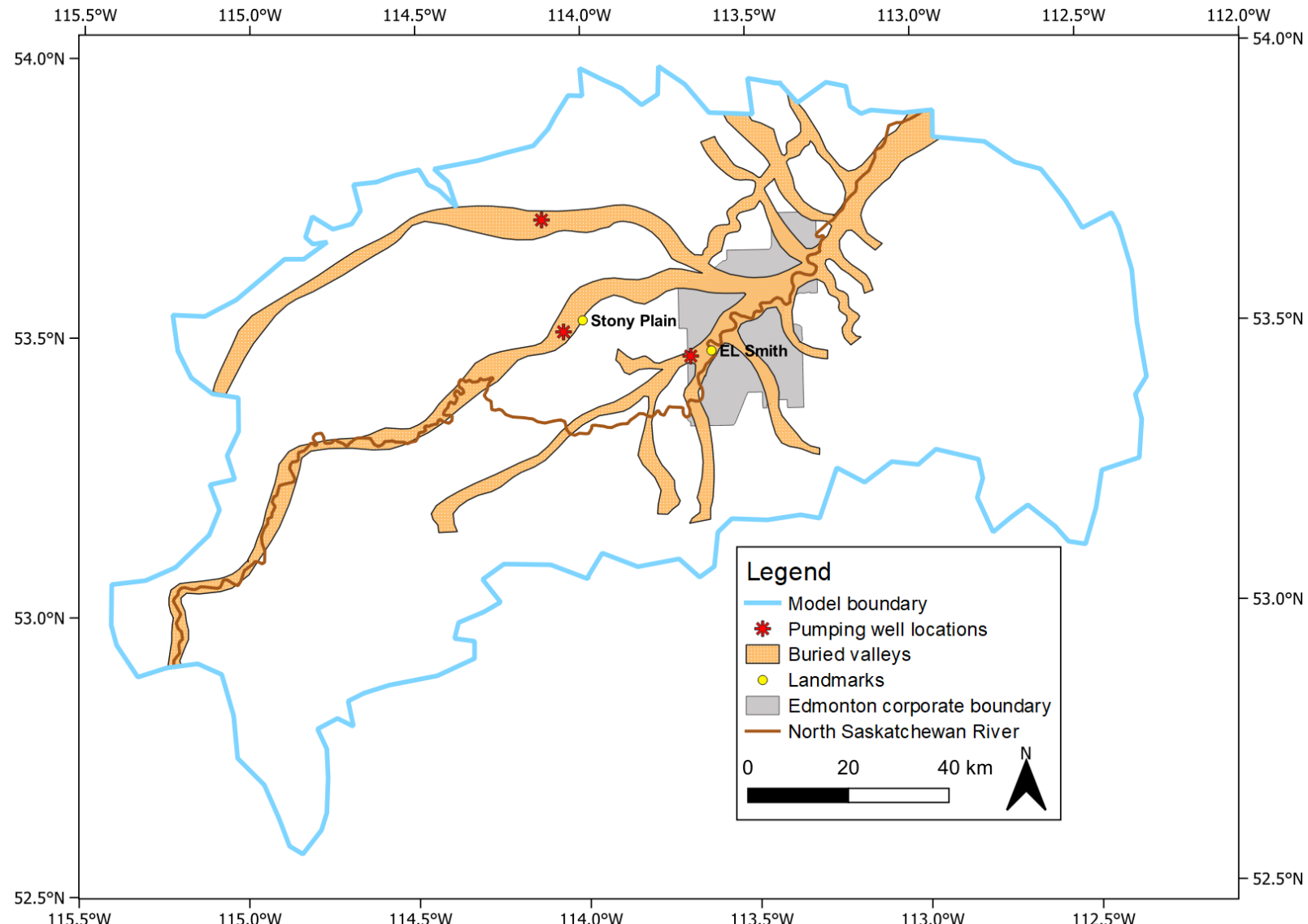


**Figure 3.6.** Pumping well network for 10 ML/day scenarios (3 and 30 days).

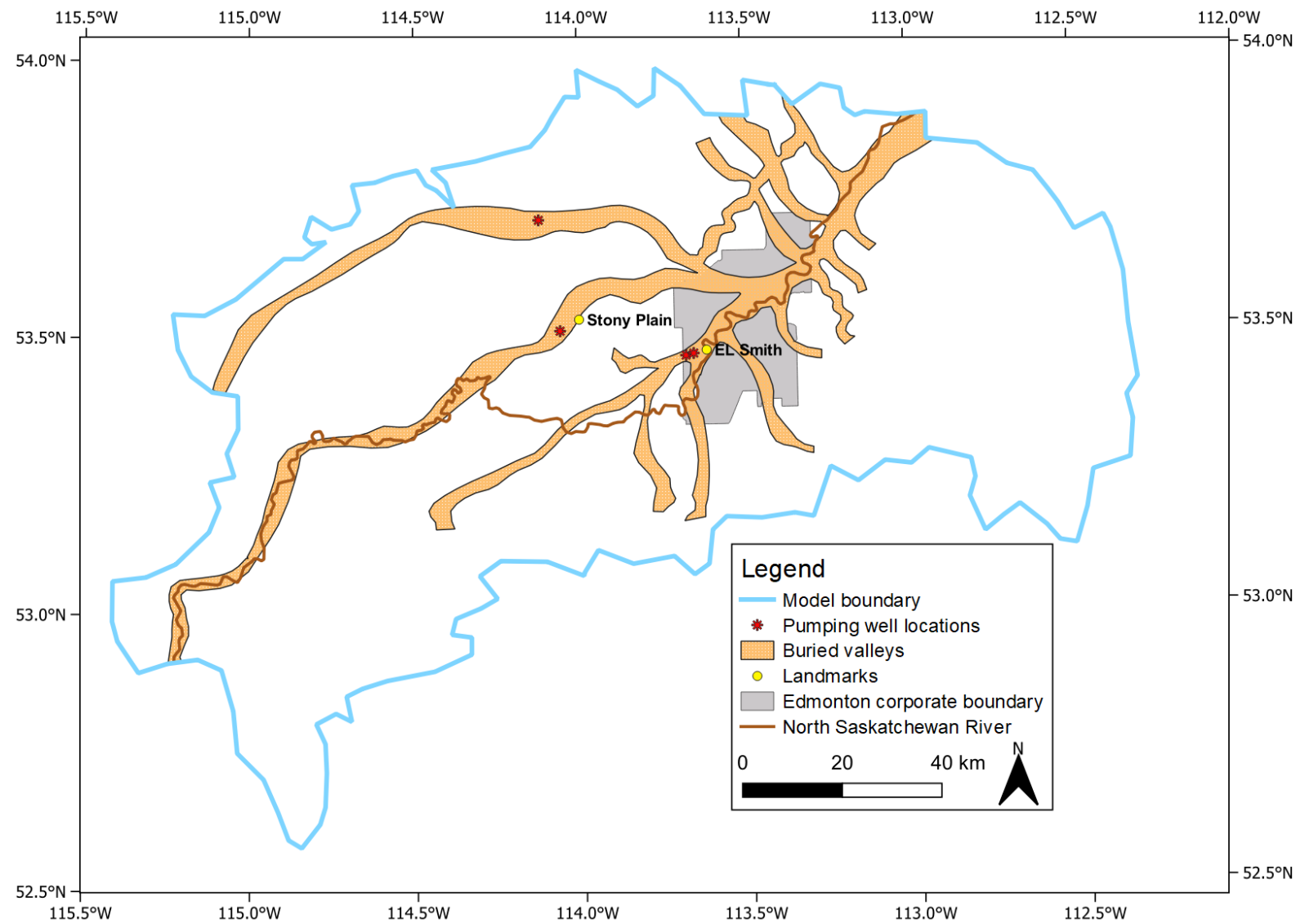


**Figure 3.7.** Pumping well network for 10 ML/day scenario, with two wells in the Stony channel (365 days).

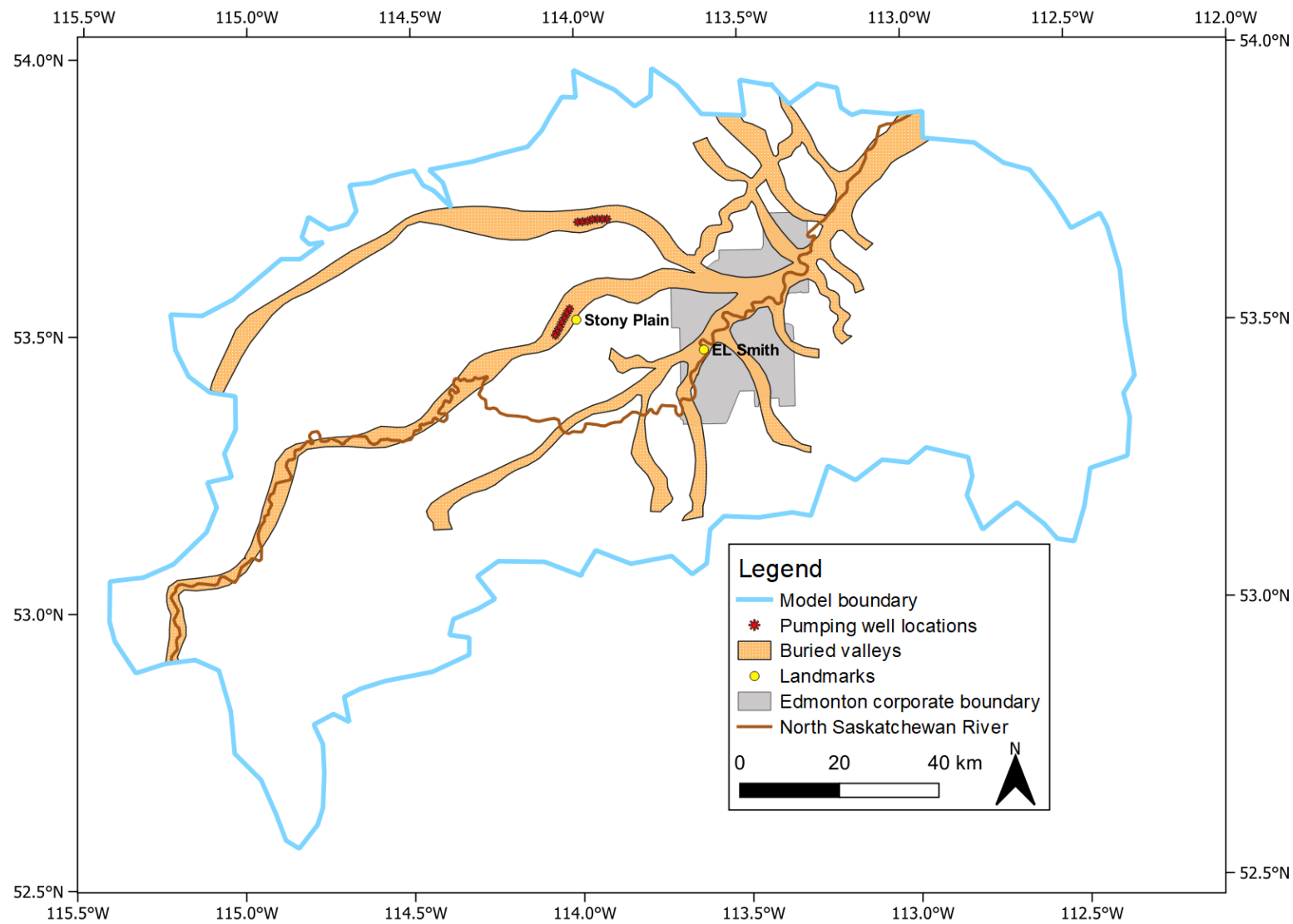


**Figure 3.8.** Pumping well network for seven pumping wells in each of the Beverly and Onoway channels for the 190 and 375 ML/day scenarios (3 days).

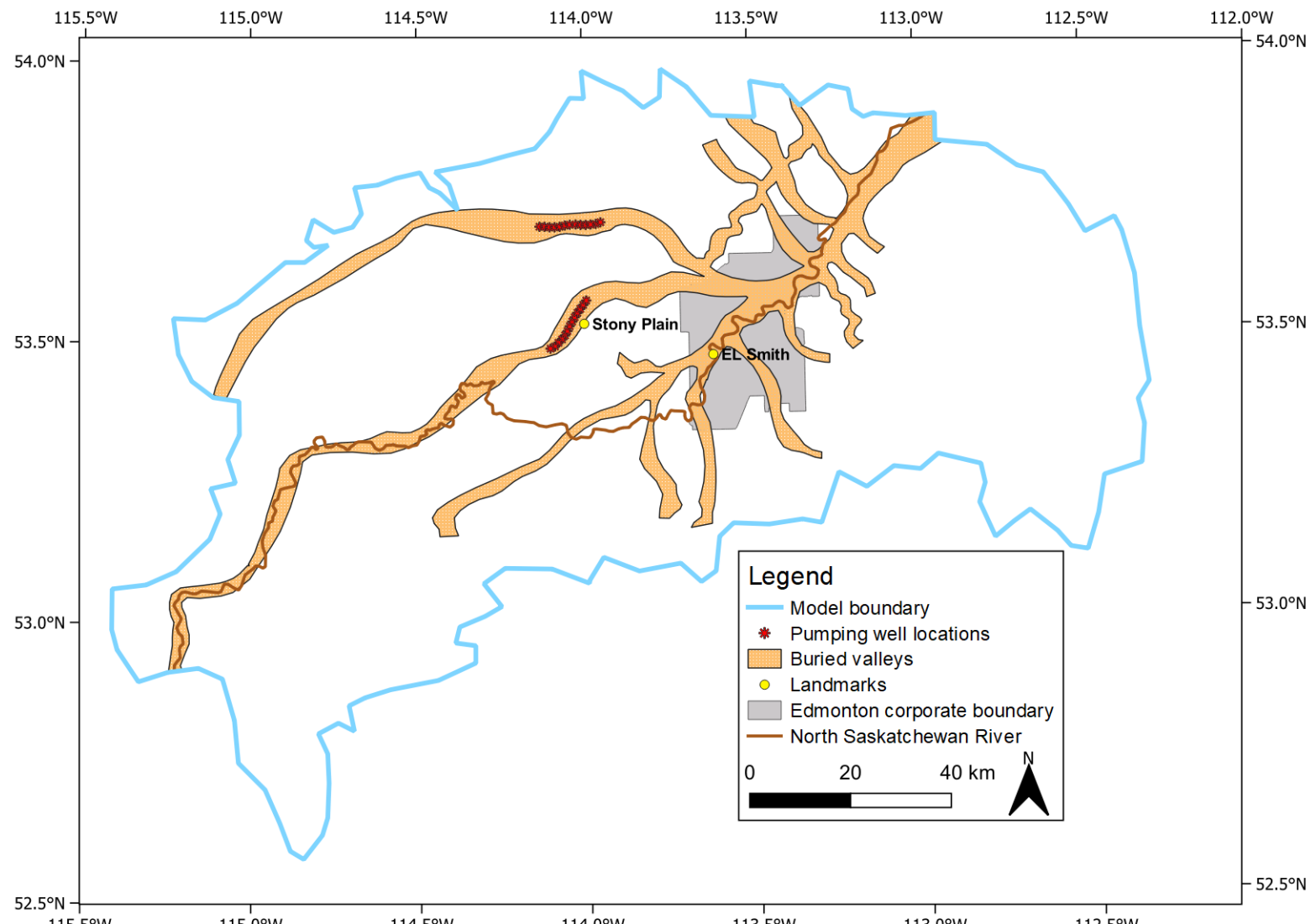


**Figure 3.9.** Pumping well network for thirteen wells in each of the Beverly and Onoway channels for the 190 and 375 ML/day scenarios (30 and 365 days).

### 3.3 Results

The maximum dimension observed from a drawdown cone was ~16 km. For clarity, results are presented as a subset of the total model area defined by a rectangle with coordinates at the north-west and south-east corners at 53.76° N, 114.2° W and 53.44° N, 113.49° W respectively (Figure 3.10).

The 10 ML/day case was feasible within all three channels tested in the model. The drawdown in layer 4 for 3, 30, and 365 days increases towards the extraction well(s) forming near circular drawdown cones in the 10 ML/day scenario (Figure 3.11; Figure 3.12; Figure 3.13). One extraction well was able to achieve a 10 ML/day withdrawal rate for all time durations in the Beverly and Onoway channels while the Stony required 2 extraction wells for 365 days (Figure 3.11; Figure 3.12; Figure 3.13). As time progresses drawdown cones become increasingly large in all channels, extending towards channel edges at 365 days (Figure 3.11; Figure 3.12; Figure 3.13).

Only the Beverly and Onoway channels can sustain the 190ML/day rate in the model. At 365 days, only the Beverly channel is able to sustain the 190ML/day extraction rate. For 3- and 30- days each channel was able to sustain 190 ML/day using seven and thirteen extraction wells, respectively (Figure 3.14; Figure 3.15). However, at 365 days, only the Beverly was able to sustain 190ML/day using thirteen wells (Figure 3.16). At each time (3, 30, 365 days), the drawdown cone is elliptical and follows the distribution of wells along the valley thalweg (Figure 3.14; Figure 3.15; Figure 3.16). After 365 days, drawdown in the Beverly becomes constrained by the lateral extent of the channel or channel edges.

The 375 ML/day case is not shown here because it was not possible under any time scenario due to well failure or dry cells at the wellbore in MODFLOW during pumping. Dry cells at the wellbore occur due to excessive drawdown that dewater sediments around the wellbore, causing the well to be unable to extract further groundwater.

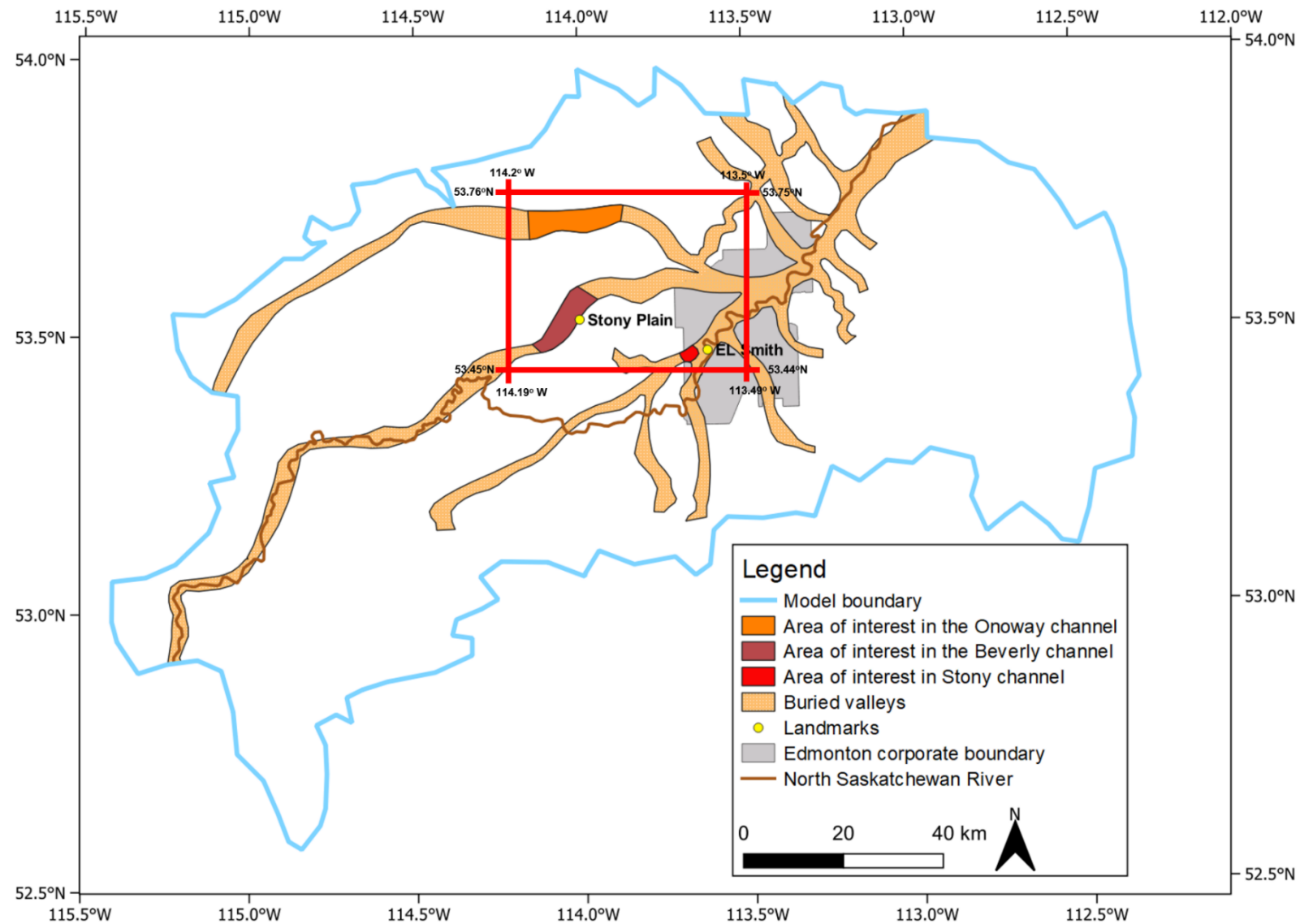


**Figure 3.10.** Model area with location of interest in red.

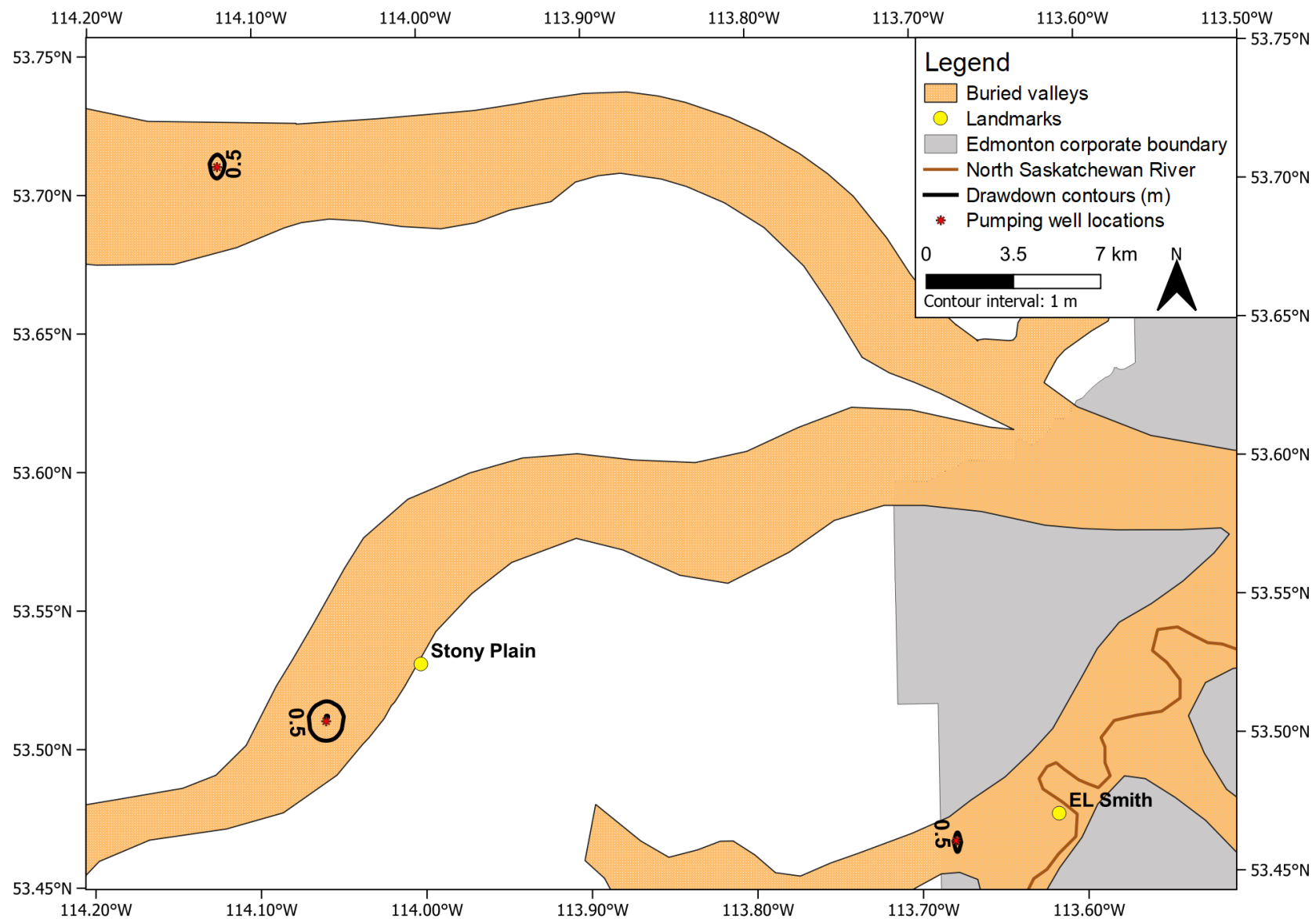


**Figure 3.11.** Drawdown contours after 3 days pumping at 10 ML/day.

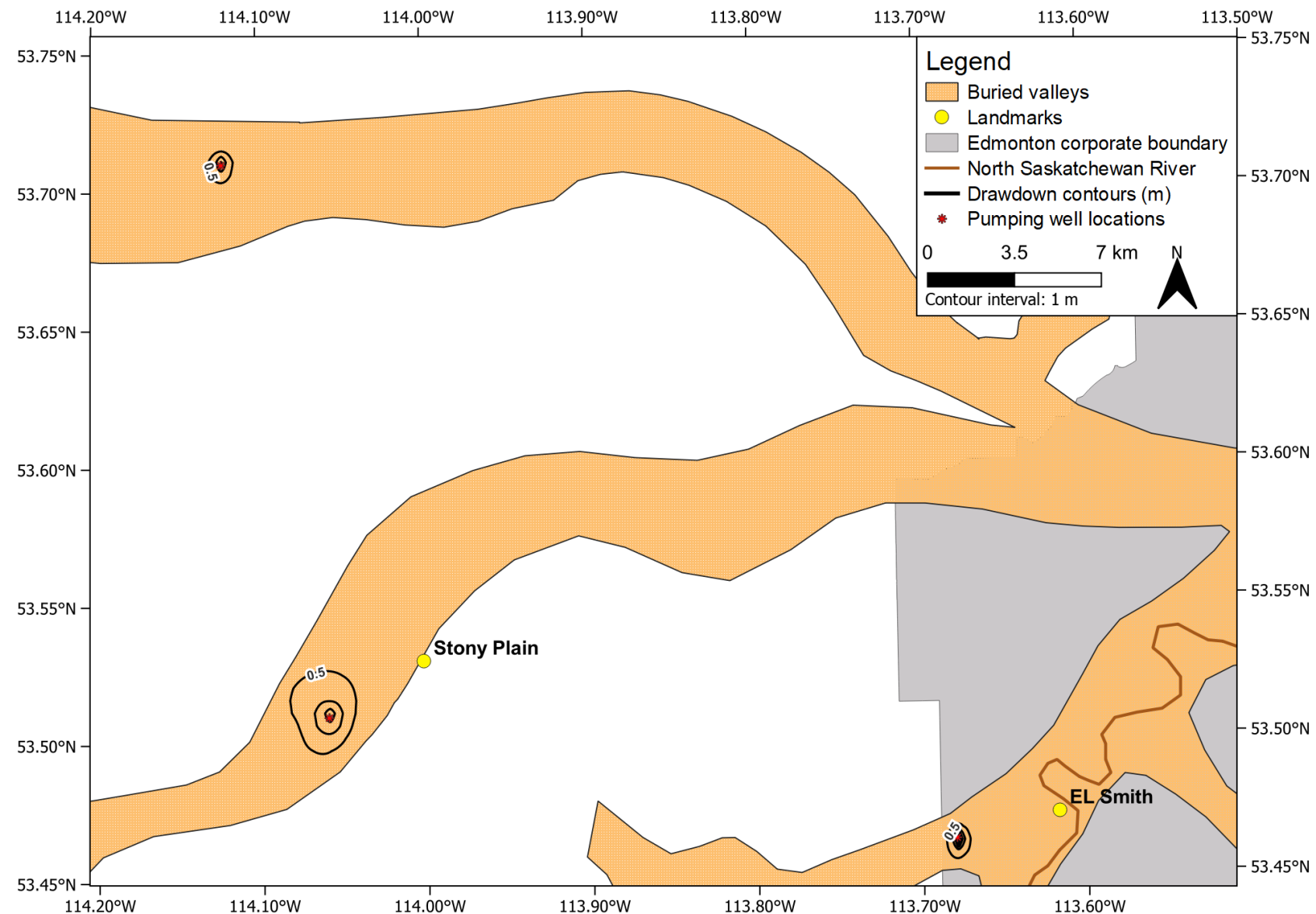


**Figure 3.12.** Drawdown contours after 30 days pumping at 10 ML/day.

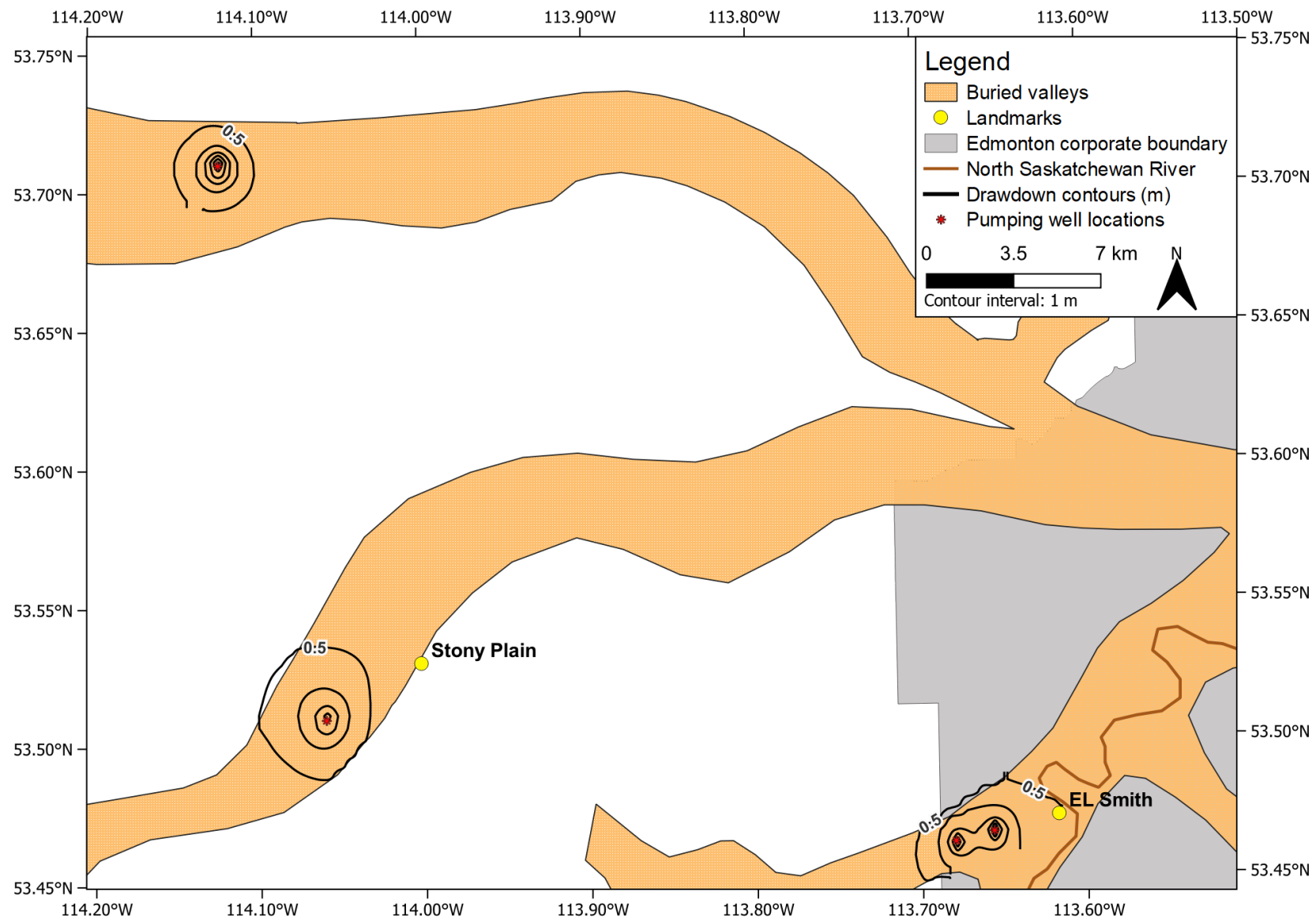


**Figure 3.13.** Drawdown contours after 365 days pumping at 10 ML/day.

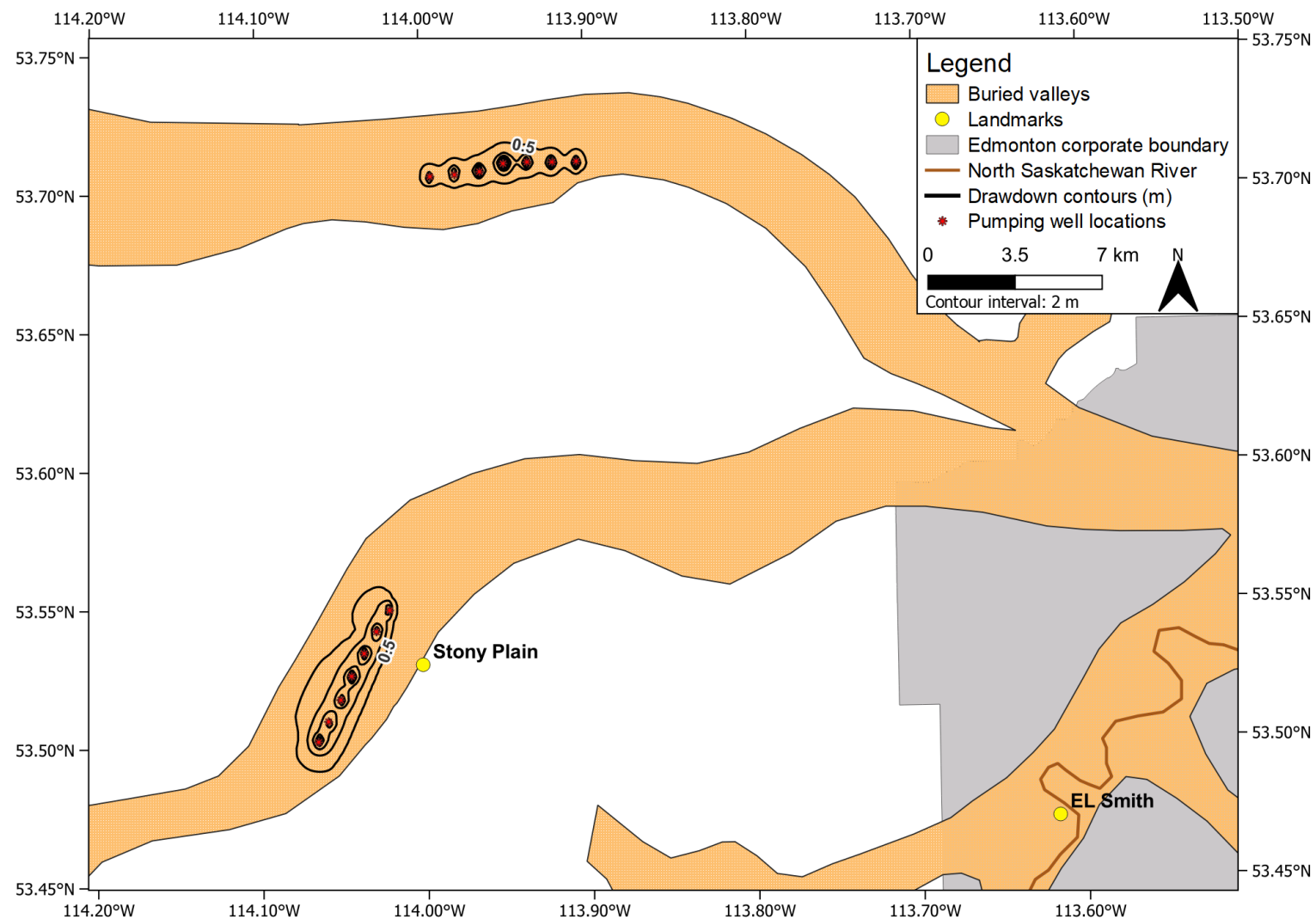


**Figure 3.14.** Drawdown contours after 3 days pumping at 190 ML/day. Note that 190 ML/day could not be pumped from the Stony Valley.

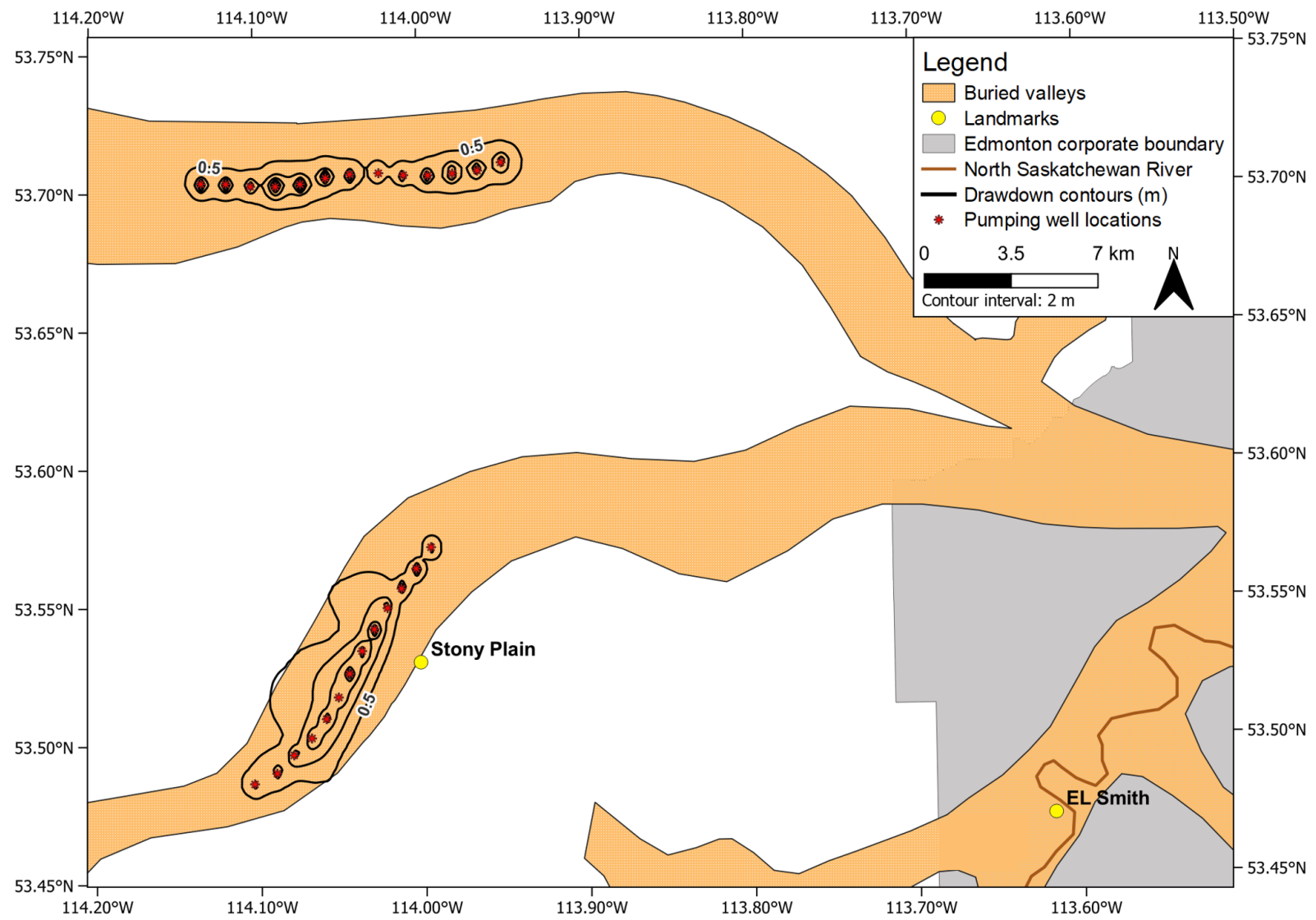


**Figure 3.15.** Drawdown contours after 30 days pumping at 190 ML/day. Note that 190 ML/day could not be pumped from the Stony Valley.

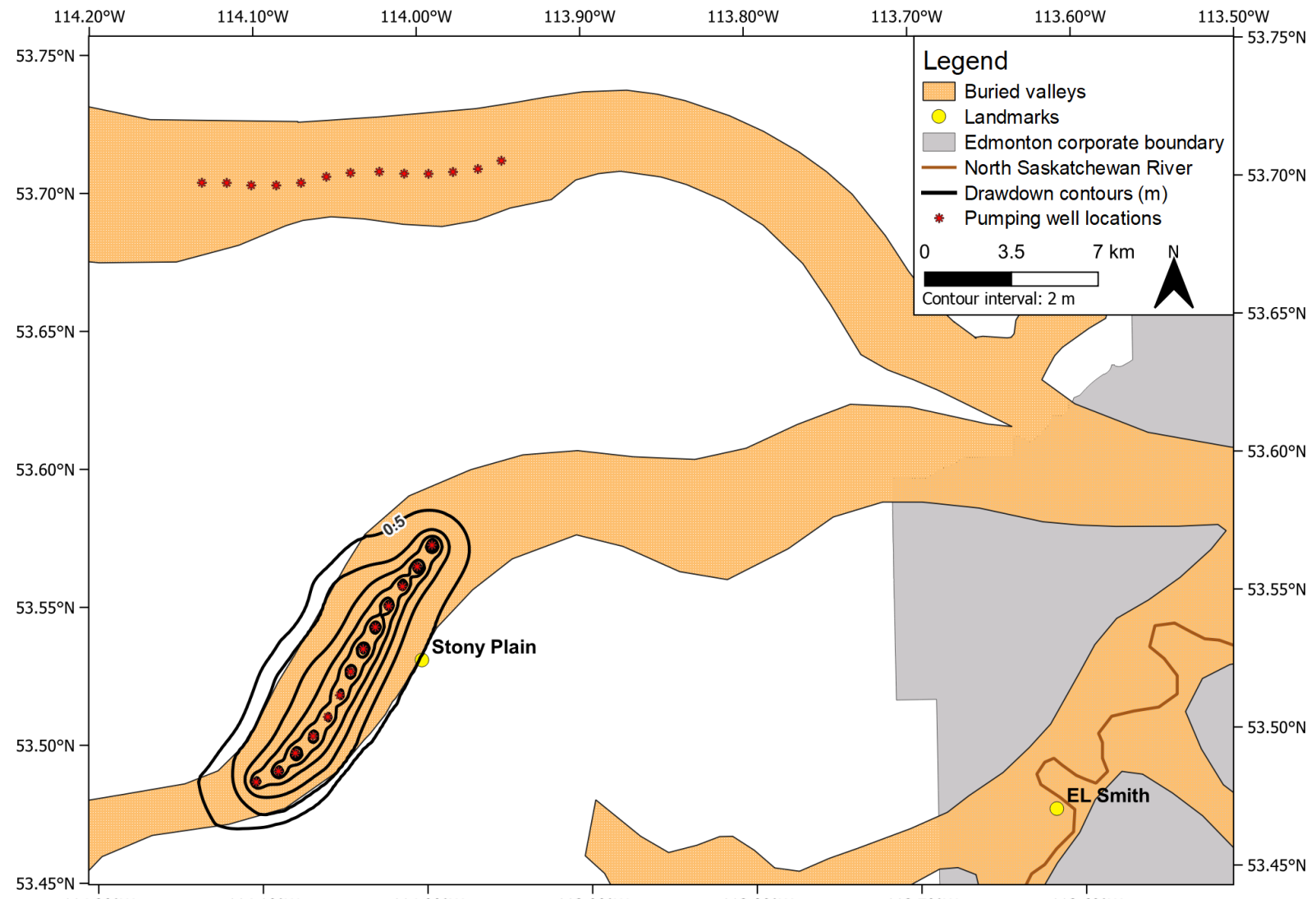


**Figure 3.16.** Drawdown contours after 365 days pumping at 190 ML/day. Note that 190 ML/day could not be pumped from the Stony and Onoway valleys.

## **3.4 Discussion**

### **3.4.1 Pumping rates**

First order hierarchization of channel ability to sustain various extraction rates under idealized conditions in buried valleys of interest was achieved (Table 3.3). Of the three channels investigated, the Beverly, the Onoway, and the Stony each responded to pumping differently and are described in turn below.

The Beverly channel was able to supply the greatest amount of water at 190 ML/day for 365 days in the current well distribution. Due to this, it is the first choice in the case of large-scale water extraction needs in a force majeure emergency scenario.

The Onoway channel was able to provide the second largest amount of water (Table 3.3). While the Onoway channel offered promising results in terms of water provided (190 ML/day for 30 days), the location tested was further from the city of Edmonton than the area of interest in the Beverly channel. Additionally, the Beverly channel could provide a greater volume of water for longer (Table 3.3). This means the Onoway channel would most likely be utilized to supplement water extraction from the Beverly channel if the need arose. Alternatively, other smaller municipalities in closer proximity to the Onoway channel such as St. Albert could utilize the channel.

The Stony channel provided the least amount of water of the three channels investigated (Table 3.3). Pumping scenarios within the Stony channel were limited to the emergency water scenario (10 ML/day) with the upper achievable extraction rate at 20 ML/day for 365 days (Table 3.3). However, despite the 10-20 ML/day limitation, the Stony channel is within ~3.5 km of E.L. Smith water treatment plant (Figure 3.12; Figure 3.13), making it an ideal consideration in an emergency scenario.

It is important to note these pumping scenarios are highly idealized and do not account for the intricacies of well field design, local permeability variation, or other groundwater users. Rather, the volumes tested at this regionalized scale provide insight into the possible variations of extractable water between channels under idealized conditions. Additionally, the goal of examining these scenarios is not to develop a pumping strategy for the buried valley aquifers. Instead, a first order approximation of achievable water rates in the channels of interest provide

regional scale hierarchization and characterization that can serve as a starting point to help guide future study and decision makers in the region.

Location	Volume/day	Time				3 days				30 days				365 days			
		10 ML	20 ML	95 ML	190 ML	375 ML	10 ML	20ML	95 ML	190 ML	375 ML	10 ML	20ML	95ML	190 ML	375 ML	
Onoway Channel	w = 1	w = 1	w = 7	w = 7			w = 1	w = 1	w = 13	w = 13		w = 1	w = 1	w = 13			
Beverly Channel	w = 1	w = 1	w = 7	w = 7			w = 1	w = 1	w = 13	w = 13		w = 1	w = 1	w = 13			
Stony Channel	w = 1	w = 1					w = 1	w = 1				w = 2					
Legend		w = # of wells used in model Note: # of wells may differ significantly in practice															
	= Probable																
	= Less Probable																
	= Not Probable																

**Table 3.3.** Relative probability table of tested pumping scenarios.

### **3.4.2 Drawdown trends in buried valley aquifers**

The response of buried valley sediments to pumping depends on transmissivity and overlying material. Transmissivity directly influences the size/shape of the drawdown cones (Figure 3.17). In this case, saturated thickness controls the effective transmissivity of channels since K is constant within and between channels. Likewise, if the material that overlies the buried valley is hydrogeologically similar in K, enhanced saturated thickness is available.

The influence of varying transmissivities on drawdown trends is more evident at early times (3, 30 days) as drawdown size and shape varies more noticeably between channels. However, at later times (365 days), drawdown expansion is controlled primarily by channel extents.

In the Beverly channel, saturated thickness, overlying material, and pumping time controlled the general drawdown trends observed (Figure 3.18; Figure 3.19). Shallow, laterally extensive drawdown cones are characteristic of the Beverly channel (Figure 3.18; Figure 3.19). This is due to it having the largest saturated thickness of the three channels at ~28.5 m in the area tested (Figure 3.17). Saturated thickness is further enhanced by the overlying pitted delta deposits for most of the area of interest. This is because pitted delta deposits have a similar K to the upper buried valleys sediments and can thus function with some vertical hydraulic continuity. The impact of this increased effective transmissivity is best demonstrated when comparing the northernmost two extraction wells with the rest of wells in the Beverly channel (Figure 3.20). In the two northernmost wells, lateral drawdown expansion is more restricted compared to the wells that underlie pitted delta deposits to the south (Figure 3.20). This illustrates how varying overlying deposit composition impacts drawdown expansion in the underlying channel. Once 365 days pumping time is reached, the primary limiting factor on drawdown expansion and shape becomes the channel boundaries (Figure 3.21).

Saturated thickness controlled the underlying drawdown trend through time, with early and late responses to pumping time visible in the Onoway channel (Figure 3.18; Figure 3.19). Drawdown cones intermediate in lateral areal extent and maximum drawdown are characteristic of the Onoway channel (Figure 3.18; Figure 3.19). This is because the Onoway has an intermediate saturated thickness for the three channels studied at ~19.7 m for the area tested. At early times (3-, 30- days) lateral expansion of the drawdown cone is primarily controlled by transmissivity. Additionally, drawdown extent does not appear to vary across the pumping domain like the

Beverly channel (Figure 3.20). This is because the Onoway channel is overlain by homogenously low K materials, contrasting the heterogenous deposits overlying the Beverly channel. However, like the Beverly channel, in the 365-day scenario drawdown expansion is limited by channel boundaries. The shift in pumping responses can be best observed when comparing the narrow, tighter drawdown cones at 3, and 30 days (Figure 3.11; Figure 3.12; Figure 3.15) with the larger expanded drawdown cones at 365 days (Figure 3.13). Therefore, the lateral extent of the drawdown cone is controlled by transmissivity at early times but at later times it becomes limited by the physical channel extent.

Only smaller pumping rates (10 to 20 ML/day) were found to be feasible in the Stony channel due to its lower transmissivity and lower static water levels (Figure 3.18). The initially lower water levels in the channel partially contribute to lower achievable withdrawal rates. This also coincides with lower saturated thickness within the Stony channel at ~16.7 m in the area tested, the lowest saturated thickness of the three channels investigated. This means drawdown is increased relative to the other channels with the areal extent of drawdown decreased by association (Figure 3.17; Figure 3.18). Steep drawdown trends and lower water levels mean that sediments around the wellbore are more likely to dry out when extracting large volumes of water. The lower transmissivity and initial hydraulic head values of the Stony channel cause it to be least prospective for large scale water withdrawal.

Each channel exhibits a unique drawdown trend dependent on hydrogeologic setting. In the hydrogeologic setting of the Beverly channel pitted delta sediments function to increase transmissivity and alter drawdown cone dimensions. Conversely, the Onoway channel is mostly confined and only has low K deposits above it with an intermediate saturated thickness. This produces a mid-range drawdown trend (Figure 3.18). Hydrogeologic conditions in the Stony channel consist of comparatively low water levels and related low saturated thickness. This results in it being least prospective for large scale water withdrawal. Overall, each buried valley has a different hydrogeologic setting that produces unique drawdown trends through time.

### **3.4.3 Implications of three-dimensional hydrogeologic setting for buried valleys**

Buried valleys play a critical role as a water resource. In a prairie setting, their ability to provide groundwater is heavily impacted by the 3-dimensional hydrogeology surrounding them. This dictates the extent of the exchange fluxes between the buried valley and the surrounding

environment. If the surrounding geology is of similar K, the buried valley and the adjoining material may function as a single hydrostratigraphic unit (Freeze & Cherry, 1979), creating enhanced pumping capacity. This is the case for pitted delta sediments overlying the Beverly channel near the town of Stony Plain. However, this also results in an increased risk of contamination. Because of the regional nature and high K of buried valleys, contaminants may travel further than expected, polluting large amounts of potable water (Bedient et al., 1999). Care must be taken to test for contamination and identify potential upstream contamination sources when considering buried valleys as a groundwater resource. If buried valleys are encased in hydrogeologic materials that are several orders of magnitude below buried valley K values as is the case for the Onoway channel and the Stony channel near E.L. Smith, they may be protected from sudden contamination (Bedient et al. 1999). Though, reduced pumping capacity will impact the extractable water volumes. Thus, when examining prairie buried valleys as a potential water source, care needs to be taken to determine the 3-dimensional hydrogeology as this ultimately impacts water availability.

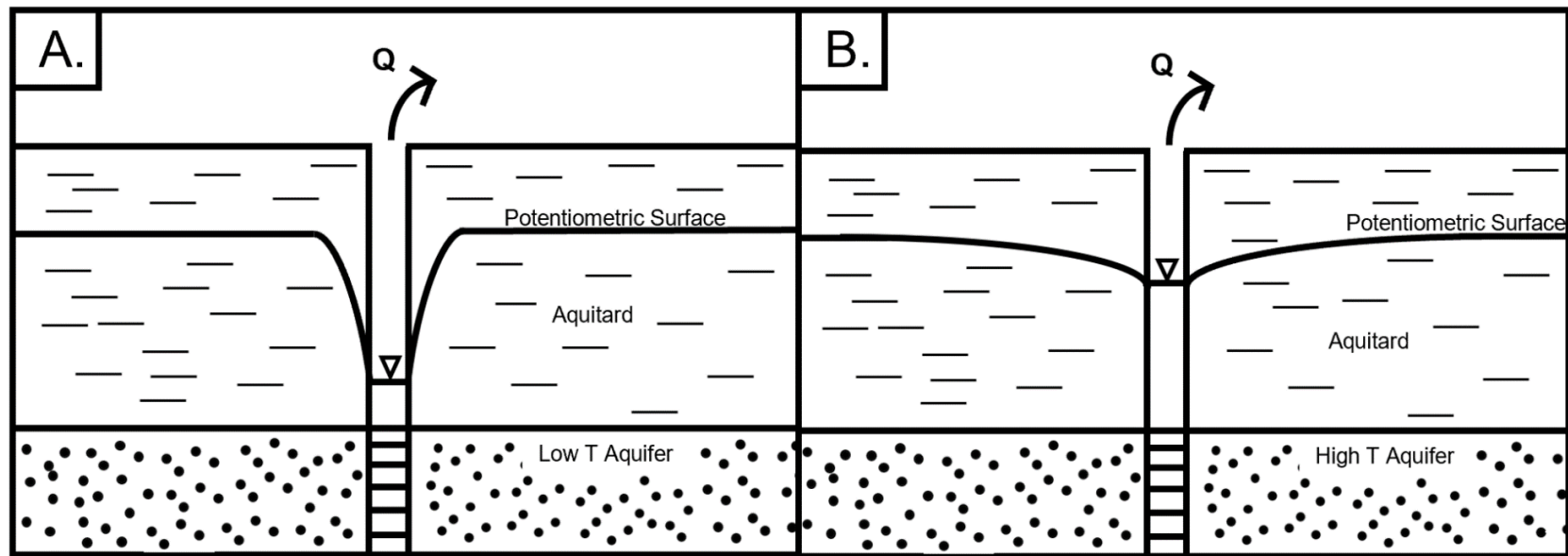


**Figure 3.17.** How transmissivity effects the shape of the drawdown cone showing A) Low transmissivity (T). B) High T. After Freeze & Cherry (1979).

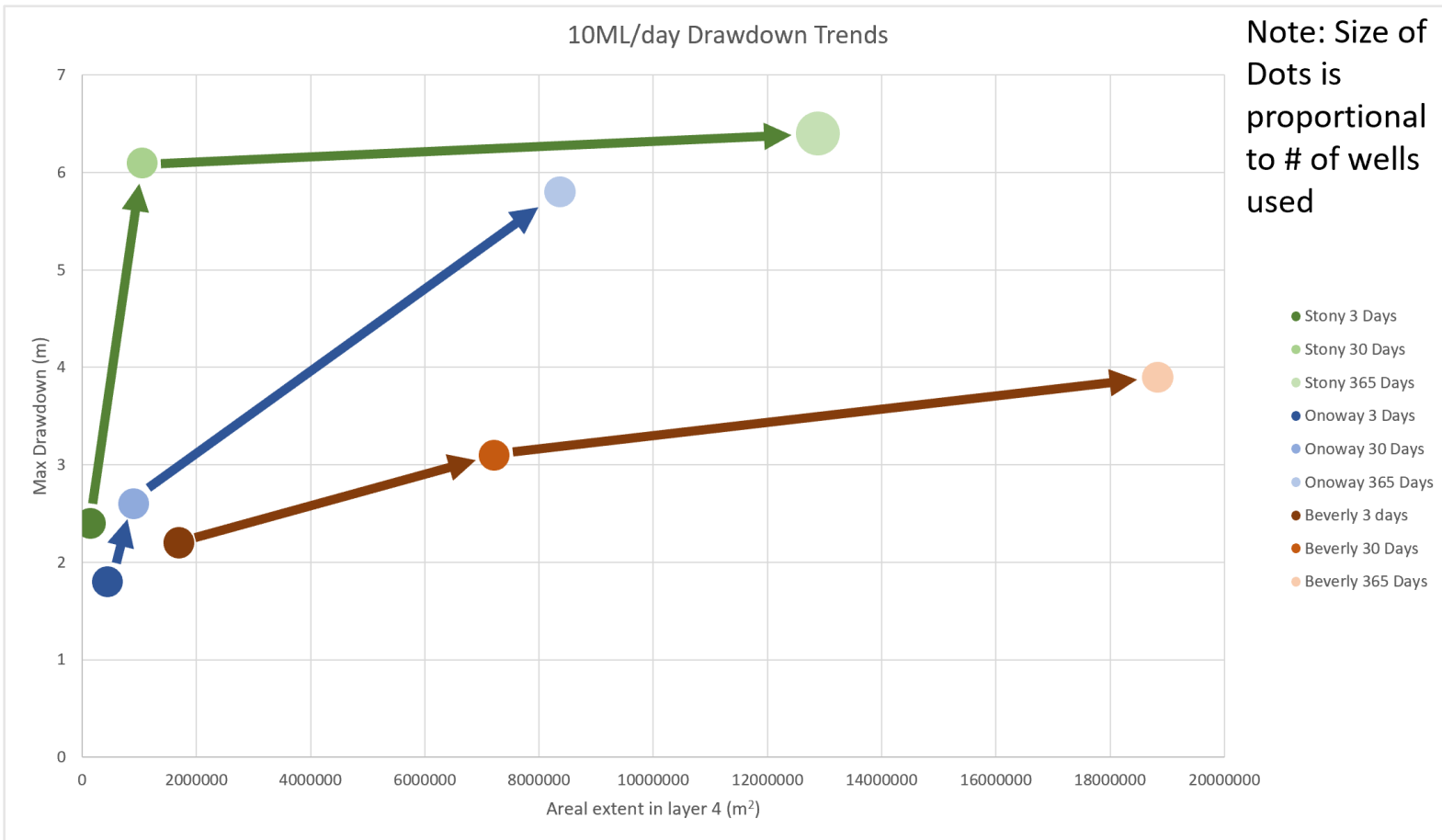


**Figure 3.18.** Drawdown trends in buried valley aquifers at 10 ML/day.

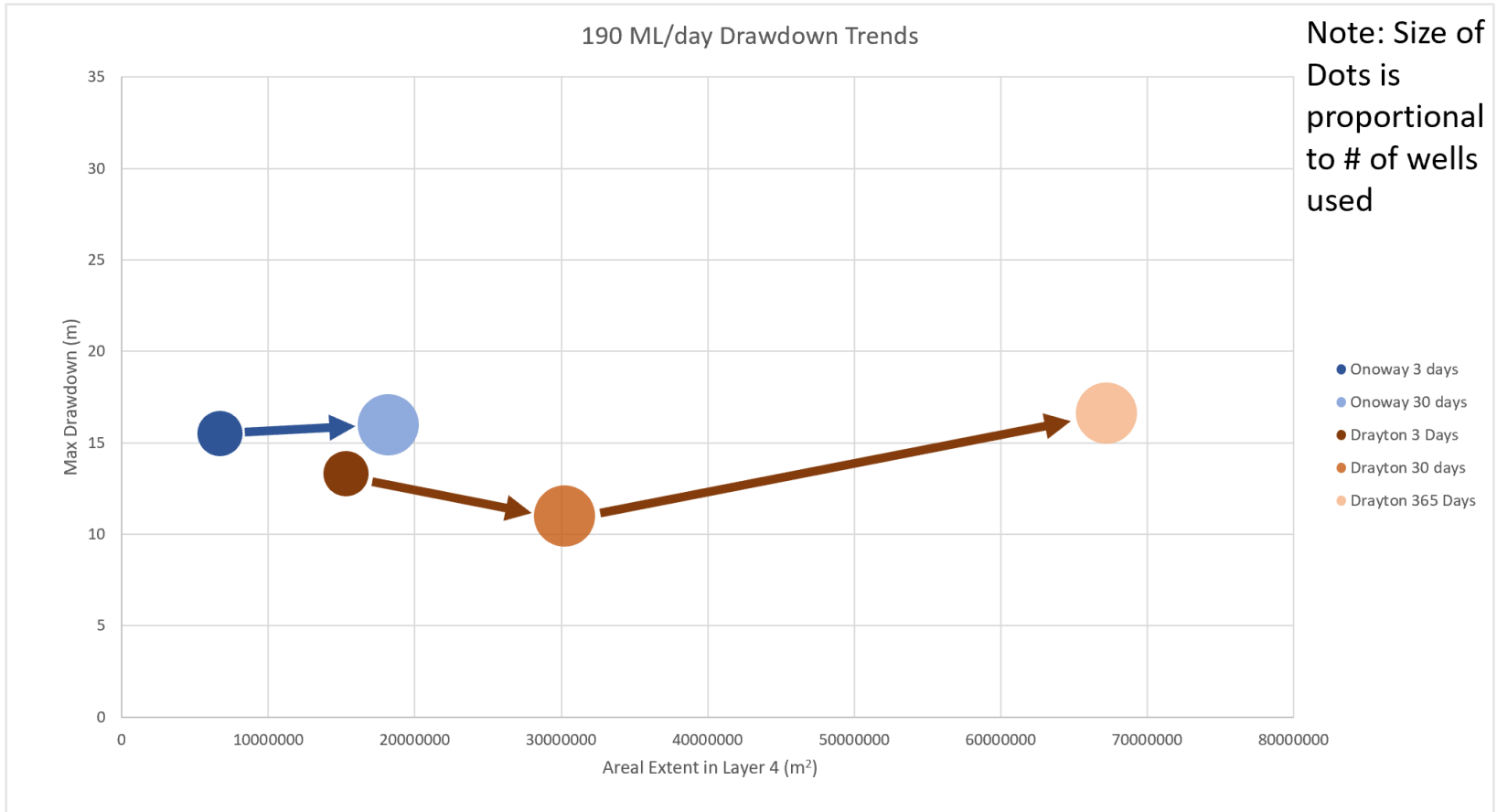


**Figure 3.19.** Drawdown trends in buried valley aquifers at 190 ML/day.

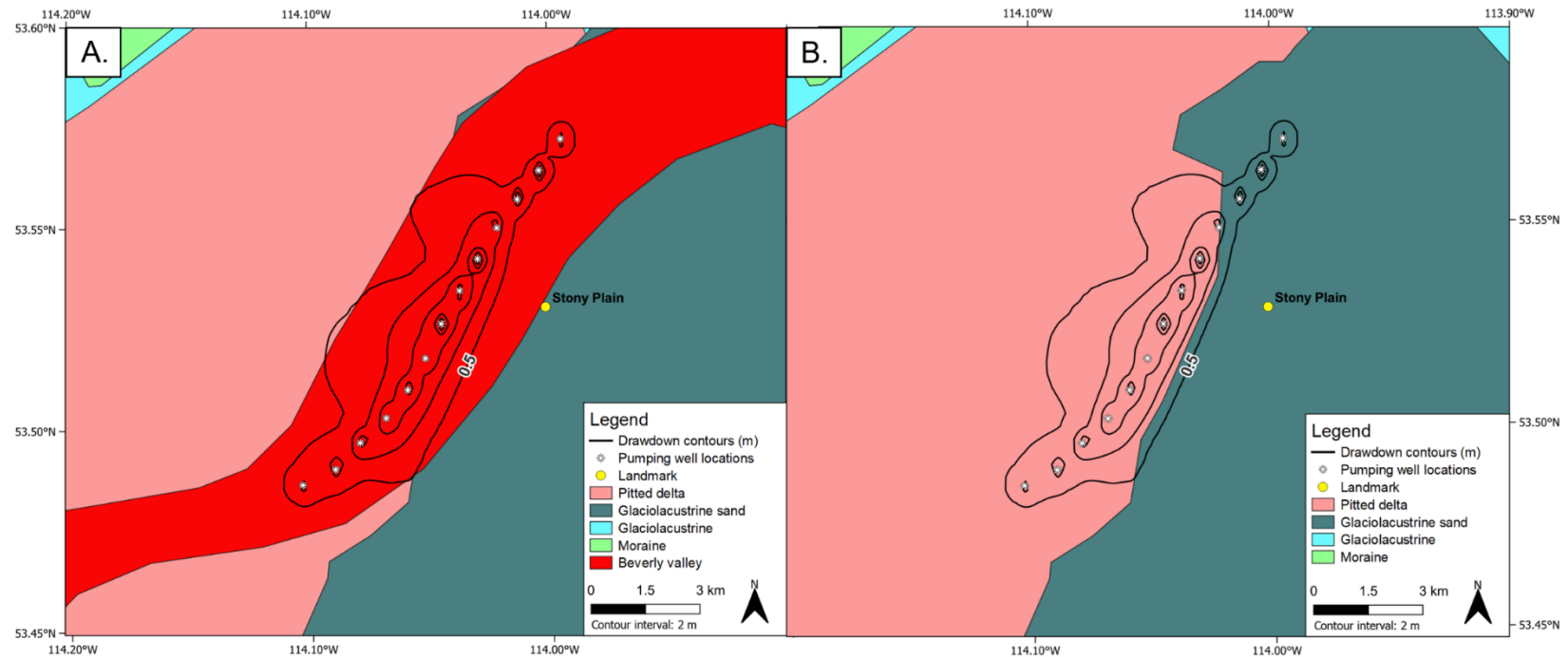


**Figure 3.20.** Drawdown extent from layer 4 in the Beverly channel after 30 days with an extraction rate of 190 ML/day with A. layer 4 geology and B. layers 1 and 2 geology overlain.

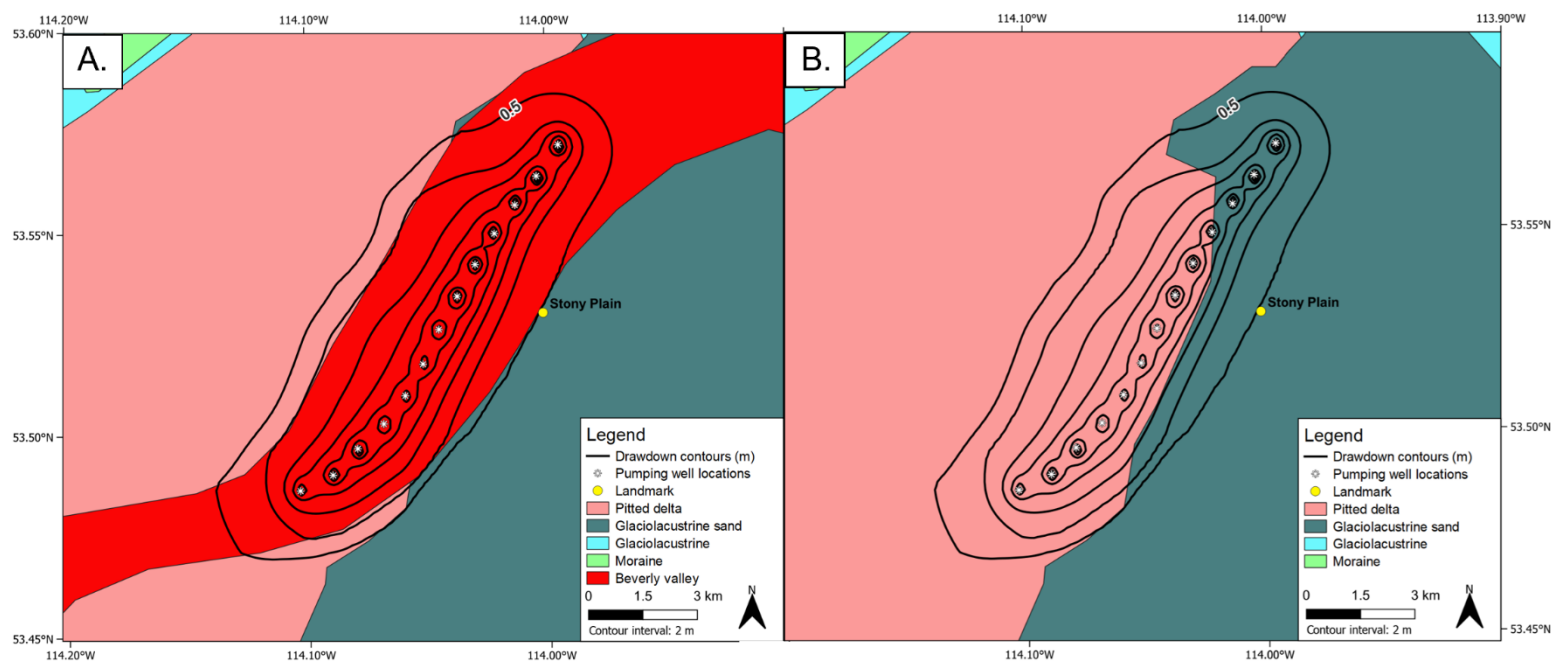


**Figure 3.21.** Drawdown extent from layer 4 in the Beverly channel after 365 days with an extraction rate of 190 ML/day with A. layer 4 geology and B. layers 1 and 2 geology overlain.

### **3.5 Conclusions**

A first order ranking system for three buried valleys of interest, the Stony, the Onoway, and the Beverly is developed based on transient groundwater modelling (Table 3.3). The three buried valleys tested varied widely in the amount and duration of water that could be provided within the constraints of the well configurations tested (Table 3.3). The Stony channel only can provide 10 ML/day for 365 days. It is enough to supply the City of Edmonton in a major emergency scenario for up to a year, providing the least amount of water among the channels tested. This is the closest to the city of Edmonton, as the area tested in the Stony channel is within ~3.5 km of the E.L. Smith Water Treatment Plant. The Onoway channel provides the second greatest volume of water at 190 ML/day for 30 days. The area tested in the Beverly channel supersedes the Onoway as it provides 190 ML/day for 365 days while also being closer to the city. However, this does not negate the importance of the Onoway channel, as it still may provide large amounts of water in a supplementary scenario or for alternate municipalities. No channel was able to provide 375 ML/day, Edmonton's current water usage for any time period.

It is important to contextualize the pumping volumes or rates tested within the model. These rates were tested in a regional scale model and local conditions may vary significantly. As previously noted, these results are intended to provide a first order regional approximation and characterization of channels tested. This provides an important assessment of regional extraction rates in context of future water needs for the city of Edmonton, while also delivering a basis (starting point) for more detailed local analysis.

Three-dimensional hydrogeology surrounding buried valleys is important to characterize when considering pumping capacity and contamination risk. For the Beverly channel near the town of Stony Plain, overlying pitted delta deposits increase the effective buried valleys saturated thickness due to their similar K value. This may lead to enhanced pumping capacity. However, while this increases pumping capacity, it also increases contamination risk from surface pollution. The Onoway channel and Stony channel near E.L. Smith Water Treatment Plant are overlain by lower K deposits such as glaciolacustrine and glacial moraine sediments. This may lower the potential pumping capacity of these buried valleys, but it also reduces the risk of contamination from surface sources. It is important to consider surrounding hydrogeology when considering large scale water resource extraction from buried valleys as this may influence channels chosen.

Buried valleys may provide part of the solution to mitigate water scarcity for the city of Edmonton from seasonal drought or contamination of the NSR. Seasonal drought is expected to become more frequent in NSR due to climate change and would result in a potential 25% reduction in surface runoff to the NSR at peak demand months (July to August) (Anis & Sauchyn, 2021). Peak demand months are also the warmest summer months and a large reduction in surface runoff may translate to an equally large reduction in river discharge. However, buried valleys may be able to supply half (190ML/d) or a quarter (95ML/d) of the city's current water usage (375ML/d) (Table 3.3) under idealized conditions. Likewise, for sudden contamination such as a chemical spill (oil and gas), buried valleys could provide adequate time (days to weeks) for the contaminated water to be remediated. This would offer increased water security for the city of Edmonton as there is currently no alternative water supply.

### 3.6 References

- Alberta Environment and Parks. (2014). *HUC Watersheds of Alberta*. [Shapefile].
- Alberta Environments and Parks. (2017). *Alberta Provincial 25 Metre Raster*. [DEM]. Retrieved from <https://open.alberta.ca/opendata/gda-c16469a2-5541-455c-bba0-63a24c0ff08a#summary>
- Andriashek, D. L. (2019). *Thalwegs of Bedrock Valleys, Alberta, Version 2 (GIS data, line features) Edition: v.2*. [Data file] Alberta Energy Regulator/Alberta Geological Survey. Retrieved from [http://ags.aer.ca/document/DIG/DIG\\_2018\\_0001.zip](http://ags.aer.ca/document/DIG/DIG_2018_0001.zip).
- Andriashek, L. D., Fenton, M. M., Root, J. D. (1979). *Surficial Geology Wabamun Lake, Alberta (NTS 83G)*. (Map 149). Edmonton, AB: Alberta Geological Survey. Retrieved from <http://ags.aer.ca/publication/map-149>.
- Anis, M. R., & Sauchyn, D. J. (2021). Ensemble projection of future climate and surface water supplies in the North Saskatchewan River basin above Edmonton, Alberta, Canada. *Water*, 13(17), 2425. <https://doi.org/10.3390/w13172425>
- Akhtar, N., Syakir Ishak, M. I., Bhawani, S. A., & Umar, K. (2021). Various natural and anthropogenic factors responsible for water quality degradation: A Review. *Water*, 13(19), 2660. <https://doi.org/10.3390/w13192660>
- Augustine, N. V. (2015). *Estimating Specific Storage and Matrix Compressibility from Barometric Efficiency in the Southern Alberta Paskapoo Aquifer System* (master's thesis). Calgary, AB: University of Calgary.
- Barnett, B., Townley, L. R., Post, V., Evans, R. E., Hunt, R. J., Peeters, L., Richardson, S., Werner, A. D., et al. (2012). (Waterlines Report Series 82). *Australian groundwater modelling guidelines*. Canberra: National Water Commission.
- Bayrock, L. A. (1972). *Surficial Geology Edmonton (83H)*. (Map 143). Edmonton, AB: Alberta Research Council.

- Bedient, P. B., Rifai, H. S., & Newell, C. J. (1999). *Ground water contamination: Transport and remediation* (2nd Edition). Prentice Hall PTR.
- Bibby, R. (1974a). *Hydrogeology of the Edmonton area (northwest segment), Alberta*. (ARC/AGS Earth Sciences Report 1974-10). Edmonton, AB: Alberta Research Council
- Bibby, R. (1974b). *Hydrogeological map of the Edmonton area, northwest segment, Alberta, NTS 83H (part)*. (Map 108). Edmonton AB: Alberta Geological Survey.
- Cathcart, J., Lorenz, K., Depoe, S., Phelan, C., Casson, J., & Jedrych, A. T. (2008). Volume 3: AESA Water Quality Monitoring Project. In *Assessment of Environmental Sustainability in Alberta's agricultural watersheds*. Palliser Environmental Services Ltd. and Alberta Agriculture and Rural Development.
- Ceroici, W.J. (1979a). *Hydrogeology of the southwest segment, Edmonton, Alberta*. (ARC/AGS Earth Sciences Report 1978-05). Edmonton AB: Alberta Research Council.
- Ceroici, W. J. (1979b). *Hydrogeological map of the Edmonton area (southwest segment), Alberta, NTS 83H (part)*. (Map 117). Edmonton AB: Alberta Geological Survey.
- Cummings, D. I., Russell, H. A., & Sharpe, D. R. (2012). *Buried valleys and till in the Canadian Prairies: Geology, hydrogeology, and origin*. (Current research - Geological Survey of Canada). Ottawa, ON: Natural Resources Canada.
- Domenico, P. A., & Mifflin, M. D. (1965). Water from low-permeability sediments and land subsidence. *Water Resources Research*, 1(4), 563–576. [http-s://doi.org/10.1029/wr001i004p00563](https://doi.org/10.1029/wr001i004p00563)
- Edmonton Power Corporation (EPCOR). (2020). *Edmonton 2020 Source Water Protection Plan*. (Report). Edmonton, AB.
- Enviroatlas. (n.d.). *Hydrologic Unit Codes: HUC 4, HUC 8, and HUC 12*. Washington, DC: United States Environmental Protection Agency. Retrieved from <https://enviroatlas.epa.gov/enviroatlas/datafactsheets/pdf/Supplemental/HUC.pdf>
- Environment Alberta. (2008, January). *Focus on Climate Change*. Retrieved from <http://open.alberta.ca/publications/0778572039#summary>

Environment and Climate Change Canada. (2017, April 10). *Canada's freshwater quality in a global context*. Canada.ca. Retrieved July 20, 2022, from <https://www.canada.ca/en/environment-climate-change/services/environmental-indicators/freshwater-quality-global-context.html>

Environment and Climate Change Canada. (2021). *Water quality in Canadian rivers: Canadian Environmental Sustainability Indicators* (Report). Retrieved from www.canada.ca/en/environment-climate-change/services/environmental-indicators/water-qualitycanadian-rivers.html

European Environmental Agency. (2020, November 23). *Climate impacts on water resources*. Retrieved July 20, 2022, from <https://www.eea.europa.eu/archived/archived-content-water-topic/water-resources/climate-impacts-on-water-resources#:~:text=The%20main%20climate%20change>

Fenton, M. M., Waters E. J., Pawley, S. M., Atkinson, N., Utting E. J., & Mckay, K. (2013). *Surficial Geology of Alberta, 1:1,000,000 scale (GIS data, polygon features)*. [Data File]. Alberta Geological Survey. Retrieved from [http://www.agi.gov.ab.ca/publications/DIG/ZIP/DIG\\_2013\\_0002.zip](http://www.agi.gov.ab.ca/publications/DIG/ZIP/DIG_2013_0002.zip)

Freeze, R. A., & Cherry, J. A. (1979). *Groundwater*. Prentice-Hall.

Government of Alberta. (n.d.a) *Alberta Water Well Information Database (or Baseline Water Well Test Database)*. [Database]. Retrieved from <http://groundwater.alberta.ca/WaterWells/d/>

Government of Alberta. (n.d.b). *Groundwater Observation Well Network*. [Database]. Retrieved April 5, 2021, from <https://www.alberta.ca/lookup/groundwater-observation-well-network.aspx>

Grisak, G. E., & Cherry, J. A. (1975). Hydrologic characteristics and response of fractured till and clay confining a shallow aquifer. *Canadian Geotechnical Journal*, 12(1), 23–43. <https://doi.org/10.1139/t75-003>

- Harbaugh, A. W. (2005). MODFLOW-2005, The U.S. Geological Survey Modular Ground-Water Model—the Ground-Water Flow Process. In *Modeling Techniques*. U.S. Geological Survey.
- Heath, R. C. (1983). *Basic Ground-Water Hydrology* (Water Supply Paper 2220). U.S. Geological Survey.
- Hughes, A. T., Smerdon, B. D., & Alessi, D. S. (2017). Hydraulic properties of the Paskapoo Formation in west-central Alberta. *Canadian Journal of Earth Sciences*, 54(8), 883–892. <https://doi.org/10.1139/cjes-2016-0164>
- Kathol, C. P., & McPherson, R. A. (1975). *Urban geology of Edmonton*. (ARC/AGS Bulletin 32, 91 p). Edmonton, AB: Alberta Research Council.
- Kaushal, S. S., Mayer, P. M., Vidon, P. G., Smith, R. M., Pennino, M. J., Newcomer, T. A., Duan, S., Welty, C. (2014). Land use and climate variability amplify carbon, nutrient, and contaminant pulses: A review with management implications. *JAWRA Journal of the American Water Resources Association*, 50(3), 585–614. <https://doi.org/10.1111/jawr.12204>
- Klassen, J., Liggett, J.E., Pavlovskii, I. and Abdurakhimova, P. (2018), *First-order groundwater availability assessment for southern Alberta* (AER/AGS Open File Report No. 2018-09). Alberta Energy Regulator/Alberta Geological Survey.
- McConnell, R.G. (1885). *Report on the Cypress Hills, Wood Mountain, and adjacent country* (Annual Report 1, Part C). Ottawa, ON: Geological Survey of Canada.
- Melnik, A. (2018). *Estevan Valley Aquifer* (Report). Moose Jaw, SA: Water Security Agency.
- Morgan, S. E., Allen, D. M., Kirste, D., & Salas, C. J. (2019). Investigating the hydraulic role of a large buried valley network on regional groundwater flow. *Hydrogeology Journal*, 27(7), 2377–2397. <https://doi.org/10.1007/s10040-019-01995-0>
- Morris, D. A., & Johnson, A. I. (1967). *Summary of Hydrologic and Physical Properties of Rock and Soil Materials, as Analyzed by the Hydrologic Laboratory of the U.S. Geological Survey* (Geological Survey Water-Supply Paper 1839-D). U.S. Geological Survey.
- Natural Resources Canada. (2020, July 14). Government of Canada. Retrieved September 09, 2020, from <https://www.nrcan.gc.ca/climate-change/impacts-adaptations/climate-change-impacts-forests/forest-change-indicators/drought/17772>

Pétré, M.-A., Rivera, A., & Lefebvre, R. (2015). Three-dimensional unified geological model of the Milk River Transboundary Aquifer (Alberta, Canada – Montana, USA). *Canadian Journal of Earth Sciences*, 52(2), 96–111. <https://doi.org/10.1139/cjes-2014-0079>

Prior, G. J., Hathway, B., Glombick, P. M., Pana D. I., Banks C. J., Hay, D. C., Schneider C. L., Grobe, M., et al. (2013). *Bedrock Geology of Alberta (GIS data, polygon features)*. [Data File]. Edmonton, AB: Alberta Geological Survey. Retrieved from [http://www.agi.gov.ab.ca/publications/DIG/ZIP/DIG\\_2013\\_0018.zip](http://www.agi.gov.ab.ca/publications/DIG/ZIP/DIG_2013_0018.zip)

Research Council of Alberta. (1978). *Edmonton Regional Utilities Study*. Alberta Environment, Pollution Control, Municipal Engineering.

Riddell, J.T.F., Moktan, H. and Jean, G. (2014). *Regional hydrology of the Edmonton–Calgary Corridor, Alberta* (AER/AGS Open File Report No. 2014-02). Edmonton, AB: Alberta Energy Regulator. Retrieved from <https://ags.aer.ca/publication/ofr-2014-02>

Riddle, A.D. (2021). *Update of the groundwater flow model for the Great Miami buried-valley aquifer in the vicinity of Wright-Patterson Air Force Base near Dayton, Ohio* (U.S. Geological Survey Scientific Investigations Report 2021–5115). 36 p. <https://doi.org/10.3133/sir20215115>.

Rubin, A. D. (2022). *Pre-Laurentide and Deglacial History of the Edmonton Region, Alberta, Canada* (master's thesis). Edmonton, AB: University of Alberta.

Seaber, R. P., Kapinos, F. P., & Knapp, L. G. (1987). *Hydrologic Unit Maps*. [Water-Supply Paper 2294]. U.S. Geological Survey. [https://pubs.usgs.gov/wsp/wsp2294/pdf/wsp\\_2294.pdf](https://pubs.usgs.gov/wsp/wsp2294/pdf/wsp_2294.pdf)

Shaver, R. B., & Pusc, S. W. (1992). Hydraulic barriers in pleistocene buried-valley aquifers. *Ground Water*, 30(1), 21–28. <https://doi.org/10.1111/j.1745-6584.1992.tb00807.x>

Sheets, R.A. (2007). Hydrogeologic setting and ground-water flow simulations of the Great Miami Basin Regional Study Area, Ohio, in Paschke, S.S., ed., *Hydrogeologic settings and ground-water flow simulations for regional studies of the transport of anthropogenic and natural contaminants to public-supply wells—studies begun in 2001—*. Washington DC: U.S. Geological Survey. <https://doi.org/10.3133/ pp1737A>.

Smerdon, B.D., Hughes, A.T. and Jean, G. (2017): *Permeability measurements of Upper Cretaceous and Paleogene bedrock cores made from 2004-2015 (tabular data, tab-delimited format, to accompany Open File Report 2016-03)*; Alberta Energy Regulator, AER/AGS Digital Data 2016-0042.

Smerdon, B. D., Mendoza, C. A., & McCann, A. M. (2005). Quantitative investigations of the hydraulic connection between a large reservoir and a buried valley aquifer in Southern Alberta. *Canadian Geotechnical Journal*, 42(5), 1461–1473. <https://doi.org/10.1139/t05-065>

Steelman, C. M., Arnaud, E., Pehme, P., & Parker, B. L. (2018). Geophysical, geological, and hydrogeological characterization of a tributary buried Bedrock Valley in Southern Ontario. *Canadian Journal of Earth Sciences*, 55(7), 641–658. <https://doi.org/10.1139/cjes-2016-0120>

Stein, R. (1976a). *Hydrogeology of the Edmonton area (northwest segment), Alberta* (Earth Sciences Report 1974-10). Edmonton, AB: Alberta Research Council.

Stein, R. (1976b). *Hydrogeological map of the Edmonton area (northeast segment), Alberta, NTS 83H* (Map 112). Edmonton, AB: Alberta Energy and Utilities Board.

Stein, R. (1982). *Hydrogeology of the Edmonton area (southeast segment), Alberta* (ARC/AGS Earth Sciences Report 1979-06). Edmonton, AB, Alberta Research Council.

Stein, R., Carlson, V. A., (1982). *Hydrogeological map of the Edmonton area (southeast segment), Alberta, NTS 83H* (Map 152). Edmonton, AB: Alberta Energy and Utilities Board.

Timoney, K. P., & Lee, P. (2009). Does the Alberta Tar Sands Industry Pollute? the scientific evidence. *The Open Conservation Biology Journal*, 3(1), 65–81. <https://doi.org/10.2174/1874839200903010065>

Tokarsky, O., (1971). *Hydrogeological map of the Rocky Mountain House area, Alberta, NTS 83B* (Map 099). Edmonton, AB: Alberta Geological Survey. Retrieved from <https://ags.ars.ca/publication/map-099>

Tyrrell, J B. (1887). *Report on a part of northern Alberta, and portions of adjacent districts of Assiniboia and Saskatchewan, embracing the country lying south of the north*

*Saskatchewan River and north of Lat. 51° 6', between Long 110° and 115° 15' west.*  
(Annual Report vol. 2, 176 pages). Ottawa, ON: Geological Survey of Canada, [http://doi.org/10.4095/296712](https://doi.org/10.4095/296712)

U.S. Geological Survey. (n.d.). *Groundwater and drought*. Retrieved April 23, 2022, from  
<https://water.usgs.gov/ogw/drought/>

van der Kamp, G., & Maathuis, H. (2011). The unusual and large drawdown response of buried-valley aquifers to pumping. *Ground Water*, 50(2), 207–215. <https://doi.org/10.1111/j.1745-6584.2011.00833.x>

WorleyParsons. (2009). *North Saskatchewan River Basin Overview of Groundwater Conditions, Issues, and Challenges* (Report No. E00088100). Edmonton, AB, North Saskatchewan Watershed Alliance.

Yang, Z., Shah, K., Laforest, S., Hollebone, B. P., Situ, J., Crevier, C., Lambert, P., Brown, C. E., et al. (2020). Occurrence and weathering of petroleum hydrocarbons deposited on the shoreline of the North Saskatchewan River from the 2016 Husky Oil Spill. *Environmental Pollution*, 258, 113769. <https://doi.org/10.1016/j.envpol.2019.113769>

## **Chapter 4: Conclusions and Future Research**

### **4.1 Conclusions**

Modelling groundwater flow systems in the Edmonton area with a focus on buried valleys demonstrates their role in regional groundwater flow, groundwater–surface water (GW-SW) interactions, and groundwater availability. The model constructed in this thesis represents the first effort to include surficial geology, newly mapped buried valley extents, and dipping bedrock geology. The combination of these elements offers a unique perspective and understanding of groundwater flow including interactions with the North Saskatchewan River (NSR). In addition, this model allows for a regional scale approximation of buried valleys potential as an alternative water resource for the city of Edmonton.

The steady state hydrogeological model described in chapter 2 demonstrates the role of buried valleys on groundwater flow, GW-SW interactions, and related baseflow variation along the NSR. Groundwater within the study area forms nested flow systems varying from regional to local-intermediate scale, driven by topography and influenced by the geological setting unique to the Western Prairies. Since buried valley aquifers have the highest hydraulic conductivity ( $K$ ) in the study area, they influence groundwater flow systems in their vicinity to conform with buried valley geometry. They receive groundwater input along their length and transmit groundwater parallel to valley thalwegs until hydrogeological conditions change along the flow path. This means that the buried valleys create meso-scale conduits for groundwater flow across the study area by linking local to intermediate scale recharge with regional flow path lengths. Buried valleys do not just influence horizontal groundwater flow directions but also vertical groundwater flow. Areas of favourable hydraulic gradient for upwards groundwater flow from bedrock deposits into buried valleys are commonly located at interpreted discharge areas. Conversely, some lakes located directly above the buried valleys often show an opposite effect, where lakes leak water downward into the buried valley systems. Lastly, the NSR receives increased baseflow along segments of its length that can be correlated to the presence of buried valleys. Increased baseflow correlated with buried valleys suggests that buried valleys increase groundwater flow to the NSR valley where paleo valleys and the modern-day river valleys coincide, potentially facilitating enhanced baseflow to the NSR. Buried valleys noticeably influence nested flow systems and GW-SW interactions

which makes them important to consider when understanding groundwater flow directions and interaction with surface water features.

The Onoway, Beverly, and Stony channels were investigated for their potential in supplying the City of Edmonton with an alternate or supplementary water supply to the NSR. Based on the transient modelling in chapter 3, the channels can be ranked according to their ability to provide water as follows: (i) the Beverly channel providing the greatest volume (up to 190ML/day for 365 days); (ii) the Onoway channel providing a similar rate but for a short period of time (up to 190ML/day for 30 days); and (iii) the Stony channel providing the least amount of water (up to 10 ML/day for 365 days).

Considering that the City of Edmonton requires about 375 ML/day, some of the buried valley aquifers may be able to provide 25% to 50% of this requirement in an idealized scenario for 30-365 days. In the event the NSR could not be used due to contamination, sourcing water from the buried valley aquifers could provide much needed time for remediation or natural attenuation. Alternatively, buried valley aquifers may be used to supplement water in the event of seasonal drought in the NSR brought on by climate change. Even the Stony channel, which had the least amount of available groundwater, could supply critical facilities (e.g., hospitals) during an emergency. Furthermore, the Stony channel is in close proximity to E.L. Smith water treatment plant, allowing groundwater from the Stony channel to be more readily linked to the current water distribution system.

A first order hierarchy is offered in chapter 3 regarding maximum water withdrawal rates under idealized conditions in the three channels investigated that can guide future study in the area. However, it is important to consider the three-dimensional hydrogeological conditions within buried valleys in this hierarchy. Surrounding geology can both increase the pumping capacity of buried valley aquifers but also increase contamination potential. The Beverly channel has both increased pumping capacity but also increased contamination potential due to surrounding pitted deltas sediments. This contrasts with the Onoway and Stony channels that may have reduced pumping capacity but may be more protected from contamination due to surrounding low K glacial deposits. This is important to consider from a water supply perspective, and a balance must be obtained between groundwater vulnerability to contamination and available quantity for extraction.

## **4.2 Future Research**

Future research can be focused on three broad categories: (1) Assessment of groundwater flow system features (2) Potential of buried valley aquifers for water supply, and (3) targeted numerical modelling. These categories and their subcategories are described below in short format.

### 1) Assessment of groundwater flow system features

#### i) Field investigation of springs along the NSR valley and their relationship to buried valleys

- Measure spring output (rates) and chemistry along the NSR
- Aggregate spring output/chemistry to river segments defined by the scale/goals of the study
- Compare spring output/chemistry between areas where the NSR valley coincides with paleo valleys (buried valleys), and where it diverts or is independent of paleo valleys
- Determine whether any changes in spring output or chemistry in the NSR valley are correlated with the presence of buried valleys
- Use the total spring output and chemistry along the NSR valley to understand the spring water contribution to the NSR and quantify/characterize any changes along the NSR

### 2) Potential of buried valley aquifers for water supply

#### i) Geophysical fieldwork (Electrical Resistivity Tomography (ERT)) to better define geometry in areas of interest

- ERT work could be completed in one or all of three channels investigated where a pumping well installation is proposed
- ERT may better constrain channel extents and identify heterogeneities for a local groundwater model or could be done in conjunction with drilling/field hydrogeological investigation (e.g., calibration of ERT measurements with rock/soil core/wireline geophysical logs)

#### ii) Hydrogeologic characterization through drilling and test well installation

- Core logs and/or geophysical logs (gamma, resistivity, etc.) may be obtained during/after the drilling process to obtain valuable sedimentological and geophysical data that can be correlated to ERT sections; possibly identifying local heterogeneities that would impact a well field
- Test well installation will enable measurement of hydraulic properties specific to a local area, which will help to determine well feasibility through real world observations

### 3) Targeted numerical modelling

#### i) Local scale groundwater model for pumping field design (informed by item 2, above)

- Create a local scale model, centered around an area where enhanced field work has been done as outlined in item 2
- Utilize the regional groundwater model of this thesis to define boundary conditions of the local scale model
- Design a well field or fence and test various configurations for optimal drawdown characteristics

#### ii) Improvement of the current regional model presented in this thesis

- Refinement of the current model conceptualization may be done to help lower run times and increase computational power in key areas
- Decreasing overall grid spacing (in areas of low hydraulic gradients), and increasing nodal count in areas where high hydraulic gradients exist may help to reduce runtimes and potentially lower residuals
- Areas where nodal counts could be increased are the NSR river valley, south-western areas of the model where steep topography dominates, and around the buried valleys
- In addition, an increased number of lakes and/or rivers/creeks could be represented in the model may help to better constrain the water table, potentially increasing accuracy

iii) Fully coupled GW-SW modelling

- A new GW-SW model could use similar conceptualization for the groundwater portion of the model but would have the benefit of simulating surface processes.
- The main advantage of a new GW-SW model would be to potentially enable better quantification of GW-SW exchange fluxes for real world applications
- Using this, a better understanding of the buried valleys role as it relates to lakes, rivers, and discharge areas may be achieved

## Bibliography

- Alberta Environment and Parks. (2014). *HUC Watersheds of Alberta*. [Shapefile].
- Alberta Environment and Parks. (2017, March 1). *Alberta Provincial 25 Metre Raster*. [DEM].  
<https://open.alberta.ca/opendata/gda-c16469a2-5541-455c-bba0-63a24c0ff08a#summary>
- Anderson, M. P., Woessner, W. W., & Hunt, R. J. (2015). *Applied groundwater modeling: Simulation of flow and Advective Transport*. Elsevier, Academic Press.
- Andriashuk, D. L. (1988). *Quaternary Stratigraphy of the Edmonton Map Area, NTS 83H*. (Open File Report 198804). Edmonton, AB: Natural Resources Division, Alberta Research Council.
- Andriashuk, D. L. (2019). *Thalwegs of Bedrock Valleys, Alberta, Version 2 (GIS data, line features) Edition: v.2*. [Data file] Alberta Energy Regulator/Alberta Geological Survey. Retrieved from [http://ags.aer.ca/document/DIG/DIG\\_2018\\_0001.zip](http://ags.aer.ca/document/DIG/DIG_2018_0001.zip).
- Andriashuk, L. D., Fenton, M. M., Root, J. D. (1979). *Surficial Geology Wabamun Lake, Alberta (NTS 83G)*. (Map 149). Edmonton, AB: Alberta Geological Survey. Retrieved from <https://ags.aer.ca/publication/map-149>.
- Anis, M. R., & Sauchyn, D. J. (2021). Ensemble projection of future climate and surface water supplies in the North Saskatchewan River basin above Edmonton, Alberta, Canada. *Water*, 13(17), 2425. <https://doi.org/10.3390/w13172425>
- Akhtar, N., Syakir Ishak, M. I., Bhawani, S. A., & Umar, K. (2021). Various natural and anthropogenic factors responsible for water quality degradation: A Review. *Water*, 13(19), 2660. <https://doi.org/10.3390/w13192660>
- Augustine, N. V. (2015). *Estimating Specific Storage and Matrix Compressibility from Barometric Efficiency in the Southern Alberta Paskapoo Aquifer System* (master's thesis). Calgary, AB: University of Calgary.
- Barnett, B., Townley, L. R., Post, V., Evans, R. E., Hunt, R. J., Peeters, L., Richardson, S., Werner, A. D., et al. (2012). (Waterlines Report Series 82.). *Australian groundwater modelling guidelines*. Canberra: National Water Commission.

- Barker, A.A., Riddell, J.T.F., Slattery, S.R., Andriashuk, L.D., Moktan, H., Wallace, S., Lyster, S., Jean, G., et al. (2011). *Edmonton-Calgary Corridor groundwater atlas* (ERCB/AGS Information Series 140, 98 p). Edmonton, AB: Energy Resources Conservation Board.
- Bayrock, L. A. (1972). *Surficial Geology Edmonton (83H)*. (Map 143). Edmonton, AB: Alberta Research Council.
- Bayrock, L.A. & Hughes, G.M. (1962). *Surficial geology of the Edmonton district, Alberta; Research Council of Alberta*. (RCA/AGS Earth Sciences Report 1962-06). Edmonton, AB, Alberta Research Council.
- Bedient, P. B., Rifai, H. S., & Newell, C. J. (1999). *Ground water contamination: Transport and remediation* (2nd Edition). Prentice Hall PTR.
- Bibby, R. (1974a). *Hydrogeology of the Edmonton area (northwest segment), Alberta*. (ARC/AGS Earth Sciences Report 1974-10). Edmonton, AB: Alberta Research Council.
- Bibby, R. (1974b). *Hydrogeological map of the Edmonton area, northwest segment, Alberta, NTS 83H (part)*. (Map 108). Edmonton AB: Alberta Geological Survey.
- Bibby, R. (1974c). *Regional chemistry and water level distribution of the near-surface groundwaters of the Edmonton area (northwest segment) Alberta*. (ARC/AGS Earth Sciences Report 1974-06). Edmonton AB, Alberta Research Council.
- Brown, C. M., Evans, D. C., Ryan, M. J., & Russell, A. P. (2013). New data on the diversity and abundance of small-bodied ornithopods (Dinosauria, ornithischia) from the Belly River Group (campanian) of Alberta. *Journal of Vertebrate Paleontology*, 33(3), 495–520. <https://doi.org/10.1080/02724634.2013.746229>
- Burns, E. R., Bentley, L. R., Hayashi, M., Grasby, S. E., Hamblin, A. P., Smith, D. G., & Wozniak, P. R. (2010). Hydrogeological implications of Paleo-fluvial architecture for the Paskapoo Formation, SW Alberta, Canada: A Stochastic analysis. *Hydrogeology Journal*, 18(6), 1375–1390. <https://doi.org/10.1007/s10040-010-0608-y>
- Cathcart, J., Lorenz, K., Depoe, S., Phelan, C., Casson, J., & Jedrych, A. T. (2008). Volume 3: AESA Water Quality Monitoring Project. In *Assessment of Environmental Sustainability in Alberta's agricultural watersheds*. Palliser Environmental Services Ltd. and Alberta Agriculture and Rural Development.

Ceroici, W.J. (1979a). *Hydrogeology of the southwest segment, Edmonton, Alberta*. (ARC/AGS Earth Sciences Report 1978-05). Edmonton AB: Alberta Research Council.

Ceroici, W. J. (1979b). *Hydrogeological map of the Edmonton area (southwest segment), Alberta, NTS 83H (part)*. (Map 117). Edmonton AB: Alberta Geological Survey.

Chunn, D., Faramarzi, M., Smerdon, B., & Alessi, D. (2019). Application of an integrated SWAT–MODFLOW model to evaluate potential impacts of climate change and water withdrawals on groundwater–surface water interactions in west-central Alberta. *Water*, 11(1), 110. <https://doi.org/10.3390/w11010110>

Cummings, D. I., Russell, H. A., & Sharpe, D. R. (2012). *Buried valleys and till in the Canadian Prairies: Geology, hydrogeology, and origin*. (Current research - Geological Survey of Canada). Ottawa, ON: Natural Resources Canada.

Demchuk, T. D., & Hills, L. V. (1991). A Re-examination of the Paskapoo Formation in the Central Alberta Plains: The Designation of Three New Members. *Bulletin of Canadian Petroleum Geology*, 39(3), 270–282.

Domenico, P. A., & Mifflin, M. D. (1965). Water from low-permeability sediments and land subsidence. *Water Resources Research*, 1(4), 563–576. <https://doi.org/10.1029/wr001i004p00563>

Edmonton Power Corporation (EPCOR). (2020). *Edmonton 2020 Source Water Protection Plan*. (Report). Edmonton, AB.

Enviroatlas. (n.d.). *Hydrologic Unit Codes: HUC 4, HUC 8, and HUC 12*. Washington, DC: United States Environmental Protection Agency. Retrieved from <https://enviroatlas.epa.gov/enviroatlas/datafactsheets/pdf/Supplemental/HUC.pdf>

Environment Alberta. (2008, January). *Focus on Climate Change*. Retrieved from <https://open.alberta.ca/publications/0778572039#summary>

Environment and Climate Change Canada. (2017, April 10). *Canada's freshwater quality in a global context*. Canada.ca. Retrieved July 20, 2022, from <https://www.canada.ca/en/environment-climate-change/services/environmental-indicators/freshwater-quality-global-context.html>

Environment and Climate Change Canada. (2021). *Water quality in Canadian rivers: Canadian Environmental Sustainability Indicators* (Report). Retrieved from [www.canada.ca/en/environment-climate-change/services/environmental-indicators/water-qualitycanadian-rivers.html](http://www.canada.ca/en/environment-climate-change/services/environmental-indicators/water-qualitycanadian-rivers.html)

Environment and Climate Change Canada. (2022, March 2). *Canadian Climate Normals 1981-2010 Station Data*. Retrieved from [https://www.climate.weather.gc.ca/climate\\_normals/results\\_1981\\_2010\\_e.html?stnID=2402&dispBack=0](https://www.climate.weather.gc.ca/climate_normals/results_1981_2010_e.html?stnID=2402&dispBack=0)

European Environmental Agency. (2020, November 23). *Climate impacts on water resources*. Retrieved July 20, 2022, from <https://www.eea.europa.eu/archived/archived-content-water-topic/water-resources/climate-impacts-on-water-resources#:~:text=The%20main%20climate%20change>

Farvolden, R., N., Meneley, W., A., Le Breton, E., G., Lennox, D., H., Meyboom, P. (1963). *Early Contributions to the Groundwater Hydrology of Alberta*. (Bulletin 12). Edmonton AB: Alberta Research Council.

Feltham, K. (1993). Quaternary sediments in central Edmonton, Alberta, Canada: Stratigraphy, distribution, and Geotechnical Implications. *Quaternary International*, 20, 13-26. doi:10.10-16/1040-6182(93)90033-c

Fenton, M. M., Waters E. J., Pawley, S. M., Atkinson, N., Utting E. J., & Mckay, K. (2013). *Surficial Geology of Alberta, 1:1,000,000 scale (GIS data, polygon features)*. [Data File]. Alberta Geological Survey. Retrieved from [http://www.agi.gov.ab.ca/publications/DIG/ZIP/DIG\\_2013\\_0002.zip](http://www.agi.gov.ab.ca/publications/DIG/ZIP/DIG_2013_0002.zip)

Freeze, R. A., & Cherry, J. A. (1979). *Groundwater*. Prentice-Hall.

Freeze, R. A., & Witherspoon, P. A. (1967). Theoretical analysis of regional groundwater flow: 2. effect of water-table configuration and subsurface permeability variation. *Water Resources Research*, 3(2), 623–634. <https://doi.org/10.1029/wr003i002p00623>

Glombick, P. (2010). *Top of the Belly River Group in the Alberta Plains: Subsurface Stratigraphic Picks and Modelled Surface*. (ERCB/AGS Open File Report No. 2010-10). Edmonton, AB: Energy Resources Conservation Board, Alberta Geological Survey.

Godfrey, J. D. (2001). *Edmonton beneath our feet: A guide to the geology of the Edmonton Region*. Edmonton, AB: Edmonton Geological Society.

Government of Alberta. (n.d.a) *Alberta Water Well Information Database (or Baseline Water Well Test Database)*. [Database]. Retrieved from <http://groundwater.alberta.ca/WaterWells/d/>

Government of Alberta. (n.d.b). *Groundwater Observation Well Network*. [Database]. Retrieved April 5, 2021, from <https://www.alberta.ca/lookup/groundwater-observation-well-network.aspx>

Grasby, S. E., Chen, Z., Hamblin, A. P., Wozniak, P. R. J., & Sweet, A. R. (2008). Regional characterization of the Paskapoo Bedrock Aquifer System, Southern Alberta. Geological Survey of Canada Contribution 2008-0479. *Canadian Journal of Earth Sciences*, 45(12), 1501–1516. <https://doi.org/10.1139/e08-069>

Grisak, G. E., & Cherry, J. A. (1975). Hydrologic characteristics and response of fractured till and clay confining a shallow aquifer. *Canadian Geotechnical Journal*, 12(1), 23–43. <https://doi.org/10.1139/t75-003>

Harbaugh, A. W. (2005). MODFLOW-2005, The U.S. Geological Survey Modular Ground-Water Model—the Ground-Water Flow Process. In *Modeling Techniques*. U.S. Geological Survey.

Harbaugh, A.W., Langevin, C.D., Hughes, J.D., Niswonger, R.N., and Konikow, L. F., (2017), MODFLOW-2005, the U.S. Geological Survey modular groundwater model: U.S. Geological Survey Software Release (Version 1.12.00) [Software]. U.S. Geological Survey. <http://dx.doi.org/10.5066/F7RF5S7G>

Heath, R. C. (1983). *Basic Ground-Water Hydrology* (Water Supply Paper 2220). U.S. Geological Survey.

Hubbert, M. K. (1940). The theory of ground-water motion. *Transactions, American Geophysical Union*, 21(2), 648. <https://doi.org/10.1029/tr021i002p00648-1>

Hughes, A. T., Smerdon, B. D., & Alessi, D. S. (2017). Hydraulic properties of the Paskapoo Formation in west-central Alberta. *Canadian Journal of Earth Sciences*, 54(8), 883–892. <https://doi.org/10.1139/cjes-2016-0164>

Hydrogeological Consultants Ltd. (1998a). *County of Lamont No. 30 Part of the North Saskatchewan River Basin Parts of Tp 051 to 058, R 15 to 20, W4M Regional Groundwater Assessment*. (Report No. 97-100). Agriculture and Agri-Food Canada, Prairie Farm Rehabilitation.

Hydrogeological Consultants Ltd. (1998b). *Lac Ste. Anne County Parts of the North Saskatchewan and Athabasca River Basins Parts of Tp 053 to 059, R 01 to 09, W5M Regional Groundwater Assessment*. (Report No. 97-112). Agriculture and Agri-Food Canada, Prairie Farm Rehabilitation.

Hydrogeological Consultants Ltd. (1998c). *Parkland County Part of the North Saskatchewan and Athabasca River Basins Parts of Tp 050 to 054, R 25, W4M to R 08, W5M Regional Groundwater Assessment*. (Report No. 97-202). Agriculture and Agri-Food Canada, Prairie Farm Rehabilitation.

Hydrogeological Consultants Ltd. (1999). *Leduc County Part of the North Saskatchewan River Basin Parts of Tp 047 to 051, R 21 to 28, W4M and R 01 to 04, W5M Regional Groundwater Assessment*. (Report No. 98-130). Agriculture and Agri-Food Canada, Prairie Farm Rehabilitation.

Hydrogeological Consultants Ltd. (2001). *Sturgeon County Part of the North Saskatchewan River Basin Parts of Tp 053 to 058, R 20 to 28, W4M & Tp 054 to 057, R 01, W5M Regional Groundwater Assessment*. (Report No. 01-100). Agriculture and Agri-Food Canada, Prairie Farm Rehabilitation.

Irish, E J W; Havard, C J. (1968). *Whitemud and Battle Formations, Kneehills Tuff Zone, a Stratigraphic Marker*. (Paper 67-63). Ottawa, ON: Geological Survey of Canada. <https://doi.org/10.4095/101442>

Kathol, C. P., & McPherson, R. A. (1975). *Urban geology of Edmonton*. (ARC/AGS Bulletin 32, 91 p). Edmonton, AB: Alberta Research Council.

Kaushal, S. S., Mayer, P. M., Vidon, P. G., Smith, R. M., Pennino, M. J., Newcomer, T. A., Duan, S., Welty, C. (2014). Land use and climate variability amplify carbon, nutrient, and contaminant pulses: A review with management implications. *JAWRA Journal of the American Water Resources Association*, 50(3), 585–614. <https://doi.org/10.1111/jawr.12204>.

Khidir, A., & Catuneanu, O. (2010). Reservoir characterization of scollard-age fluvial sandstones, Alberta Foredeep. *Marine and Petroleum Geology*, 27(9), 2037–2050. <http://doi.org/10.1016/j.marpetgeo.2010.05.001>

Klassen, J., Liggett, J.E., Pavlovskii, I. and Abdurakhimova, P. (2018), *First-order groundwater availability assessment for southern Alberta* (AER/AGS Open File Report No. 2018-09). Alberta Energy Regulator/Alberta Geological Survey.

Land Information Services Division. (1988). *Specifications and Procedures Manual*. Alberta Forestry, Lands, and Wildlife.

MacCormack, K. E., Atkinson, N., & Lyster, S. (2015). *Bedrock Topography of Alberta* (Map 602). Edmonton, AB: Alberta Geological Survey.

Marvel, K., Cook, B. I., Bonfils, C., Durack, P. J., Smerdon, J. E., & Williams, A. P. (2019). Twentieth-century emergence of an externally forced signal in global hydroclimate. *Nature*, 569, 59–65.

McConnell, R.G. (1885). *Report on the Cypress Hills, Wood Mountain, and adjacent country* (Annual Report 1, Part C). Ottawa, ON: Geological Survey of Canada.

Melnik, A. (2018). *Estevan Valley Aquifer* (Report). Moose Jaw, SA: Water Security Agency.

Morgan, S. E., Allen, D. M., Kirste, D., & Salas, C. J. (2019). Investigating the hydraulic role of a large buried valley network on regional groundwater flow. *Hydrogeology Journal*, 27(7), 2377–2397. <https://doi.org/10.1007/s10040-019-01995-0>

Morris, D. A., & Johnson, A. I. (1967). *Summary of Hydrologic and Physical Properties of Rock and Soil Materials, as Analyzed by the Hydrologic Laboratory of the U.S. Geological Survey* (Geological Survey Water-Supply Paper 1839-D). U.S. Geological Survey

Mossop, G. D., Shetsen, I., Dawson, F. M., Evans, C. G., Marsh, R., Richardson, R., Power, B., Sweet, A. R., et al. (1994). Chapter 24 - Uppermost Cretaceous and Tertiary Strata of the Western Canada Sedimentary Basin. In *Geological atlas of the western canada sedimentary basin*. Calgary, AB: Canadian Society of Petroleum Geologists.

Natural Resources Canada. (2020, July 14). Government of Canada. Retrieved September 09, 2020, from <https://www.nrcan.gc.ca/climate-change/impacts-adaptations/climate-change-impacts-forests/forest-change-indicators/drought/17772>

Organisation for Economic Co-operation and Development (OECD). (2013). Chapter 3: Climate change adaptation for water systems in OECD countries. In *Water and climate change adaptation: Policies to navigate Uncharted Waters*. <https://doi.org/10.1787/9789264200449-7-en>

Ozoray, G.F. (1972). *Hydrogeology of the Wabamun Lake area, Alberta* (RCA/AGS Earth Sciences Report 1972-08). Edmonton, AB, Research Council of Alberta.

Pétré, M.-A., Rivera, A., & Lefebvre, R. (2015). Three-dimensional unified geological model of the Milk River Transboundary Aquifer (Alberta, Canada – Montana, USA). *Canadian Journal of Earth Sciences*, 52(2), 96–111. <https://doi.org/10.1139/cjes-2014-0079>

Post, V. E., & von Asmuth, J. R. (2013). Review: Hydraulic head measurements—new technologies, Classic Pitfalls. *Hydrogeology Journal*, 21(4), 737–750.

Prior, G. J., Hathway, B., Glombick, P. M., Pana D. I., Banks C. J., Hay, D. C., Schneider C. L., Grobe, M., et al. (2013). *Bedrock Geology of Alberta (GIS data, polygon features)*. [Data File]. Edmonton, AB: Alberta Geological Survey. Retrieved from [http://www.agso.v.ab.ca/publications/DIG/ZIP/DIG\\_2013\\_0018.zip](http://www.agso.v.ab.ca/publications/DIG/ZIP/DIG_2013_0018.zip)

Research Council of Alberta (1978). *Edmonton Regional Utilities Study* (Vol. IV Groundwater). Edmonton, AB: Alberta Environment and RPA Consultant Limited.

- Riddell, J.T.F., Moktan, H. and Jean, G. (2014). *Regional hydrology of the Edmonton–Calgary Corridor, Alberta* (AER/AGS Open File Report No. 2014-02). Edmonton, AB: Alberta Energy Regulator. Retrieved from <https://ags.aer.ca/publication/ofr-2014-02>
- Riddle, A.D. (2021). *Update of the groundwater flow model for the Great Miami buried-valley aquifer in the vicinity of Wright-Patterson Air Force Base near Dayton, Ohio* (U.S. Geological Survey Scientific Investigations Report 2021–5115). 36 p. <https://doi.org/10.3133/sir20215115>.
- Rubin, A. D. (2022). *Pre-Laurentide and Deglacial History of the Edmonton Region, Alberta, Canada* (master's thesis). Edmonton, AB: University of Alberta.
- Seaber, R. P., Kapinos, F. P., & Knapp, L. G. (1987). *Hydrologic Unit Maps*. [Water-Supply Paper 2294]. U.S. Geological Survey. [https://pubs.usgs.gov/wsp/wsp2294/pdf/wsp\\_2294.pdf](https://pubs.usgs.gov/wsp/wsp2294/pdf/wsp_2294.pdf)
- Shaver, R. B., & Pusc, S. W. (1992). Hydraulic barriers in pleistocene buried-valley aquifers. *Ground Water*, 30(1), 21–28. <https://doi.org/10.1111/j.1745-6584.1992.tb00807.x>
- Sheets, R.A. (2007). Hydrogeologic setting and ground-water flow simulations of the Great Miami Basin Regional Study Area, Ohio, in Paschke, S.S., ed., *Hydrogeologic settings and ground-water flow simulations for regional studies of the transport of anthropogenic and natural contaminants to public-supply wells—studies begun in 2001—*. Washington DC: U.S. Geological Survey. <https://doi.org/10.3133/ pp1737A>.
- Smerdon, B.D., Hughes, A.T. and Jean, G. (2017). Permeability measurements of Upper Cretaceous and Paleogene bedrock cores made from 2004-2015 (tabular data, tab-delimited format, to accompany Open File Report 2016-03) (AER/AGS Digital Data 2016-0042). Edmonton, AB: Alberta Energy Regulator.
- Smerdon, B. D., Mendoza, C. A., & McCann, A. M. (2005). Quantitative investigations of the hydraulic connection between a large reservoir and a buried valley aquifer in Southern Alberta. *Canadian Geotechnical Journal*, 42(5), 1461–1473. <https://doi.org/10.1139/t05-065>
- Steelman, C. M., Arnaud, E., Pehme, P., & Parker, B. L. (2018). Geophysical, geological, and hydrogeological characterization of a tributary buried Bedrock Valley in Southern Ontario.

*Canadian Journal of Earth Sciences*, 55(7), 641–658. <https://doi.org/10.1139/cjes-2016-0120>

Stein, R. (1976a). *Hydrogeology of the Edmonton area, (northeast segment), Alberta* (ARC/AGS Earth Sciences Report 1976-01). Edmonton, AB, Alberta Energy and Utilities Board.

Stein, R. (1976b). *Hydrogeological map of the Edmonton area (northeast segment), Alberta, NTS 83H* (Map 112). Edmonton, AB: Alberta Energy and Utilities Board.

Stein, R. (1982). *Hydrogeology of the Edmonton area (southeast segment), Alberta* (ARC/AGS Earth Sciences Report 1979-06). Edmonton, AB, Alberta Research Council.

Stein, R., Carlson, V. A., (1982). *Hydrogeological map of the Edmonton area (southeast segment), Alberta, NTS 83H* (Map 152). Edmonton, AB: Alberta Energy and Utilities Board.

Timoney, K. P., & Lee, P. (2009). Does the Alberta Tar Sands Industry Pollute? the scientific evidence. *The Open Conservation Biology Journal*, 3(1), 65–81. <https://doi.org/10.2174/1874839200903010065>

Tokarsky, O., (1971). *Hydrogeological map of the Rocky Mountain House area, Alberta, NTS - 83B* (Map 099). Edmonton, AB: Alberta Geological Survey. Retrieved from <https://ags.agr.ca/publication/map-099>

Tóth, J. (1962). A theory of groundwater motion in small drainage basins in central Alberta, Canada. *Journal of Geophysical Research*, 67(11), 4375–4388. <https://doi.org/10.1029/jz067i011p04375>

Tóth, J. (1963). A theoretical analysis of groundwater flow in small drainage basins. *Journal of Geophysical Research*, 68(16), 4795–4812. <https://doi.org/10.1029/jz068i016p04795>

Tóth, J. (1970). A conceptual model of the groundwater regime and the hydrogeologic environment. *Journal of Hydrology*, 10(2), 164–176. [https://doi.org/10.1016/0022-1694\(70\)90186-1](https://doi.org/10.1016/0022-1694(70)90186-1)

Tyrrell, J B. (1887). *Report on a part of northern Alberta, and portions of adjacent districts of Assiniboia and Saskatchewan, embracing the country lying south of the north Saskatchewan River and north of Lat. 51° 6', between Long 110° and 115° 15' west.*

(Annual Report vol. 2, 176 pages). Ottawa, ON: Geological Survey of Canada, [http://doi.org/10.4095/296712](https://doi.org/10.4095/296712)

U.S. Geological Survey. (n.d.). *Groundwater and drought*. Retrieved April 23, 2022, from [http://water.usgs.gov/ogw/drought/](https://water.usgs.gov/ogw/drought/)

van der Kamp, G., & Maathuis, H. (2011). The unusual and large drawdown response of buried-valley aquifers to pumping. *Ground Water*, 50(2), 207–215. <https://doi.org/10.1111/j.1745-6584.2011.00833.x>

Von Hauff, H. M. (2004). *Three-dimensional numerical modelling of the Wagner Natural Area Groundwater Flow System* (master's thesis). Edmonton, AB: University of Alberta.

Winter, T. C. (1976). Numerical simulation analysis of the interaction of lakes and Ground Water. *Professional Paper*. <https://doi.org/10.3133/pp1001>

WorleyParsons. (2009). *North Saskatchewan River Basin Overview of Groundwater Conditions, Issues, and Challenges* (Report No. E00088100). Edmonton, AB, North Saskatchewan Watershed Alliance.

Yang, Z., Shah, K., Laforest, S., Hollebone, B. P., Situ, J., Crevier, C., Lambert, P., Brown, C. E., et al. (2020). Occurrence and weathering of petroleum hydrocarbons deposited on the shoreline of the North Saskatchewan River from the 2016 Husky Oil Spill. *Environmental Pollution*, 258, 113769. <https://doi.org/10.1016/j.envpol.2019.113769>

Zaremehrjardy, M., Victor, J., Park, S., Smerdon, B., Alessi, D. S., & Faramarzi, M. (2022). Assessment of snowmelt and groundwater-surface water dynamics in mountains, foothills, and plains regions in northern latitudes. *Journal of Hydrology*, 606, 127449. <https://doi.org/10.1016/j.jhydrol.2022.127449>

Zektser I. S., & Everett, L. G. (2006). *Ground Water Resources of the world and their use*. National Ground Water Association Press.